

Even-point Multi-loop Unitarity and its Applications: Exponentiation, Anomalies and Evanescence

John Joseph M. Carrasco,¹ Nicolas H. Pavao¹

¹*Department of Physics and Astronomy, Northwestern University, Evanston, Illinois 60208, USA*

ABSTRACT: We identify novel structure in newly computed multi-loop amplitudes and quantum actions for even-point effective field theories, including both the nonlinear sigma model (NLSM) and double-copy gauge theories such as Born-Infeld and its supersymmetric generalizations. We exploit special properties of all even-point theories towards efficient unitarity based amplitude construction. We find evidence that the leading IR divergence of NLSM amplitudes exponentiates. We then systematically compute the two-loop anomalous behavior of Born-Infeld, and find that the counterterms required to restore $U(1)$ behavior at loop-level in the Born-Infeld theory can be constructed via a symmetric-structure double-copy. We also demonstrate that the one-minus $(-+++)$ two-loop amplitude vanishes upon the introduction of an evanescent operator. In addition to these pure photon counterterms, we verify through explicit calculation that the anomalous matrix elements that violate $U(1)$ duality invariance can be alternatively cancelled by summing over internal $\mathcal{N} = 4$ DBIVA superfields. Finally we find that $\mathcal{N} = 4$ Dirac-Born-Infeld-Volkov-Akulov (DBIVA) amplitudes permit double-copy construction through two-loop order by reproducing our unitarity based result with a double copy between color-dual $\mathcal{N} = 4$ super-Yang-Mills and our two-loop NLSM amplitudes. This result provides strong evidence for the existence of a color-dual representations for NLSM beyond one-loop. We conclude with an overview of how D -dimensional four-photon counterterms can be constructed in generality with the symmetric-structure double-copy, and outline a convenient way of counting evanescent operators using Hilbert series as generating functions.

Contents

1	Introduction	2
2	Review	4
2.1	Color-dressed and ordered amplitudes	4
2.2	Color-Kinematics Duality and the Double-Copy	5
2.3	4D Spinor Helicity vs. D -dimensions	7
2.4	One-loop integral basis and tensor reduction	8
2.5	Even-point Effective Field Theories	10
2.6	On-shell Unitarity methods	15
3	Even-point Multi-loop Unitarity	18
3.1	Multi-loop recursive integrals	20
3.2	Two-loop tensor reduction	21
3.3	Gauge-invariant basis tensors	25
4	Loop-level results	28
4.1	NLSM via EMU	29
4.1.1	One-loop	29
4.1.2	Two-loop	31
4.2	DBIVA via EMU	35
4.2.1	One-loop DBIVA	36
4.2.2	Two-loop Born-Infeld	42
4.2.3	Two-loop $\mathcal{N} = 4$ DBIVA	44
4.3	DBIVA via double copy	46
4.3.1	One-loop $\mathcal{N} = 4$ DBIVA	47
4.3.2	Two-loop $\mathcal{N} = 4$ DBIVA	47
5	Effective Actions	48
5.1	Anomaly cancellation	49
5.1.1	One-loop	49
5.1.2	Two-loop	50
5.2	Double copy construction	52
5.2.1	Symmetric-structure double-copy	52
5.2.2	Higher-spin \otimes Adler Zero	53
5.3	Evanescient operator counting	54
6	Conclusions	56

1 Introduction

Recent decades have seen significant advances in our ability to compute scattering amplitudes to higher orders in perturbation theory. At the epicenter of this explosion in the generation of sharp S -matrix data is the unitarity method [1–3], which bypasses the standard Feynman diagram approach by constructing higher order amplitudes directly from lower order on-shell information. At one-loop, the unitarity method allows one to extract amplitudes by directly computing a series of unitarity cuts [4]. On-shell methods have furthermore unveiled novel amplitude-level structure, like the duality between color and kinematics [5] and associated double-copy construction [6], which are frequently obscured by the traditional classical Lagrangian description of the theories. While much of the research in perturbative calculations thus far has focused on gauge theory and gravity, recent literature has investigated to what extent the S -matrix of effective field theory is constrained by on-shell data [7–24].

In this paper we make the quantum leap to the multi-loop sector of effective field theory. Namely we study even-point (EP) effective field theory (EFT) at the multi-loop level using a combination of generalized unitarity [1–3] and the double-copy construction [5, 6]. The EFTs that we consider are the nonlinear sigma model (NLSM) and a related family of gauge theories involving Born-Infeld theory and supersymmetric generalizations known as Dirac-Born-Infeld-Volkov-Akulov (DBIVA) theories. These families are known at tree-level to be double-copies between NLSM and Yang-Mills theories with varying amounts of supersymmetry. While we focus on these specific examples, the methods we develop can be used for perturbative calculations in any even point effective field theory.

The motivation for this work is three-fold. First, perturbative calculations in NLSM and DBIVA effective field theories are in many ways significantly simpler than the typical multi-loop calculations of more phenomenological theories, like quantum-chromodynamics (QCD). As we will show, the multi-loop amplitudes for these theories allow us to recycle many of the D -dimensional integration tools that are so powerful at one-loop order. To approach this problem, we expand on the now standard approach of Forde [4], that computes one-loop amplitudes directly from 4D unitarity cuts. In section 3 we’ll show that there are only two basis integrals needed at two-loop four-point for even point effective field theory amplitudes. In the spirit of one-loop unitarity, the integral coefficients can be directly extracted from EMU and tensor reduction. Our method of Even-point Multi-loop Unitarity (EMU) is a D -dimensional approach to integrand construction. This allows us to compute a large catalog of D -dimensional two-loop amplitudes, which provides fertile ground for cultivating insights about the multi-loop structure of effective field theories. The perturbative depth of our calculations sheds light on the exponential structure of IR divergences for NLSM amplitudes through two-loops, the anomalous behavior $U(1)$ duality invariance through two-loop order in DBIVA theories, as well as the emergence of evanescent operators relevant for anomaly cancellation in pure Born-Infeld theory. We believe these surprisingly rich physical structures could serve as a theoretical laboratory for future studies of the interplay between effective field theory operators and perturbative calculations in quantum field theory.

The second motivation is that very little is known about the duality between color and kinematics at multi-loop level for generic models in the web of theories [25]. For a comprehensive review of color-dual representations, see refs. [25–27] and references therein. While there has been tremendous success of applying the color-kinematics duality to $\mathcal{N} = 4$ super-Yang-Mills, for which color-dual integrands are known through four-point four-loop [28–30], five-point through three-loops, and to seven-point at one-loop [31–33], there are many obstructions for generic gauge/gravity theories. Presently, the state-of-the-art for nonlinear sigma model (NLSM) color-dual numerators come from the *XYZ* model of Cheung and Shen [34], while D -dimensional integrands for pure Yang-Mills have only been identified through five-point one-loop [35]. At present, there are no known D s-dimensional representations for either of these theories at two-loop that globally manifest the duality between color and kinematics, despite attempts in the literature [36–39]. Furthermore, similar bottlenecks exists for less-than-maximal $\mathcal{N} < 2$ sYM [40]. While there have been a number of recent developments in constructing manifestly color-dual Feynman rules [41–47], a precise definition the kinematic algebra off-shell remains elusive. Considering the known tree-level double-copy relationships between NLSM and DBIVA and higher-derivative corrections [48, 49], all of the amplitudes we compute should in principle participate in a double-copy formulation of our results. At the very least, the amplitudes we compute will serve as important checks on future breakthroughs in multi-loop studies of color-dual representations. In addition to traditional double-copy construction, we find that the quantum effective actions generated by loop effects permit a rather compact construction in terms of symmetric-structure double-copy, which was introduced in recent work by the authors [50].

Finally, DBIVA effective field theories touch a wide range research areas at the forefront of high energy physics. Of more formal interest, is the presence of quantum anomalies that violate the $U(1)$ duality invariance, which the theory enjoys at tree-level [51]. The presence of these $U(1)$ anomalies in gravity is closely linked to ultraviolet divergences computed at loop-level [52–55]. It has been argued that cancelling these anomalous matrix elements with R^n counterterms can lead to enhanced UV cancellations [56–58]. This relationship has been demonstrated both for pure Einstein-Hilbert gravity [59–61], and also for less than maximal $\mathcal{N} \leq 4$ supergravity [62]. While DBIVA theories are themselves ultraviolet divergent in $D = 4$, due to their simplicity they serve as an essential laboratory for probing anomaly cancellation at high loop order. Moreover, in addition to their formal theory relevance, DBI has garnered wide phenomenological interest in cosmology, both for sourcing non-gaussianities in CMB bispectrum [63–65], and for their consistency with the observed CMB tensor mode suppression [66–70]. Thus, with inflationary data on the horizon, understanding the perturbative structure of DBI could be particularly relevant for modeling early universe quantum fluctuations.

The outline of the paper is as follows: in section 2, we will provide a review of the on-shell methods and integration techniques needed to probe the multi-loop physics studied in this paper. Then in section 3, we introduce the method of Even-point Multi-loop Unitarity (EMU) and compute the two-loop tensor integrals needed in this work. In section 4, we

present our results, beginning with a warm-up calculation in section 4.1 where we construct the integrands for NLSM through NNLO in the effective coupling, and compute the fully integrated amplitudes. We show that in $D = 2 - 2\epsilon$, the leading IR divergences of the theory exponentiate. With the scaffolding of D -dimensional integration in hand, we then compute two-loop amplitudes for $\mathcal{N} = 4$ DBIVA theory and pure-photon Born-Infeld theory in section 4.2. There we compute the anomalies present beyond one-loop order. Then, using the NLSM integrands of section 4.1, we perform a multi-loop double-copy to $\mathcal{N} = 4$ DBIVA observables with the color-dual basis numerators available in the literature in section 4.3. After computing the catalog of two-loop amplitudes, we study the construction of quantum effective actions in section 5 as they relate to the anomalous matrix elements present in two-loop Born-Infeld amplitudes. We demonstrate in section 5.1 that the one-minus anomaly at two-loop requires the introduction of an evanescent operator at $\mathcal{O}(\alpha'^4)$. Then in section 5.2 we take the opportunity to discuss the application of symmetric-structure double copy to cancel these anomalies, along with their relationship to higher-spin modes as studied in a recent work by the authors. Finally, in section 5.3 we lay out a Hilbert series framework for counting evanescent operators at general orders in mass-dimension. To conclude, in section 6 we discuss many directions of future work and summarize the insights gained from this study.

2 Review

2.1 Color-dressed and ordered amplitudes

Here we provide an overview of the amplitudes nomenclature and organizational principles we use throughout the work. When working with scattering amplitudes, \mathcal{A} , in an on-shell framework it is convenient to introduce the following graphical description at general multiplicity, n , and loop order, L ,

$$\mathcal{A}_{n,L} = \int \prod_{i=1}^L \frac{d^D l_i}{(2\pi)^D} \sum_g \frac{1}{S_g} \frac{\mathcal{N}_g}{D_g} \quad (2.1)$$

As written above, S_g are the internal symmetry factors for a Feynman diagram, g , the propagator structure is captured by the denominator function, D_g , and the theory-dependent interaction vertices determine numerator functions, \mathcal{N}_g . As written the numerator functions carry all non-propagator kinematic information and any color-data that would be encoded in the interaction Feynman rules of the theory. By color-data we mean the typical weighting of feynman diagrams by the representation of the particles described. Most of the theories we describe are defined in the adjoint, so the color-data involves the usual dressing of vertices with antisymmetric structure constants, f^{abc} . Although, as we will see, it will be useful to describe certain counterterms in terms of symmetric d^{abc} color-weights,

For gauge theories, it is often useful to further decompose the full, or color-dressed, amplitudes of eq. (2.1) into purely kinematic building blocks where the color information is stripped away. For example, at tree level, gauge theory n -point amplitudes can be re-expressed in terms

of a trace basis decomposition as follows:

$$\mathcal{A}_{n,\text{tree}} = \sum_{\sigma \in S^{n-1}} \text{Tr}(T^1 T^{\sigma(2)} \dots T^{\sigma(n)}) A_n(1, \sigma(2), \dots, \sigma(n)) \quad (2.2)$$

where the sum is taken over the inequivalent orderings of group theory generator traces. A similar decomposition applies to one-loop gauge theory amplitudes, which we will describe in section 4. The color-ordered functions, A_n , are called partial amplitudes, as they only contain on-shell information for a particular color ordering. However, like full amplitudes, they factor on poles to lower-point partial amplitudes. For vector theories partial amplitudes are independently gauge invariant since they weight linearly independent color traces.

When expressed in this form, many gauge theories reveal hidden redundancy that is obscured by the color-dressed amplitude formulation of eq. (2.1). The $(n-1)!$ partial amplitudes for a large catalog [25] of adjoint gauge theories, including Yang-Mills and NLSM, are linearly related to a smaller set of basis amplitudes. The first such set of partial amplitude relations identified by Kleiss and Kluijff [71], known formally as KK relations, relates amplitudes different color orderings and signature to a basis of $(n-2)!$ partial amplitudes:

$$A(1, \alpha, n, \beta) = (-1)^{|\alpha|} \sum_{\sigma \in \alpha \sqcup \beta^T} A(1, \sigma, n) \quad (2.3)$$

where β^T denotes the inverse ordering of β , and \sqcup is the shuffle product that runs over ordered permutations of α and β^T . More recently, Bern, Johansson and one of the authors, (BCJ) further identified a set of kinematic relations that reduced the size of n -point partial amplitude basis down to $(n-3)!$ via BCJ relations [5]:

$$\sum_{i=2}^{n-1} k_1 \cdot (k_2 + \dots + k_i) A(2, \dots, i, 1, \dots, n) = 0 \quad (2.4)$$

Underlying both sets of amplitude relations are hidden graphical principles that manifest the amplitude level redundancy of eq. (2.3) and eq. (2.4), which we describe in the next section. Before moving on, we emphasize that everything described thus far applies in arbitrary space-time dimensions. As such, the aforementioned nomenclature and organization are well suited for constructing loop integrands compatible with dimensional regularization.

2.2 Color-Kinematics Duality and the Double-Copy

To apprehend this graph-based structure for color-dressed theories, we first rewrite the full amplitude of eq. (2.1) as a sum over cubic graphs, as follows:

$$\mathcal{A}_{n,L} = \int \prod_{i=1}^L \frac{d^D l_i}{(2\pi)^D} \sum_{g \in \Gamma_{n,L}^{(3)}} \frac{1}{S_g} \frac{C_g N_g}{D_g} \quad (2.5)$$

where N_g and C_g are the kinematic numerators and color factors, respectively, and $\Gamma_{n,L}^{(3)}$ denotes the set of cubic diagrams at n -point L -loop. In this formulation of the amplitude,

contact diagrams are absorbed into cubic graphs by multiplying by inverse propagators. The procedure of assigning contact diagrams to cubic graphs is referred to as generalized gauge freedom [5]. In practice, there are many different ways to assign contact diagrams to cubic graphs.

The gauge theories that we study in this paper have sufficient generalized gauge freedom to assign contact diagrams to kinematic numerators such that at every multiplicity at tree level one can write the amplitude in terms of N_g that obey the same algebraic relations as the color factors, C_g . For color factors that are composed of adjoint structure constants, f^{abc} they must be anti-symmetric around vertices, and be related by Jacobi relations about each edge. For $SU(N_c)$ we can take $f^{abc} \propto \text{Tr}(T^a[T^b, T^c])$ for arbitrary representation T of the gauge group. We will also consider generalization beyond the adjoint to color-weights that can include d^{abc} and associated algebraic relations. For $SU(N_c)$ we can take $d^{abc} \propto \text{Tr}(T^a\{T^b, T^c\})$. Symmetric-structure color obey symmetric algebraic relations rather than anti-symmetric ones. When a gauge theory can be expressed in a form such that the color and kinematic factors obey the same algebraic relations, we call such theories color-dual. For ordered amplitudes the ability to find kinematic numerators that obey antisymmetry and Jacobi relations is one-to-one with the ordered amplitudes satisfying KK and BCJ relations, respectively.

An important consequence of color-kinematics duality is the ability to double-copy [5] color-dual numerators with each other preserving simultaneously factorization of ordered-amplitudes as well as gauge-invariance. Because cubic-graph color-weights are not linearly independent, gauge-invariance of the full amplitude is encoded in algebraic relation between the color factors. Thus, equipped with a set of color-dual numerators, \tilde{N}_g , that obey the same algebraic relations as C_g , we can make the simple replacement, $C_g \rightarrow \tilde{N}_g$, giving a new gauge invariant amplitude, \mathcal{M} , as follows:

$$\mathcal{M}_{n,L} = \int \prod_{i=1}^L \frac{d^D l_i}{(2\pi)^D} \sum_{g \in \Gamma_{n,L}^{(3)}} \frac{1}{S_g} \frac{\tilde{N}_g N_g}{D_g} \quad (2.6)$$

Note that \mathcal{M} is colorless. It satisfies manifest gauge invariance on the N_g side of the double copy due to the algebraic properties of \tilde{N}_g . In the event that \tilde{N}_g also belongs to a vector theory, then \mathcal{M} describes amplitudes in a gravitational theory. In such a case the gauge invariance of constituent \mathcal{A} and $\tilde{\mathcal{A}}$ conspire to generate linearized diffeomorphism invariance. As long as both kinematic factors obey the same algebraic constraints as the color algebra, this double copy construction works for integrands at the multi-loop level since it globally manifests color-kinematics on all possible unitarity cuts.

Throughout the text we will reserve \mathcal{M} to denote double-copy amplitudes. As shorthand, when the kinematic weights of two theories, X and Y , participate in the double copy

construction of \mathcal{M}^{XY} we will use the outer-product to mean double copy construction as in,

$$\mathcal{M}^{XY} = X \otimes Y \equiv \int \prod_{i=1}^L \frac{d^D l_i}{(2\pi)^D} \sum_{g \in \Gamma_{n,L}^{(3)}} \frac{1}{S_g} \frac{N_g^X N_g^Y}{D_g}. \quad (2.7)$$

At tree-level, such double-copy construction in the adjoint case can be understood equivalently [[**REFs NEEDED**]] in terms of a KLT or momentum kernel matrix $S(a|b)$ and a BCJ spanning set of ordered amplitudes for each of the X and Y theories,

$$X \otimes Y = \sum_{a,b \in S_{n-3}(2,\dots,n-2)} A^X(1, \{a\}, n, n-1) S(a|b) A^Y(1, \{b\}, n-1, n), \quad (2.8)$$

where the sum runs over both sets a, b of $(n-3)!$ distinct ordered amplitudes. No such momentum kernel has been constructed yet for the symmetric case.

As we will see, double-copy construction between symmetric color-dual kinematic numerators [50] is quite natural for capturing Born-Infeld counterterms needed for anomaly cancellation beyond one loop. Indeed, many of the higher derivative counterterms captured by double-copying symmetric kinematic factors are inaccessible¹ to the traditional double copy between adjoint kinematics. We will describe this non-adjoint color-dual double-copy in more detail in section 5.2, where we will explicate the tension between local symmetric numerators and higher-spin adjoint numerators.

2.3 4D Spinor Helicity vs. D -dimensions

All the amplitude methods we have discussed thus far are valid in arbitrary dimension. This has a number of advantages that we will touch upon when reviewing integrand construction towards dimensionally regulated amplitudes in section 2.6. While most of our calculations will be carried out completely agnostic to the spacetime dimension, the vector amplitudes we compute will have 4D symmetries that will be completely obscured by D -dimensional kinematics. It is useful therefore to also consider 4D kinematics.

When working with boson kinematics in arbitrary dimensions, we will employ formal Lorentz covariant polarizations, ε_a^μ , and momenta, k_a^μ . The mostly minus signature will be used throughout. The only restrictions we will place on physical momenta and polarizations are the standard on-shell constraints: momentum conservation and the null-momenta condition,

$$\sum_a k_a^\mu = 0 \quad k_a^2 = 0 \quad (2.9)$$

Furthermore, we will take external polarizations ε_a formal and transverse throughout:

$$\varepsilon_a \cdot k_a = 0 \quad (2.10)$$

¹As identified in ref. [50] they can technically be described in terms of adjoint double-copy but between presumably unphysical theories that require factorization involving higher-spin exchange.

Dimensions will generically be away from four, $D = 4 - 2\epsilon$, with ϵ arbitrary.

As noted, it will be convenient to take $D \rightarrow 4$ in certain circumstances after integration. In such cases we will employ appropriate spinor-helicity variables. Here we apply the same conventions of ref. [73], which we quote now. For massless momenta k_a , and k_b we have

$$s_{ab} = (k_a + k_b)^2 = \langle ab \rangle [ba] \quad (2.11)$$

the component definition of our spinor bracket that are consistent with the conventions above,

$$\langle ab \rangle = \frac{(a_1 + ia_2)(b_0 + b_3) - (b_1 + ib_2)(a_0 + a_3)}{\sqrt{(a_0 + a_3)(b_0 + b_3)}} \quad (2.12)$$

$$[ab] = \frac{(b_1 - ib_2)(a_0 + a_3) - (a_1 - ia_2)(b_0 + b_3)}{\sqrt{(a_0 + a_3)(b_0 + b_3)}} \quad (2.13)$$

where the a_i are component values of the four-vector, $k_a^\mu = (a_0, a_1, a_2, a_3)$.

Four-dimensional polarization dot products with fixed helicity states can be mapped as follows:

$$\begin{aligned} k_a \cdot \varepsilon_b^{(+)} &= \frac{\langle qa \rangle [ab]}{\sqrt{2} \langle qb \rangle} & k_a \cdot \varepsilon_b^{(-)} &= -\frac{[qa] \langle ab \rangle}{\sqrt{2} [qb]} \\ \varepsilon_a^{(-)} \cdot \varepsilon_b^{(+)} &= -\frac{\langle qa \rangle [qb]}{[qa] \langle qb \rangle} & \varepsilon_a^{(\pm)} \cdot \varepsilon_b^{(\pm)} &= 0 \end{aligned} \quad (2.14)$$

where q^μ is some null reference momentum that all polarizations are projected along.

While all four-dimensional equivalence relayed in this paper can be achieved analytically, in practice it is often much more convenient to verify equivalence numerically.

2.4 One-loop integral basis and tensor reduction

It is well known that one-loop amplitudes are spanned by a small basis of scalar integrals [4, 109, 110]. This property can be exposed via a D -dimensional integral reduction algorithm due to Passarino and Veltman [74]. The basis of irreducible scalar products (ISPs) that include loop momenta grows in lock step with the number of propagators. Explicitly, an N -gon integral can have $N - 1$ factors of $(k_i \cdot l)$, due to momentum conservation, and exactly one factor of l^2 ; this matches the number of N -gon propagators.

Furthermore, factors of $(\epsilon_i \cdot l)$ can be mapped to tensor structures with factors of $(\epsilon_i \cdot k_j)(k_i \cdot l)/(k_i \cdot k_j)$ using polarization completeness relations [56]. Thus, any N -gon tensor integral permits a partial fraction decomposition in terms of inverse propagators, and thus can be mapped to a scalar basis of integrals:

$$T_{\mu_1 \mu_2 \dots \mu_r} I_N^{\mu_1 \mu_2 \dots \mu_r} = \sum_{M=1}^N C_M I_M \quad (2.15)$$

where $T_{\mu_1 \mu_2 \dots \mu_r}$ and C_M are functions exclusively of external kinematics. This relationship holds D -dimensionally for any r -rank N -gon one-loop integral. Thus, any one-loop amplitude can be expressed completely in terms of a basis of one-loop integrals. This special property of

one-loop integration is not the case for generic loop order, where the basis of ISPs grows faster than number of inverse propagators. As such, any universal integral basis beyond one-loop must include integrals with non-unit exponents for **JJ: powers of** the propagators.

The remarkable simplicity of one-loop amplitudes is even more dramatic in a fixed space-time dimension. In $D = 4$, the kinematic projection to a basis of scalar integrals saturates at the box integral due to the appearance of Gram determinants. Roughly speaking, N -gon integral coefficients of eq. (2.44) come dressed with a factor of \mathcal{G}_N ,

$$\mathcal{G}_N = \det(k_i \cdot k_j) \quad (2.16)$$

where k_i are the external momenta flowing into the N -gon integral. In fixed spacetime dimension, D , the momenta are D -component vectors and thus the Lorentz product matrix $(k_i \cdot k_j)$ must have a null space for $N > D$. As a result, $C_M \neq 0$, only when $M \leq D + 1$. Furthermore, in $D = 4 - 2\epsilon$ dimensions, any scalar pentagon integral can be rewritten up to $\mathcal{O}(\epsilon)$ in terms of five pinched scalar box integrals [111]. All the information of one-loop 4D amplitudes can therefore be completely determined by evaluating up to box integrals, regardless of the multiplicity. We will demonstrate in the next section how this can be used in 4D integral construction.

The last important feature of one-loop basis integrals is that many of them can be evaluated in arbitrary dimension for a very general set of parameters appearing in the exponents of the propagators. **JJ: Save Boxed for our key results?** Take for example the D -dimensional triangle and bubble integrals that we will use throughout the text:

$$\begin{aligned} I_{2,(K)}^{(\alpha_1, \alpha_2)} &= \int \frac{d^{2D}l}{(2\pi)^{2D}} \frac{1}{[l^2]^{\alpha_1} [(l+K)^2]^{\alpha_2}} \\ &= i \left[-\frac{K^2}{4\pi} \right]^D \frac{\Gamma(D - \alpha_1) \Gamma(D - \alpha_2) \Gamma(\alpha_{12} - D)}{[K^2]^{\alpha_{12}} \Gamma(\alpha_1) \Gamma(\alpha_2) \Gamma(2D - \alpha_{12})} \\ I_{3,(K_{12})}^{(\alpha_1, \alpha_2, \alpha_3)} &= \int \frac{d^{2D}l}{(2\pi)^{2D}} \frac{1}{[l^2]^{\alpha_1} [(l+K_1)^2]^{\alpha_2} [(l+K_{12})^2]^{\alpha_3}} \\ &= i \left[-\frac{K_{12}^2}{4\pi} \right]^D \frac{\Gamma(D - \alpha_{12}) \Gamma(D - \alpha_{23}) \Gamma(\alpha_{123} - D)}{[K_{12}^2]^{\alpha_{123}} \Gamma(\alpha_1) \Gamma(\alpha_3) \Gamma(2D - \alpha_{123})} \end{aligned} \quad (2.17)$$

where we have introduced the notation $\alpha_{12\dots n} = \alpha_1 + \alpha_2 + \dots + \alpha_n$, and have taken $D \rightarrow 2D$ to make the expressions more compact. The above integral expressions hold for massless external kinematics, $K_i^2 = 0$, which applies to all the integrals needed for the physical processes described in the text.

The existence of closed form expressions, like those in eq. (2.46), while common for one-loop integrals, are incredibly rare for higher loop order outside of very specialized kinematic regimes. Luckily, in this work, the integral basis at four-point two-loop order for even-point theories can be reconstructed from the one-loop expressions in eq. (2.46). This is a special

$$\Omega_{(2,4)} = \left\{ \text{diagram 1}, \text{diagram 2} \right\}$$

Figure 1. Recursive one-loop integrals contributing to the two-loop four-point calculation in even-point effective field theories, we refer to as the ostrich integral and double-bubble from left to right.

property of we refer to as recursively one-loop amplitudes, which we can exemplify in the simple context of scalar ϕ^{2k} theory.

Consider the interactions needed to construct two loop amplitudes for the generic arbitrarily weighted ϕ^{2k} -scalar theory:

$$\mathcal{L}_{\phi^{2k}} = \frac{1}{2}(\partial\phi)^2 + c_4\phi^4 + c_6\phi^6 + c_8\phi^8 + \dots \quad (2.18)$$

The two-loop amplitude for ϕ^{2k} theory is simply generated by evaluating the following set of scalar 1-particle-reducible (1PI) integrals:

$$\begin{aligned} \mathcal{M}_{\phi^{2k}}^{2\text{-loop}} = & \frac{c_4^3}{4} \text{diagram 1} + \frac{c_4^3}{2} \text{diagram 2} + \frac{c_8}{4} \text{diagram 3} \\ & + \frac{c_4 c_6}{6} \text{diagram 4} + \text{perms}(1, 2, 3, 4) \end{aligned} \quad (2.19)$$

Since the external states are massless, only the first two integrals, those appearing in Fig. 1, are non-vanishing in dimensional regularization – the rest are scaleless. Therefore the above even-point perturbative predictions of ϕ^{2k} is equivalent to ϕ^4 theory at four-point through two-loop order:

$$\mathcal{M}_{\phi^{2k}}^{2\text{-loop}} \equiv \mathcal{M}_{\phi^4}^{2\text{-loop}} \quad (2.20)$$

In addition to being perturbatively equivalent to the quartic sector of the theory at two-loop, we can see above that the integrals for the Feynman diagrams in eq. (2.21) are recursively one-loop. In other words, to integrate the full amplitude at two-loop, we only need the iterated basis of one-loop integrals. This observation comes with the added advantage of permitting the application of one-loop Passarino-Veltman tensor reduction [74] to two loop integrals. This property of recursively one-loop integrals will dramatically simplify the higher derivative even point theories that we consider in this work.

2.5 Even-point Effective Field Theories

In this section we provide a catalog of the even-point effective field theories studied in this paper. We will define the Lagrangian, \mathcal{L} , to be the integrand of the action, S , when working

in spacetime coordinate frame:

$$S = \int d^D x \mathcal{L} \quad (2.21)$$

Some theories in this work, like Volkov-Akulov and supersymmetric extensions of Born-Infeld, have natural formulations in terms of vielbeins that depend on fermionic degrees of freedom. For such theories, it is useful to distinguish between the coordinate independent actions, and the coordinate-dependent Lagrangians.

Nonlinear Sigma Model The simplest effective field theory that we will consider in this work is the nonlinear sigma model (NLSM). The NLSM Lagrangian can be expressed in terms of the chiral current, $j_\mu = U^\dagger \partial_\mu U$, as follows,

$$\mathcal{L}^{\text{NLSM}} = \frac{1}{2} \text{tr}[(\partial_\mu U)^\dagger (\partial^\mu U)] = \frac{1}{2} \text{tr} \left[\frac{(\partial_\mu \pi)(\partial^\mu \pi)}{(1 - f_\pi^{-2} \pi^2)^2} \right] \quad (2.22)$$

where the trace is over the color indices of the gauge group, $\pi \equiv \pi^a T^a$, and on the right hand side we have applied the Cayley parameterization to the $SU(N_c)$ group elements, $U = \frac{1 + \pi/f_\pi}{1 - \pi/f_\pi}$, where f_π is the dimensionful pion decay width. This theory is the unique two-derivative EFT that is invariant under constant shifts of the pion field in color space:

$$\pi^a \rightarrow \pi^a + c^a \quad (2.23)$$

We could also consider higher derivative generalizations of the NLSM that are invariant under the shift symmetry of eq. (2.25). Such EFTs correspond to the so-called chiral limit **JJ**: **Maybe cite Jara's collaborator -JJ** of chiral perturbation theory [75, 76], describing massless pion scattering below the chiral symmetry breaking scale of QCD.

$$\mathcal{L}^{\text{XPT}} = \frac{1}{2} \text{tr}[(\partial_\mu U)^\dagger (\partial^\mu U)] + \frac{\beta_1}{f_\pi^2} \text{tr}[(\partial_\mu U)^\dagger (\partial^\mu U)]^2 + \frac{\beta_2}{f_\pi^2} \text{tr}[\partial_\mu U^\dagger \partial_\nu U] \text{tr}[\partial_\mu U^\dagger \partial_\nu U] + \dots \quad (2.24)$$

By construction, each of the higher derivative operators appearing above are invariant under the shift symmetry of eq. (2.25). These higher derivative generalizations of NLSM have been studied both in the context of the S -matrix bootstrap [77–79], and soft theorem bootstraps of refs. [8–12]. Considering the relevance of eq. (2.26) in Standard Model pion scattering, the amplitudes for $SU(2)$ NLSM have been computed through two-loop order [80–82]. In this work, we add to the literature by computing the two-loop amplitudes of eq. (2.24) for arbitrary $SU(N_c)$ color structure. In doing so, we show that the IR divergences of the theory exponentiates in the large N_c limit.

Born-Infeld Photons and Dirac Scalars The second even-point EFT we will study is Born-Infeld theory [83]. This theory describes the dynamics of open string endpoints with $U(1)$ charge attached to a D -dimensional spacetime with Dirichlet boundary conditions. Given the stringy dynamics orthogonal to the spacetime, the electric field generated by the

charged endpoints has a maximum field strength of order the inverse string tension, $1/\alpha'$. The effective Lagrangian for this theory

$$\alpha'^2 \mathcal{L}^{\text{BI}} = 1 - \sqrt{\det(\eta_{\mu\nu} + \alpha' F_{\mu\nu})}. \quad (2.25)$$

A close cousin of Born-Infeld theory is the dimensionally reduction to Dirac scalars, which describes a D -dimensional spacetime propagating in a $(D+1)$ -dimensional background:

$$\alpha'^2 \mathcal{L}^{\text{DBI}} = 1 - \sqrt{\det(\eta_{\mu\nu} + \alpha'^2 \partial_\mu \varphi \partial_\nu \varphi)} \quad (2.26)$$

where φ is the spacetime coordinate in the orthogonal space. This theory is uniquely determined by considering the most general polynomial of $X = (\partial\varphi)^2$, $P(X)$, constrained to be invariant under the field redefinition [10]:

$$\varphi \rightarrow \varphi + c + b^\mu (x_\mu + \varphi \partial_\mu \varphi) \quad (2.27)$$

When the transformation law leaves the polynomial $P(X)$ theory invariant, there are an additional $D+1$ conserved charges, and the Poincaré symmetry of $P(X)$ EFT is promoted from D to $(D+1)$ dimensions. One can verify that applying eq. (2.29) to eq. (2.28) shifts the Lagrangian by a total derivative [84]. Similar to the soft theorem constraints on the building blocks of NLSM and χ PT, the DBI action can be bootstrapped by requiring the amplitudes vanish at $\mathcal{O}(p^2)$ when taking external momentum, p , soft [10].

Volkov-Akulov Fermions and Supersymmetry Now we will describe the supersymmetric extensions of the Born-Infeld action given above in eq. (2.27). First we start by defining the theory of shift symmetric fermions first written down by Volkov, Akulov (VA) [85]. The easiest way to define this shift symmetric theory is by first constructing manifestly symmetric 1-forms, and constructing a volume form in the veirbein frame. That is, define a 1-form, $\omega^m = e_\mu^m dx^\mu$, where the veirbein (frame fields), e_μ^m , are expressed in terms of the fermion fields, λ , as follows:

$$e_\mu^m = \delta_\mu^m + i\bar{\lambda}\Gamma^m \overset{\leftrightarrow}{\partial}_\mu \lambda = \delta_\mu^m + i(\bar{\lambda}\Gamma^m \partial_\mu \lambda - \partial_\mu \bar{\lambda}\Gamma^m \lambda) \quad (2.28)$$

This frame field is manifestly invariant under the superspace shift:

$$\delta\lambda \rightarrow \eta \quad \delta\bar{\lambda} \rightarrow \bar{\eta} \quad \delta x^\mu \rightarrow x^\mu - i(\bar{\lambda}\Gamma^\mu \eta - i\bar{\eta}\Gamma^\mu \lambda) \quad (2.29)$$

The Volkov-Akulov action in the veirbein frame is then simply the fermionic world-volume integral over the D -form [86],

$$S^{\text{VA}} = \int \omega^1 \wedge \omega^2 \wedge \cdots \wedge \omega^D. \quad (2.30)$$

This is not dissimilar from the construction of the pure scale DBI action above. Likewise, we can write the Lagrangian in the spacetime coordinate from akin to eq. (2.27) and eq. (2.28).

Transforming back into spacetime coordinates, yields the following Lagrangian density for self interaction VA fermions upto four-point interactions:

$$\alpha'^2 \mathcal{L}^{\text{VA}} = \det(e_\mu^m) = i\bar{\lambda} \overleftrightarrow{\not{\partial}} \lambda + \frac{1}{2}(\bar{\lambda}\Gamma^\mu \partial^\nu \lambda)(\bar{\lambda}\Gamma_\mu \partial_\nu \lambda) + \mathcal{O}(\partial^4 \lambda^6). \quad (2.31)$$

A convenient choice of field redefinition was proposed by Komargodski and Seiberg (KS) [87, 88], which defines a new fermion field, $\psi = \psi(\lambda, \bar{\lambda})$, in a way that is perturbatively equivalent to the VA fermions. This construction is equivalent to a theory of nilpotent chiral superfields [89–91], relevant for the construction of α -attractor models of inflation [92]. Applying the KS nonlinear field redefinition yields the considerably simpler Lagrangian for VA theory:

$$\alpha'^2 \mathcal{L}^{\text{VA}} = i\bar{\psi} \not{\partial} \psi + \frac{1}{2}\bar{\psi}^2 \partial^2 \psi^2 + \frac{1}{4}\psi^2 \bar{\psi}^2 \partial^2 \psi^2 \partial^2 \bar{\psi}^2 \quad (2.32)$$

With the world-volume formulation of VA theory in hand, we can also trivially construct the action for maximal $\mathcal{N} = 1$ supersymmetric Born-Infeld theory in $D = 10$ [93, 94]. We simply replace the flat space background of eq. (2.27) with the fermionic background of eq. (2.33),

$$S_{\mathcal{N}=1}^{\text{DBIVA}} = \int \omega^1 \wedge \omega^2 \wedge \cdots \wedge \omega^{10} \sqrt{\det(\eta_{mn} + \alpha F_{mn})} \quad (2.33)$$

It is worth noting that the fermion-vector interaction is introduced via the non-minimal coupling between the field strength and the fermionic spacetime metric. This differs from the linearly realized supersymmetry of super-Yang-Mills theory, which minimally couples the vector mode to the chiral fermion. This non-minimal coupling is a requirement of supersymmetry due to the even-point nature abelian vector theories like Born-Infeld.

The action above in eq. (2.35) can be similarly re-expressed in terms of our canonical spacetime coordinates, giving us the following flat-space Lagrangian for maximally supersymmetric Born-Infeld theory in $D = 10$:

$$\alpha'^2 \mathcal{L}^{\text{DBIVA}}_s = \sqrt{\det(\eta_{\mu\nu} - \alpha' F_{\mu\nu} + \alpha'^2(\bar{\lambda}\Gamma_\mu \partial_\nu \lambda) - \alpha'^4(\bar{\lambda}\Gamma^\rho \partial_\mu \lambda)(\bar{\lambda}\Gamma_\rho \partial_\nu \lambda))}. \quad (2.34)$$

To recover the $D = 4$ theory, we simply dimensionally reduce in a way that preserves the maximum number of supercharges, which is $\mathcal{N} = 4$ in $D = 4$. While this is obscured at the level of the Lagrangian, implementing a dimensional reduction that preserves the supercharges of eq. (2.36) is rather straight forward in an on-shell framework.

$$\mathcal{M}^{\text{DBIVA}} = A^{\text{NLSM}} \otimes A^{\text{sYM}} \quad (2.35)$$

Since the double copy construction holds D -dimensionally at tree-level [25], double-copying maximal sYM with NLSM will yield the analogous spectrum of maximally supersymmetry DBIVA theory, whether in $D = 10$, as described above, or in $D = 4$, as we will study in this work.

Abelian Open String Similar to the amplitudes of DBIVA theories described above, the tree-level amplitudes for the open superstring (OSS) [95, 96] likewise permit a double copy construction [97]. To construct open-superstring amplitudes we simply double copy maximally supersymmetric super-Yang-Mills (sYM) and Chan-Paton dressed Z -theory amplitudes [49, 98, 99], as follows,

$$A^{\text{OSS}} = Z \otimes A^{\text{sYM}} \quad (2.36)$$

where \otimes implements the field theory double copy [5, 72] described above. Moreover, the amplitudes of DBIVA emerge from the above construction as the field theory limit of the abelian open superstring [100]. To recover the abelian sector, one simply sums over all Chan-Paton color orderings on the side of the bi-colored Z -theory amplitudes that obey string monodromy relations. In the field theory limit, the observables for so-called abelian Z -theory are simply the amplitudes generated by the NLSM Lagrangian [49]. That is, given a n -point amplitude in Z -theory, with field theory ordering $a = (a_1, a_2, \dots, a_n)$ and string theoretic color ordering $A = (A_1, A_2, \dots, A_n)$, one finds the following relation:

$$A^{\text{NLSM}}(a_1, a_2, \dots, a_n) \equiv \lim_{\alpha' \rightarrow 0} (\alpha')^{2-n} Z_{\times}(a_1, a_2, \dots, a_n) \quad (2.37)$$

where Z_{\times} are abelian Z -theory amplitudes of [49], defined by summing all possible orderings of Chan-Paton factors:

$$Z_{\times}(a_1, a_2, \dots, a_n) \equiv \sum_{A \in S^{n-1}} Z_{(A_1, \dots, A_{n-1}, n)}(a_1, a_2, \dots, a_n) \quad (2.38)$$

Since the field theory limit of abelian Z -theory produces NLSM amplitudes, the field theory limit of the abelian OSS, gives rise to DBIVA observables at leading order:

$$\begin{aligned} \lim_{\alpha' \rightarrow 0} Z_{\times} &= A^{\text{NLSM}} \otimes A^{\text{BAS}} \equiv A^{\text{NLSM}} \\ \Rightarrow \lim_{\alpha' \rightarrow 0} A_{\times}^{\text{OSS}} &= A^{\text{NLSM}} \otimes A^{\text{sYM}} \equiv A^{\text{DBIVA}} \end{aligned} \quad (2.39)$$

Additional details on the bi-colored Z -theory amplitudes these string-theoretic double-copy constructions can be found in [49, 97–99, 101] and references therein. We emphasize that that NLSM and DBIVA are the two theories that we will focus on in this work. However, the methods that we develop in the next section apply much more broadly to the full catalog of even-point theories.

Duality Invariance and Higher Derivatives In addition to the perturbative structure of these theories, four-dimensional DBIVA amplitudes have an additional special property that we will study in this work. At tree-level, the amplitudes generated by eq. (2.27) and eq. (2.35) exhibit $U(1)$ duality invariance [102, 103]. A theory is said to exhibit this on-shell 4D symmetry when the effect of rotating field strengths, $F^{\mu\nu}$, into the dual-fields, $G^{\mu\nu}$, defined below,

$$G^{\mu\nu} = \epsilon^{\mu\nu\rho\sigma} \frac{\partial \mathcal{L}}{\partial F^{\rho\sigma}}, \quad (2.40)$$

leaves the equations of motion invariant [104, 105]. This dynamical symmetry gives rise to a 4D helicity selection rule [103] whereby tree-level matrix elements outside the aligned-helicity sector vanish on-shell

$$\mathcal{M}_{(n_-, n_+)}^{\text{DBIVA}} = 0 \quad \Leftrightarrow \quad n_- \neq n_+, \quad (2.41)$$

where $n_{(+)}$ and $n_{(-)}$ is the number of external positive and negative helicity photons, respectively. For $\mathcal{N} = 0$ pure Born-Infeld theory [83, 106], this symmetry is violated at four-point one-loop in the all-plus (+ + + +) helicity sector [107]. In the text, we will show how this anomaly is propagated to two-loop, and demonstrate that $U(1)$ duality invariance is further broken in the $(- + + +)$ configuration beyond one-loop.

It is worth noting that in the case of supersymmetric DBIVA, at four-points, $U(1)$ symmetry is promoted to an R -symmetry, and is protected perturbatively to all orders by supersymmetric Ward Identities [108]. We will show this explicitly in the case of $\mathcal{N} = 4$ DBIVA through two-loop. However, we note that this supersymmetric enhancement of $U(1)$ duality does not carry over to higher multiplicity, where R -symmetry permits non-vanishing matrix elements outside the split helicity sector. To see one such example of this, we need not look any further than the abelianized OSS described above. At higher-multiplicity and higher orders in α' , the manifestly supersymmetric abelian OSS violates $U(1)$ duality. It would be fascinating if these higher derivative violations of $U(1)$ duality in OSS spectrum are precisely those needed to cancel anomalous behavior at the quantum level of higher multiplicity amplitudes. **JJ: Maybe some more words here? I'm not sure what we're saying – are we talking about stuff required to eat up anomalous 6-point behavior?** We see this as a natural future direction and application of the methods we develop in this work.

2.6 On-shell Unitarity methods

Above we have reviewed the known behavior of one-loop integral bases in $D = 4$ spacetime dimensions. In this section we will briefly demonstrate why traditional 4D unitarity methods are so powerful – and why we must go beyond them to accommodate the multi-loop calculations of interest in this work.

Integrands from 4D Cuts Applying one-loop integral reduction in 4D tells us that any one-loop massless amplitude, for which tadpoles are scaleless, can be expressed in terms of box, triangle, and bubble diagrams, with each integral weighted by dimensionally-dependent functions of kinematics:

$$\mathcal{A}^{1\text{-loop}} = \sum_{N=2}^4 C_N(D) I_N^D = \sum_{N=2}^4 C_N(4) I_N^D + \mathcal{R} \quad (2.42)$$

where the scalar basis-integrals, I_N^D , are evaluated in $D = 4 - 2\epsilon$, and \mathcal{R} is a rational term that emerges from series expanding around $\epsilon = (4 - D)/2$. To construct integral coefficients, C_N , we make use of the Optical Theorem for the S -matrix, which states that,

$$S^\dagger S = \mathbb{I} \quad \Rightarrow \quad 2 \text{Im}(T) = T^\dagger T \quad (2.43)$$

where $S = \mathbb{I} + iT$. Applying relation to eq. (2.47) allows us to identify the imaginary part of $\mathcal{A}^{1\text{-loop}}$ with the imaginary parts of each basis integral weighted by the respective 4D coefficient, $C_N(4)$:

$$\text{Im}(\mathcal{A}^{1\text{-loop}}) = \sum_{N=2}^4 C_N(4) \text{Im}(I_N^D) \quad (2.44)$$

JJ: Wording. Application of the optical theorem to constrain on-shell amplitudes is known as the unitarity method [1, 3]. In order to isolate each $C_N(4)$ appearing in eq. (2.47), we must employ generalized unitarity, which places particular internal legs on-shell. That is, for each internal loop propagator, $1/P_i^2$, that we wish to take on-shell, we make the following replacement inside the integral:

$$\frac{i}{P_i^2 + i\delta} \rightarrow 2\pi\delta^{(+)}(P_i^2) \quad (2.45)$$

This replacement of the internal propagators will select out the requisite imaginary parts needed to determine the integral coefficients. This approach to one-loop amplitude construction was systematized in ref. [4], which demonstrated how to directly extract the integrand coefficients directly from 4D cuts:

$$C_4^{(P_i P_j P_k)} \sim \begin{array}{c} \begin{array}{cc} P_i & P_j \\ \bullet & \bullet \\ | & | \\ \bullet & \bullet \\ | & | \\ P_k & \end{array} \end{array} \quad (2.46)$$

$$C_3^{(P_i P_j)} \sim \begin{array}{c} \begin{array}{c} P_i \\ \bullet \\ | \\ \bullet \end{array} \end{array} \quad (2.47)$$

$$C_2^{(P_i)} \sim \begin{array}{c} \begin{array}{c} \bullet \\ \diagup \quad \diagdown \\ \bullet \end{array} \end{array} \quad (2.48)$$

where exposed legs are summed over all internal states crossing the cut, and the labels P_i are external momentum scales flowing into the specified cuts. The subtractions account for the overlapping information in the respective N -gon cuts. By momentum conservation, the momentum flow in the unlabeled vertex is completely determined by the other $N - 1$ vertices.

As a concrete example, consider the 4D cut construction of the bubble coefficient for pure

Born-Infled theory:

$$\begin{array}{c} - \\ \diagup \quad \diagdown \\ \text{---} \quad \text{---} \\ \diagdown \quad \diagup \\ + \end{array} \quad \begin{array}{c} + \\ \diagdown \quad \diagup \\ \text{---} \quad \text{---} \\ \diagup \quad \diagdown \\ - \end{array} = \sum_{h_i \in \text{states}} \mathcal{M}^{\text{BI}}(1^-, 2^-, l_2^{h_2}, l_1^{h_1}) \mathcal{M}^{\text{BI}}(-l_1^{\bar{h}_1}, -l_2^{\bar{h}_2}, 3^+, 4^+) \quad (2.49)$$

$$= \langle 12 \rangle^2 [l_2 l_1]^2 \langle l_1 l_2 \rangle^2 [34]^2 \quad (2.50)$$

$$= [(l_1 + l_2)^2]^2 \langle 12 \rangle^2 [34]^2 \quad (2.51)$$

$$= s_{12}^2 \langle 12 \rangle^2 [34]^2 \quad (2.52)$$

where in the last step we have made the replacement $(l_1 + l_2) = -(k_1 + k_2)$ by momentum conservation. Determining the leading behavior of the 1-loop Born-Infled amplitude thus amounts to specifying all possible 4D cuts.

While this method is incredible powerful, as we can see from eq. (2.49) it misses a key piece of the amplitude – namely, the rational terms, \mathcal{R} . For some theories like $\mathcal{N} = 4$ super-Yang-Mills in $D = 4$ [2], rational terms are absent because the loop power counting for an N -gon cut is bounded to be less than $N - 2$. However, for generic theories of interest in this paper, like Born-Infled, rational terms are present and necessary for extracting anomalous matrix elements and higher-loop sub-divergences. While there are methods developed to extract these rational terms at one-loop using μ -integrals [109], at generic loop order evaluating these μ -integrals becomes increasingly complicated. For this reason, to perform the multi-loop calculations in this paper, we will employ cut construction in general dimensions [112, 113].

Integrands from D -dimensional Cuts The presence of 4D rational terms in the amplitude is due to the appearance of $(D - 4)$ factors. By constructing integrands D -dimensionally, we can guarantee that our integral coefficients are sensitive to these overall factors. Rather than summing over internal 4D states, we will instead compute D -dimensional cuts using the formal polarizations described in section 2.3. The D -dimensional analog of eq. (2.54) asserts that the one-loop integrand $\mathcal{I}_{1\text{-loop}}$ of pure Born-Infled theory should satisfy the following constraint:

$$\text{Cut}(\mathcal{I}_{1\text{-loop}}) = \sum_{h_i \in \text{states}} \mathcal{M}_4^{\text{BI}}(l_1^{h_1}, -l_2^{\bar{h}_2}) \mathcal{M}_4^{\text{BI}}(l_2^{h_2}, -l_1^{\bar{h}_1}), \quad (2.53)$$

where $\text{Cut}(\mathcal{I}_{1\text{-loop}})$ extracts the kinematic numerator by imposing a maximal cut on the one-loop integrand

$$\text{Cut}(\mathcal{I}_{1\text{-loop}}) \equiv l_1^2 l_2^2 (\mathcal{I}_{1\text{-loop}}) \Big|_{l_1^2, l_2^2 \rightarrow 0}. \quad (2.54)$$

To carry out the sum over formal polarization states in eq. (2.58) we apply the following D -dimensional completeness relation for on-shell polarizations,

$$\sum_{\text{states}} \varepsilon_{(l)}^\mu \varepsilon_{(-l)}^\nu = \eta^{\mu\nu} - \frac{l^\mu q^\nu + l^\nu q^\mu}{l \cdot q}, \quad (2.55)$$

with null reference momentum, $q^2 = 0$. The dependence of q is a gauge choice that disappears when on-shell kinematic constraints are imposed. At loop level, the state-sum of eq. (2.60)

can potentially lead to dimension dependence in the D -dimensional integrand. This is due to terms that contain products of internal polarizations:

$$\begin{aligned}
\mathcal{I}_{1\text{-loop}} &\supset \sum_{\text{states}} \varepsilon_{(l)}^\mu \varepsilon_{(-l)}^\nu \eta_{\mu\nu} \\
&= \left(\eta^{\mu\nu} - \frac{l^\mu q^\nu + l^\nu q^\mu}{l \cdot q} \right) \eta_{\mu\nu} \\
&= D_s - 2
\end{aligned} \tag{2.56}$$

where D_s is the spin-dimension of the internal photons, and where $D_s - 2$ just counts the number of photon states. To calculate the loop-level amplitudes in this work, we use dimensional regularization to regulate the integrals. In this work we adopt the conventions of [114, 115] and take the spin-dimension, D_s , to be the same as the dimension appearing in dimensional regularization, $D = 4 - 2\epsilon$. We will use them interchangeably throughout. The appearance of these D -dependent factors in the state sum are the source of rational terms in the Born-Infeld S -matrix. Throughout the text, we will use the generalized unitarity cut condition of eq. (2.58) to fix our multiloop integrands. With this in hand, in the spirit of Forde’s one-loop cut construction, we will now systematize the procedure for capturing all the cut information needed for even-point theories at the multiloop order.

3 Even-point Multi-loop Unitarity

In this section we will describe the methods we have developed to compute the multi-loop results of this paper. We begin by introducing the notion of Even-point Multi-loop Unitarity (EMU), which is an organizational principle at the foundation of our unitarity-based integrand construction. EMU is an extension of the method of maximal cuts [116], which is a hierarchical approach to perturbative calculations [117]. EMU is a constructive algorithm aimed at capturing all the perturbative information needed at general loop order and multiplicity. We describe the algorithm below, and provide a 2-loop 4-point example that we choose to study in this paper.

Even-point Multi-loop Unitarity (EMU)

- **Step 0** – At n -point l -loop, enumerate all 1-particle-irreducible (1PI) graphs constructed from $(n + 2l - 2)/2$ four-point vertices. We call these diagrams the maximal cut (MC) diagrams. Graphs with higher-point blobs are grouped into the $N^k\text{MC}$ category, where k is the number of collapsed internal propagators relative to the MC graphs.
- **Step 1** – Culling from $N^k\text{MC} \rightarrow \partial N^k\text{MC}$:
 - **Step 1A** – Discard all diagrams at the given order $N^k\text{MC}$ that capture scale-less behavior from **internal** kinematics. For massless theories, this amounts to

throwing out diagrams that contain one of the following internal nodes:



(3.1)

- **Step 1B** – Discard all diagrams at the given order $N^k MC$ that capture scaleless behavior from **external** kinematics. At n -point, this amounts to rejecting diagrams that contain $n - 1$ external edges attached to a single blob:



(3.2)

- **Step 2** – Collapsing from $\partial N^k MC \rightarrow N^{k+1} MC$: If the culling procedure of Step 1 produces an empty set of graphs, $\partial N^k MC = \emptyset$, then the routine terminates. If not, collapse one of the internal propagators for all diagrams in all topologically distinct ways. Collapsing a propagator simply means merging the two nodes connected by that propagator's edge and removing that edge all together. So the resulting graph will have one less internal edge and one less internal node. This collapsing step will take the $\partial N^k MC$ set of diagrams to $N^{k+1} MC$. Once there, repeat Step 1A and 1B until the routine terminates.

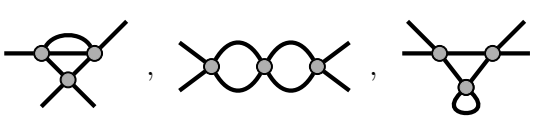
This procedure for collecting all the cut information using EMU can be represented diagrammatically as a sequence of culling and collapsing as follows:

$$MC_{(l,n)} \xrightarrow{S_1^1} \partial MC_{(l,n)} \xrightarrow{S_2^2} \dots \xrightarrow{S_2^2} N^k MC_{(l,n)} \xrightarrow{S_1^1} \partial N^k MC_{(l,n)} \equiv \emptyset \quad (3.3)$$

After applying EMU and collecting all the diagrams up to some order $N^k MC_{(l,n)}$, the set of cuts² we use to fully constrain the n -point l -loop integrand, $\Omega_{(l,n)}$, is the intersection of these sequence of unitarity cuts:

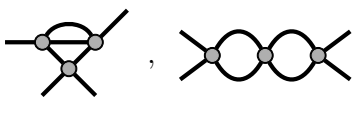
$$\Omega_{(l,n)} = \bigcap_{i=0}^k \partial N^i MC_{(l,n)} \quad (3.4)$$

Taking the intersection accounts for the overlapping information stored in the cut diagrams at different orders in $N^k MC$. As a concrete example, let's consider the case of two-loop four-point of interest in this paper. First, we obtain the following set of diagrams at the MC level built from three four-point vertices:

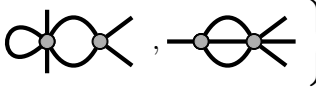
$$MC_{(2,4)} = \left\{ \text{Diagram 1}, \text{Diagram 2}, \text{Diagram 3} \right\} \quad (3.5)$$


²Strictly speaking only the $N^k MC_{(l,n)}$ cuts are required as they represent a spanning set. **JJ: Spanning discussion, change needed??**

Each blob corresponds to an on-shell tree-level amplitude from the even point theory of interest. The third diagram is scaleless on support of dimensional regularization, and thus we discard it in Step 1A. This gives the following restricted set of MC diagrams:

$$\partial\text{MC}_{(2,4)} = \left\{ \text{Diagram 1}, \text{Diagram 2} \right\} \quad (3.6)$$


Since $\partial\text{MC}_{(2,4)}$ is not empty, we proceed to Step 2. After throwing out the scaleless diagram in $\text{MC}_{(2,4)}$, this leads to the following set of N^1MC diagrams for two-loop four-point:

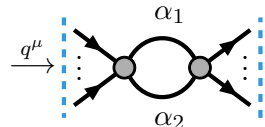
$$\text{N}^1\text{MC}_{(2,4)} = \left\{ \text{Diagram 3}, \text{Diagram 4} \right\} \quad (3.7)$$


Now the first diagram is discarded in Step 1A, and the second diagram is discarded in Step 1B. Thus, we need not consider any next-to-maximal cuts for two-loop four-point amplitudes in even point theories. Since $\partial\text{N}^1\text{MC}_{(2,4)} = \emptyset$, this concludes the EMU cut construction.

As we can see from the diagrams that contribute at two-loops four-point in eq. (3.6), even point theories can be fully constructed from convolutions of one-loop integrals. As described earlier, we call such integrals recursively one-loop since we can iteratively apply one-loop unitarity and tensor reduction methods in order to recover the full multi-loop structure. In the next two sections, we first illustrate the recursive behavior of convolution integrals, and then use their properties to develop multi-loop tensor reduction methods that we use throughout the paper.

3.1 Multi-loop recursive integrals

As we found above in our example of EMU, the only diagrams that contribute at two-loop four-point are those given in Fig. 1. Due to the bubble integral insertions, both of these integrals can be evaluated in terms of the one-loop basis integrals of eq. (2.46). This is a direct consequence of the single-scale nature of bubble insertions. Since internal bubbles are single-scale, they will only contribute additional powers of inverse propagators. This has the effect of shifting an L -loop convolution integral to $(L - 1)$ -loop order, with a propagator power determined by the mass-dimension of the evaluated bubble integral. Explicitly, we can evaluate a D -dimensional nested bubble with internal momentum, q^μ , flowing into the diagram,

$$\text{Diagram} \sim [q^2]^{D/2 - \alpha_1 - \alpha_2} \quad (3.8)$$


where α_1 and α_2 are the degree of the denominators appearing in the bubble integral. For example, consider a banana integral diagram constructed from six-point contacts that would appear in a higher-loop application of EMU at three-loop order with external momentum

$q^\mu = (k_1 + k_2)^\mu$. Evaluating the simplest case where all $\alpha_i = 1$, we find that eq. (3.8) readily yields the following sequence:

$$\begin{array}{c} \xrightarrow{k_{12}^\mu} \text{Diagram 1} \sim \text{Diagram 2} \sim \text{Diagram 3} \sim s_{12}^{3D/2-4} \end{array} \quad (3.9)$$

$\alpha_1=1$ $\alpha_2=D/2-2$ $\alpha_3=D/2-2$
 $\alpha_4=1$ $\alpha_4=1$ $\alpha_4=1$

Where for simplicity, we have dropped the Γ -function dependent factors at each step in the evaluation. This procedure of evaluating bubble integrals at successively orders also works for tensor bubble-integral insertions as well. As we'll show in this next section, such tensor bubble insertions can be reduced to scalars integrals via Passarino-Veltman [74]. While there are a number of tensor reduction algorithms available in the literature [118–125], our ability to use Passarino-Veltman on the recursive integrals of Fig. 1 will prove useful for evaluating terms with factors of $(\varepsilon_i \cdot l_j)$, which include formal polarizations. This procedure will aid in our pursuit of extracting the rational part of the two-loop Born-Infeld amplitudes that we study in section 4.2.2.

3.2 Two-loop tensor reduction

First we will study the canonical one-loop case needed for the nested bubble integrals described above, and then show that it naturally generalizes to the two-loop for the recursive integrals of interest. We begin with a general expression for the rank- n tensor bubble:

$$I_2^{\mu_1 \dots \mu_n}(K) = \int \frac{d^D l}{(2\pi)^D} \frac{l^{\mu_1} l^{\mu_2} \dots l^{\mu_n}}{l^2(l+K)^2} \quad (3.10)$$

$$= \sum_{m+2k=n} a_{(m,k)} \mathcal{T}_{\text{bub}}^{(m,k)}, \quad (3.11)$$

where we have introduced the following shorthand for the symmeterized rank- $(m+2k)$ tensor:

$$\mathcal{T}_{\text{bub}}^{(m,k)} \equiv K^{(\mu_1} \dots K^{\mu_m} \eta^{\mu_1 \mu_2} \dots \eta^{\mu_{2k-1} \mu_{2k}}) \quad (3.12)$$

By contracting the tensor integral with the internal scale, K^μ , and the metric, $\eta^{\mu\nu}$, we obtain the following two constraint equations:

$$K_{\mu_1} I_2^{\mu_1 \dots \mu_n}(K) = \int \frac{d^D l}{(2\pi)^D} \frac{(K \cdot l) l^{\mu_2} \dots l^{\mu_n}}{l^2(l+K)^2} = -\frac{K^2}{2} I_2^{\mu_2 \dots \mu_n}(K) \quad (3.13)$$

$$\eta_{\mu_1 \mu_2} I_2^{\mu_1 \dots \mu_n}(K) = \int \frac{d^D l}{(2\pi)^D} \frac{l^{\mu_2} \dots l^{\mu_n}}{(l+K)^2} = 0 \quad (3.14)$$

Performing the same contractions on the symmeterized tensor defined above in eq. (3.12) yields the following:

$$K \cdot K_{\text{sym}}^{\otimes(m)} \eta_{\text{sym}}^{\otimes(k)} = K^2 \mathcal{T}_{\text{bub}}^{(m-1,k)} + (m+1) \mathcal{T}_{\text{bub}}^{(m+1,k-1)} \quad (3.15)$$

$$\eta \cdot K_{\text{sym}}^{\otimes(m)} \eta_{\text{sym}}^{\otimes(k)} = K^2 \mathcal{T}_{\text{bub}}^{(m-2,k)} + [D + 2(m+k-1)] \mathcal{T}_{\text{bub}}^{(m,k-1)} \quad (3.16)$$

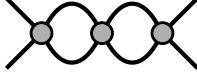


Figure 2. Graphical depiction of the the double-bubble integral. Every exposed internal edge represents a propagator in the integrand.

These linear relations can be used to line up the coefficients with distinct tensor structures, which gives the following:

$$0 = \sum a_{(m,k)} \left[K^2 \mathcal{T}_{\text{bub}}^{(m-1,k)} + (m+1) \mathcal{T}_{\text{bub}}^{(m+1,k-1)} + \frac{K^2}{2} \mathcal{T}_{\text{bub}}^{(m,k)} \right] \quad (3.17)$$

$$= \sum \left[a_{(m+2,k)} K^2 + a_{(m,k+1)} (m+1) + a_{(m+1,k)} \frac{K^2}{2} \right] \mathcal{T}_{\text{bub}}^{(m+1,k)} \quad (3.18)$$

and similarly so for the metric contraction:

$$0 = \sum a_{(m,k)} \left[K^2 \mathcal{T}_{\text{bub}}^{(m-2,k)} + [D + 2(m+k-1)] \mathcal{T}_{\text{bub}}^{(m,k-1)} \right] \quad (3.19)$$

$$= \sum \left[a_{(m+2,k)} K^2 + a_{(m,k+1)} [D + 2(m+k)] \right] \mathcal{T}_{\text{bub}}^{(m,k)} \quad (3.20)$$

Treating the distinct tensor structures as basis elements, we thus conclude the following set of linear relations between the coefficients for the rank- n tensor bubble:

$$0 = K^2 a_{(m+2,k)} + [D + 2(m+k)] a_{(m,k+1)}, \quad (3.21)$$

$$0 = K^2 a_{(m+2,k)} + (m+1) a_{(m,k+1)} + \frac{1}{2} K^2 a_{(m+1,k)}, \quad (3.22)$$

where $D = \eta_{\mu\nu} \eta^{\mu\nu}$. These constraints can be rearranged to give the following recursive definition for the coefficients $a_{(m,k)}$:

$$\boxed{\begin{aligned} a_{(m,k)} &= - \left[\frac{K^2}{D + 2(m+k-1)} \right] a_{(m+2,k-1)} \\ a_{(m,0)} &= - \left[\frac{D + 2(m-2)}{2(D+m-3)} \right] a_{(m-1,0)} \\ a_{(0,0)} &= I_2(K) \end{aligned}} \quad (3.23)$$

The base step is simply the scalar bubble integral, $a_{(0,0)} = I_2(K)$. Constructing $a_{(m,k)}$ from this recursive definition, the one-loop integrand of eq. (2.58) that contains factors of $(l \cdot \varepsilon_i)$ and $(l \cdot k_i)$ can be expressed completely in terms of the bubble integral, $I_2(K)$, weighted by dimension dependent numerical factors and external vector kinematics.

We note that these coefficients are also sufficient to evaluate the contribution from the double-bubble integral whose propagator structure is sketched in Fig. ???. This is best demonstrated with an explicit example. Consider the following integral, $I_{2\text{bub}}^{\text{ex}}$, that functionally

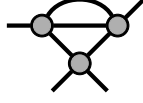


Figure 3. Graphical depiction of the the ostrich integral. Every exposed internal edge represents a propagator in the integrand.

captures terms that could appear in the cut construction of the double-bubble integral at two-loop:

$$I_{2\text{bub}}^{\text{ex.}} \equiv \int \frac{d^D l_1 d^D l_2}{(2\pi)^{2D}} \frac{(l_1 \cdot l_2)^2 (l_1 \cdot v_1) (l_2 \cdot v_2)}{l_1^2 (l_1 + k_{12})^2 l_2^2 (l_2 + k_{12})^2} \quad (3.24)$$

where v_i is a stand-in for external kinematics, ε_i or k_i . While the numerator mixes factors of l_1 and l_2 , the denominator can be separated. This allows us to re-express the above integral completely in terms of iterated tensor bubbles of eq. (2.46):

$$I_{2\text{bub}}^{\text{ex.}} = I_2^{\alpha\beta\gamma}(s_{12}) I_2^{\mu\nu\rho}(s_{12}) \eta_{\alpha\beta} \eta_{\mu\nu} v_{1\gamma} v_{2\rho}. \quad (3.25)$$

Then, by applying eq. (3.11), and plugging in the expressions for $a_{(m,k)}$, the kinematic numerator of $I_{2\text{bub}}^{\text{ex.}}$ no longer mixes loop momenta. Thus, the integral is separable and can be expressed as a product of scalar bubbles integrated over l_1 and l_2 .

A similar procedure can be applied to the ostrich type diagrams of Fig. ???. However, the integration procedure is a little more delicate than the $I_{2\text{bub}}^{\text{ex.}}$ of eq. (??). As $I_{2\text{bub}}^{\text{ex.}}$ could be expressed as an iterated bubble, we only needed to consider integer powers of the denominators when constructing the recursion relations. In contrast, ostrich integrals will lead to non-integer, ϵ -dependent powers of loop propagators. We are therefore interested in performing a tensor reduction on the triangle integral,

$$I_{3,x}^{\mu_1 \dots \mu_n}(K_{12}) = \int \frac{d^D l}{(2\pi)^D} \frac{l^{\mu_1} l^{\mu_2} \dots l^{\mu_n}}{l^2 (l + K_1)^{2x} (l + K_{12})^2} \quad (3.26)$$

$$= \sum_{m+l+2k=n} a_{(m,l,k)}^x \mathcal{T}_{\text{tri}}^{(m,l,k)}, \quad (3.27)$$

with $K_{12} = K_1 + K_2$ introduced as shorthand notation. We note that x is a non-integer value that will inherit dependence on ϵ from integrating over the internal bubble, $I_2^{4-2\epsilon}(l + K_1) \sim [(l + K_1)^2]^{-\epsilon}$, and the symmetrized triangle tensor takes the following definition:

$$\mathcal{T}_{\text{tri}}^{(m,l,k)} \equiv K_1^{(\mu_1} \dots K_1^{\mu_m} K_2^{\mu_1} \dots K_2^{\mu_l} \eta^{\mu_1 \mu_2} \dots \eta^{\mu_{2k-1} \mu_{2k}}). \quad (3.28)$$

Given this definition, when we perform the tensor contractions over K_1 and K_2 , the degree of x will get shifted:

$$K_{1\mu_1} I_{3,x}^{\mu_1 \dots \mu_n} = \int \frac{d^D l}{(2\pi)^D} \frac{(K_1 \cdot l) l^{\mu_2} \dots l^{\mu_n}}{l^2 (l + K_1)^{2x} (l + K_{12})^2} = \frac{1}{2} I_{3,x-1}^{\mu_2 \dots \mu_n} \quad (3.29)$$

$$K_{2\mu_1} I_{3,x}^{\mu_1 \dots \mu_n} = \int \frac{d^D l}{(2\pi)^D} \frac{(K_2 \cdot l) l^{\mu_2} \dots l^{\mu_n}}{l^2 (l + K_1)^{2x} (l + K_{12})^2} = -\frac{1}{2} \left[I_{3,x-1}^{\mu_2 \dots \mu_n} + K_{12}^2 I_{3,x}^{\mu_2 \dots \mu_n} \right] \quad (3.30)$$

where for our purposes, external momenta are taken to be null, $K_1^2 = K_2^2 = 0$. By construction, contracting with the metric will yield a scaleless integral, giving us the following constraint:

$$\eta_{\mu_1 \mu_2} I_{3,x}^{\mu_1 \dots \mu_n} = \int \frac{d^D l}{(2\pi)^D} \frac{l^{\mu_2} \dots l^{\mu_n}}{(l + K_1)^{2x} (l + K_{12})^2} = 0 \quad (3.31)$$

Note that in the above contractions with K_1 and K_2 the degree of the denominator get's shifted from $x \rightarrow x - 1$. For normal one-loop triangle integral reductions for which $x = 1$, this would lead to a tensor bubble that we have computed in the previous section,

$$K_{1\mu_1} I_{3,x=1}^{\mu_1 \dots \mu_n} = \frac{1}{2} I_2^{\mu_2 \dots \mu_n} \quad (3.32)$$

$$K_{2\mu_1} I_{3,x=1}^{\mu_1 \dots \mu_n} = -\frac{1}{2} \left[I_2^{\mu_2 \dots \mu_n} + K_{12}^2 I_{3,x=1}^{\mu_2 \dots \mu_n} \right] \quad (3.33)$$

However, since the two-loop integration leads to ϵ -dependence, this will now induce additional factors of scalar $I_{3,\epsilon-n}$ final tensor reduction. Proceeding with the computation, these integral constraints can be similarly applied to our symmeterized tensors, yielding the following set of contractions:

$$K_1 \cdot \mathcal{T}_{\text{tri}}^{(m,l,k)} = \frac{1}{2} K_{12}^2 \mathcal{T}_{\text{tri}}^{(m,l-1,k)} + (m+1) \mathcal{T}_{\text{tri}}^{(m+1,l,k-1)} \quad (3.34)$$

$$K_2 \cdot \mathcal{T}_{\text{tri}}^{(m,l,k)} = \frac{1}{2} K_{12}^2 \mathcal{T}_{\text{tri}}^{(m-1,l,k)} + (l+1) \mathcal{T}_{\text{tri}}^{(m,l+1,k-1)} \quad (3.35)$$

$$\eta \cdot \mathcal{T}_{\text{tri}}^{(m,l,k)} = K_{12}^2 \mathcal{T}_{\text{tri}}^{(m-1,l-1,k)} + [D + 2(m+k+l-1)] \mathcal{T}_{\text{tri}}^{(m,l,k-1)} \quad (3.36)$$

Keeping this in mind, we obtain the following linear relations between the coefficients,

$$\begin{aligned} 0 &= 2(m+1) a_{(m,l,k+1)}^x + s_{12} a_{(m+1,l+1,k)}^x - a_{(m+1,l,k)}^{x-1} \\ 0 &= 2(l+1) a_{(m,l,k+1)}^x + s_{12} [a_{(m+1,l+1,k)}^x + a_{(m,l+1,k)}^x] + a_{(m,l+1,k)}^{x-1} \\ 0 &= [D + 2(m+l+k)] a_{(m,l,k+1)}^x + s_{12} a_{(m+1,l+1,k)}^x \end{aligned} \quad (3.37)$$

Just as was done for the scalar bubble, these functional expressions can be rearranged to construct family of recursion relations for the tensor coefficients:

$$\begin{aligned}
a_{(m,l,k)}^x &= - \left[\frac{s_{12}}{D + 2(m + l + k - 1)} \right] a_{(m+1,l+1,k-1)}^x \\
a_{(m,l,0)}^x &= - \left[\frac{D + 2(m + l - 2)}{D + 2(m - 2)} \right] \left[\frac{1}{s_{12}} a_{(m-1,l,0)}^{x-1} + a_{(m-1,l,0)}^x \right] \\
a_{(0,l,0)}^x &= \frac{1}{s_{12}} a_{(0,l-1,0)}^{x-1} \\
a_{(0,0,0)}^x &= I_{3,x}(K_{12})
\end{aligned} \tag{3.38}$$

This system of equations uniquely fixes the rank- n triangle tensor integral in eq. (3.26) with non-integer powers in the denominator. Using these integral reduction formulae, both the one-loop and two-loop integrals can be expressed completely in terms of scalar one-loop bubble and scalar triangle integrals, which we are provided in eq. (2.46) of the previous section. Before proceeding to our results, we will introduce a bit of notation that will be relevant for capturing loop-level contributions to the amplitude.

3.3 Gauge-invariant basis tensors

The final bit of machinery we introduce for the multi-loop calculations of this paper is a spanning set of D -dimensional four-photon on-shell tensor structures. All of the vector integrands constructed in the following sections will be fixed on D -dimensional cuts, and projected to a basis of D -dimensional photon tensors. The purpose of proceeding in this way has a number of advantages over the traditional on-shell approach of fixing on 4D cuts. Firstly, it makes dimensional dependence of dimensional regularization absolutely manifest. This makes the procedure of computing rational terms (see for example, [109]) significantly more algorithmic than the standard approaches in $D = 4$ that we reviewed in section 2.5.

In addition, by projecting to a D -dimensional basis of tensor structures, we can more easily track the one-loop divergences that propagate to two-loop order. This is due to the existence of evanescent operators, those which vanish when plugging in 4D states, but are non-vanishing in general dimensions. As we will see in pure Born-Infeld amplitudes of section 4.2, these so-called evanescent operators are the cause of two-loop divergences that are obscured when looking at the one-loop behavior in $D = 4$ exclusively. Tracking divergences introduced by evanescent operators has been an active area of research Standard Model effective field theory (SMEFT) [126–130], the UV behavior of quantum gravity [56, 131, 132], and more generally as an area of formal theory interest [133–137]. Below we will give a concrete example of an evanescent operator expressed with notation used in the text to provide some justification for our D -dimensional tensor basis.

First, we will use the pair of D -dimensional tensor structure, $f_{ij}f_{kl}$ and f_{ijkl} defined previously in [50],

$$f_{ij} = \frac{1}{2} \text{tr}[F_i F_j] \quad f_{ijkl} = \text{tr}[F_i F_j F_k F_l] \tag{3.39}$$

where $F_i^{\mu\nu} = k_i^\mu \epsilon_i^\nu - k_i^\nu \epsilon_i^\mu$ are linearized field strengths, and the trace is taken over spacetime indices. With these vector building blocks, there are exactly four D -dimensional four-photon local amplitudes one can write down at $\mathcal{T}(k^8)$:

$$\mathcal{T}_{(2,0)}^{F^2 F^2} = s_{12}^2 f_{12} f_{34} + \text{cyc}(2, 3, 4) \quad (3.40)$$

$$\mathcal{T}_{(2,0)}^{F^4} = s_{12}^2 f_{1324} + \text{cyc}(2, 3, 4) \quad (3.41)$$

$$\mathcal{T}_{(0,1)}^{F^2 F^2} = s_{13} s_{14} f_{12} f_{34} + \text{cyc}(2, 3, 4) \quad (3.42)$$

$$\mathcal{T}_{(0,1)}^{F^4} = s_{13} s_{14} f_{1324} + \text{cyc}(2, 3, 4) \quad (3.43)$$

where the Mandelstam invariants are defined as $s_{ij} = (k_i + k_j)^2$. The index subscripts correspond to powers of Mandelstam invariants that are easily generalized,

$$\boxed{\begin{aligned} \mathcal{T}_{(x,y)}^{F^2 F^2} &\equiv s_{12}^x (s_{13} s_{14})^y f_{12} f_{34} + \text{cyc}(2, 3, 4), \\ \mathcal{T}_{(x,y)}^{F^4} &\equiv s_{13}^x (s_{12} s_{14})^y f_{1234} + \text{cyc}(2, 3, 4), \\ \mathcal{T}_{(x,y)}^{F^3} &\equiv \sigma_3^x \sigma_2^y [st A_{(s,t)}^{F^3}], \end{aligned}} \quad (3.44)$$

with $\sigma_3 = s_{12} s_{13} s_{14} / 8$ and $\sigma_2 = (s_{12}^2 + s_{13}^2 + s_{14}^2) / 8$.

The important takeaway from eq. (3.40) is that one can write down four independent Lorentz invariant photon tensor structures at this mass-dimension. However, this obscures the 4-dimensional freedom at this mass dimension. In fact, there are only three distinct helicity structures in $D = 4$. One particular basis for which the space of these helicity structures is provided below:

$$\mathcal{T}_{(++++)}^{4D} = (s_{12}^4 + s_{13}^4 + s_{14}^4) \frac{[12][34]}{\langle 12 \rangle \langle 34 \rangle} \quad (3.45)$$

$$\mathcal{T}_{(---+)}^{4D,1} = (s_{13}^2 + s_{14}^2) \langle 12 \rangle^2 [34]^2 \quad (3.46)$$

$$\mathcal{T}_{(---+)}^{4D,2} = s_{12}^2 \langle 12 \rangle^2 [34]^2 \quad (3.47)$$

Above we have used the spinor helicity variable conventions of ref. [73] described in section 2.3. Immediately we can see that the full D -dimensional basis must have a non-trivial null space when projected down to $D = 4$. Given that the 4D helicity space is overdetermined, we are able to define the following evanescent amplitude $\mathcal{T}^{\text{ev.}}$ that vanishes when constrained to any 4D states:

$$\mathcal{T}^{\text{ev.}} \equiv \mathcal{T}_{(2,0)}^{F^2 F^2} - \mathcal{T}_{(0,1)}^{F^2 F^2} + \mathcal{T}_{(0,1)}^{F^4} \quad (3.48)$$

Again, using the helicity projection rules of eq. (??) one can verify that this indeed vanishes in $D = 4$, while clearly non-vanishing in general dimension. This behavior will be particularly relevant for interpreting the loop level results where $D = 4 - 2\epsilon$. To see why, let's consider

a pedagogical example where a 4D divergent evanescent operator is inserted into a one-loop bubble integral. That is, suppose we have a two-loop integral for which we need to integrate the following quantity:

$$\begin{array}{c} \mathcal{T}^{\text{ev.}} \quad \mathcal{T}^{\text{arb.}} \\ \text{diagram: a bubble with a dark blob on the left and a light blob on the right, connected by a wavy line} \end{array} = \sum_{\text{states}} \int \frac{d^D l}{(2\pi)^D} \frac{\mathcal{T}_{(1,2,\bar{l}_1,\bar{l}_2)}^{\text{ev.}} \mathcal{T}_{(l_1,l_2,3,4)}^{\text{arb.}}}{l^2(l+k_{12})^2} \quad (3.49)$$

where $\bar{l}_1 = -l_1 = l$ and $\bar{l}_2 = -l_2 = -(l+k_{12})$, the evanescent amplitude $\mathcal{T}^{\text{ev.}}$, which could be the result of an unspecified loop integral, we dress the darker blob with, and a generic arbitrary vector structure $\mathcal{T}^{\text{arb.}}$ is dressing the light blob. Exposed legs are taken to be on-shell.

As an easy example, we can take the vector insertion on the right hand side to be $\mathcal{T}_{(1234)}^{\text{arb.}} \equiv f_{12}f_{34}$. By applying the state sum and tensor reduction formulae from the previous sections, this can be evaluated explicitly. The result is given,

$$\begin{array}{c} \mathcal{T}^{\text{ev.}} \quad \mathcal{T}^{f^2} \\ \text{diagram: a bubble with a dark blob on the left and a light blob on the right, connected by a wavy line} \end{array} = \frac{(D_s - 4)(D_s - 3)}{8(D_s - 1)} s_{12}^4 I_2(k_{12}) f_{12} f_{34} \quad (3.50)$$

$$= -\frac{i}{192\pi^2} s_{12}^4 f_{12} f_{34} + \mathcal{O}(\epsilon) \quad (3.51)$$

where $I_2(k_{12})$ is the scalar bubble integral in the s_{12} -channel, and in the second line we have plugged in $D = 4 - 2\epsilon$. Thus far, this is exactly what we should expect. Since the amplitude $\mathcal{T}^{\text{ev.}}$ vanishes in $D = 4$, the 4-dimensional cut above must vanish. The Optical Theorem thus disallows imaginary parts from logarithms that would appear post integration. This physical constraint is imposed by the factor of $(D - 4)$, which absorbs the divergence of $I_2(k_{12})$ and pushes the logarithm to be subleading at $\mathcal{T}(\epsilon)$.

However, suppose that $\mathcal{T}^{\text{ev.}}$ came dressed with a $1/\epsilon$ -divergence from some nested integral in a full two-loop calculation. That is, suppose the operator insertion came from the leading divergence of a one-loop integral, such that,

$$\mathcal{M}^{\text{1-loop}}|_{\text{div.}} \sim \begin{array}{c} \text{diagram: a single vertex with four external wavy lines} \end{array} \Big|_{\text{div.}} = \frac{1}{\epsilon} \mathcal{T}_{(1234)}^{\text{ev.}} \quad (3.52)$$

In which case, the two-loop contribution would be divergent despite the vanishing 4D cut between the evanescent operator and the example operator, \mathcal{T}^{f^2} , chosen above:

$$\begin{array}{c} \frac{1}{\epsilon} \mathcal{T}^{\text{ev.}} \quad \mathcal{T}^{f^2} \\ \text{diagram: a bubble with a dark blob on the left and a light blob on the right, connected by a wavy line} \end{array} \Big|_{\text{div.}} = -\frac{1}{\epsilon} \frac{i}{192\pi^2} s_{12}^4 f_{12} f_{34} \quad (3.53)$$

Thus, it is critically important that we track the full D -dimensional contribution when probing for divergences at multi-loop order. To this end, we will introduce a basis of four-photon vector

building blocks to be used throughout the text when computing loop-level divergences. There are only three distinct vector building blocks needed to span photon effective operators at four-point – those given above in eq. (3.40), which span the $(\pm\pm\pm\pm)$ and $(\pm\pm\mp\mp)$ helicity sectors, and the single insertion of F^3 tensor permutation invariant, $stA_{(s,t)}^{F^3}$, which captures the $(\pm\pm\pm\mp)$ helicity configurations. This leads naturally to the class of higher derivative D -dimensional photon operators indexed by x and y to indicated higher powers of Mandelstam invariants given in eq. (3.53).

The F^3 vector permutation invariant, $stA_{(s,t)}^{F^3}$, can be expressed concisely in terms of $\mathcal{T}_{(x,y)}^{F^2F^2}$ as follows,

$$stA_{(s,t)}^{F^3} = \frac{\mathcal{T}_{(0,2)}^{F^2F^2} - g_1g_2g_3g_4}{s_{12}s_{13}s_{14}}, \quad (3.54)$$

where $g_i \equiv 2k_{i-1}^\mu F_i^{\mu\nu} k_{i+1}^\nu$. While not obvious when expressed in this form, the numerator of the above tensor structure is proportional to the permutation invariant in the denominator, $\mathcal{T}_{(0,2)}^{F^2F^2} - g_1g_2g_3g_4 \sim \sigma_3$, and thus it is local by construction. This set of operators completely spans the space of D -dimensional permutation invariant photon effective operators, thereby allowing us to write an on-shell effective amplitude parameterized by numeric Wilson coefficients, $a_{(x,y)}$, as,

$$\boxed{\mathcal{M}_4^{\text{photon-EFT}} = \sum_{x,y} a_{(x,y)}^{F^2F^2} \mathcal{T}_{(x,y)}^{F^2F^2} + a_{(x,y)}^{F^4} \mathcal{T}_{(x,y)}^{F^4} + a_{(x,y)}^{F^3} \mathcal{T}_{(x,y)}^{F^3}} \quad (3.55)$$

In ref. [50] it was demonstrated that this photonic effective field theory (EFT) amplitude permits a double copy construction by either introducing a set of d^{abc} -type symmetric algebraic structures, or more traditional adjoint f^{abc} -type kinematics but at the cost of factorizing over higher spin modes. While we will comment on the double-copy properties of this amplitude in section 5.2, for now we will just stress that these D -dimensional operators will serve as an useful basis for capturing divergences and anomalies in the Born-Infeld S -matrix. With that, we are prepared to proceed to the loop level results.

4 Loop-level results

We now apply the even-point multi-loop unitarity approach introduced in section 3 to constructing two-loop amplitudes in NLSM and DBIVA theories and reducing them to an appropriate basis of integrals. We will evaluate the D -dimensional scalar integrals in the dimension of interest. We will focus primarily on $D = 4 - 2\epsilon$ for DBIVA amplitudes, but we will also consider $D = 2 - 2\epsilon$, which is the dimension for which NLSM is critical. We will then project D -dimensional tensor structures along defined 4D spinor helicity states using the conventions described in section 2.3. This will clarify where anomalous matrix elements contribute for non-supersymmetric BI, which has a classically conserved $U(1)$ symmetry.

We begin with an instructive example of NLSM pions through two-loop order. These amplitudes can serve as the scaffolding for constructing $\mathcal{N} = 4$ DBIVA integrands using the

double copy even without explicitly finding a color-dual representation. As we will demonstrate, an exciting realization of our results is that the loop-level double copy construction of $\mathcal{N} = 4$ DBIVA is consistent with the results that we compute directly via unitarity. This is the first application of double-copy construction for multi-loop amplitudes for non-gravitational theories. Furthermore, it suggests that there should exist a color-dual representation of two-loop NLSM integrands, a representation that has yet to be constructed explicitly.

4.1 NLSM via EMU

We begin with the color-dressed NLSM tree amplitudes that will serve as the kinematic building blocks to appear in our unitarity construction. For our purposes, a convenient color basis is the so-called half-ladder basis of Del Duca, Dixon and Maltoni (DDM) [138],

$$\mathcal{A}_n^{\text{NLSM}} = \sum_{\sigma \in S^{n-2}} C_{(1\sigma n)}^{\text{H.L.}} A_{(1\sigma n)}^{\text{NLSM}}. \quad (4.1)$$

The half-ladder color factors are defined in terms of the antisymmetric structure constants as,

$$C_{(1\sigma n)}^{\text{H.L.}} \equiv f^{1\sigma_2\beta_2} f^{\beta_2\sigma_3\beta_3} \dots f^{\beta_{n-1}\sigma_n-1n}. \quad (4.2)$$

In the above expression, each half ladder dresses a color-ordered amplitude $A_{(1\sigma n)}^{\text{NLSM}}$. At four-point, it is well known that the ordered amplitude for NLSM is simply,

$$A_{(1234)}^{\text{NLSM}} = f_\pi^{-2} s_{13}. \quad (4.3)$$

In which case, the full four-point amplitude can be expressed completely in terms of the s -channel and u -channel color factors,

$$\mathcal{A}_{(1|23|4)}^{\text{NLSM}} = f_\pi^{-2} \left(C_{(1234)}^{\text{H.L.}} s_{13} + C_{(1324)}^{\text{H.L.}} s_{12} \right). \quad (4.4)$$

The t -channel color factor satisfies a Jacobi identity with the s - and u -channel diagrams, $c_t \equiv C_{(2341)}^{\text{H.L.}} = C_{(1234)}^{\text{H.L.}} - C_{(1324)}^{\text{H.L.}}$, and thus can be chosen so that it does not contribute to the full color-dressed amplitude. In this work, we use the convention $s = (k_1 + k_2)^2$, $t = (k_2 + k_3)^2$ and $u = -s - t$. The color-dressed amplitude is entirely bose-symmetric, but we use the subscript $(1|23|4)$ to emphasize a functional choice of the $1|\sigma|4$ half-ladder basis.

4.1.1 One-loop

At one-loop, the unitarity construction of gauge theory amplitudes is particularly simple, since the color factors can be decomposed into a DDM-like ordered color basis. That is, all color factors, C_g associated with the following cubic representation of the integrand:

$$\mathcal{A}_n^{1\text{-loop}} = \int \prod_{i=1}^L \frac{d^D l_i}{(2\pi)^D} \sum_{g \in \Gamma^{(3)}} \frac{1}{S_g} \frac{C_g N_g}{D_g} \quad (4.5)$$

can be expressed uniquely as a sum over a canonical ordering of color factors by iteratively applying the color jacobi identity. In doing so, all 1-loop color factors, $C_g^{1\text{-loop}}$, can be expressed as a sum over n -gon integrand factors, $C_{(a_1 A_2 \dots a_n)}^{n\text{-gon}}$ in the following way,

$$C_g^{1\text{-loop}} = \sum_{\sigma \in S^{n-1}} \beta_g^{(\sigma)} C_{(\sigma_1 \sigma_2 \dots \sigma_{n-1} n)}^{n\text{-gon}} \quad (4.6)$$

where $\beta_g^{(\sigma)}$ are factors of $\{-1, 0, 1\}$ depending on the color structure of the diagram, $C_g^{1\text{-loop}}$. The n -gon basis diagrams take the following definition in terms of adjoint structure constants, f^{abc} :

$$C_{(a_1 A_2 \dots a_n)}^{n\text{-gon}} \equiv f^{b_1 a_1 b_2} f^{b_2 a_2 b_3} \dots f^{b_n a_n b_1} \quad (4.7)$$

This allows us to express the one-loop amplitudes in terms of a sum over the $(n-1)!$ distinct color factors, weighted by the contributions from the color-ordered Feynman diagrams:

$$\mathcal{A}_n^{1\text{-loop}} = \sum_{\sigma \in S^{n-1}} C_{(\sigma n)}^{n\text{-gon}} A_{(\sigma n)}^{1\text{-loop}}. \quad (4.8)$$

As this is a minimal basis we will consider cuts that allow a targeted identification of each color-weight's coefficients.

Construction Using the four-point tree-level NLSM amplitude, and following the reasoning of section 3, it is straightforward to write down an off-shell integrand associated with the one-loop bubble:

$$\begin{array}{c} 2 \\ \diagup \quad \diagdown \\ \text{---} \bullet \quad \bullet \text{---} \\ \diagdown \quad \diagup \\ 1 \quad \quad 4 \end{array} \quad 3 = \int \frac{d^D l}{(2\pi)^D} \frac{\sum_{\text{states}} \mathcal{A}_{(\bar{l}_1|12|\bar{l}_2)}^{\text{NLSM}} \mathcal{A}_{(l_2|34|l_1)}^{\text{NLSM}}}{l^2(l+k_{12})^2}. \quad (4.9)$$

We define the internal loop momenta as, $\bar{l}_1 = -l_1 = l$ and $\bar{l}_2 = -l_2 = -(l+k_{12})$. The integrand numerator can be easily evaluated, yielding the following expression:

$$\sum_{\text{states}} \mathcal{A}_{(\bar{l}_1|12|\bar{l}_2)}^{\text{NLSM}} \mathcal{A}_{(l_2|34|l_1)}^{\text{NLSM}} = 4f_\pi^{-4} C_{(1234)}^{\text{box}} [(k_2 \cdot \bar{l}_1)(k_3 \cdot l_1) + (k_1 \cdot \bar{l}_1)(k_4 \cdot l_1)] \quad (4.10)$$

$$+ 4f_\pi^{-4} C_{(1243)}^{\text{box}} [(k_1 \cdot \bar{l}_1)(k_2 \cdot \bar{l}_1) + (k_3 \cdot l_1)(k_4 \cdot l_1)] \quad (4.11)$$

Again, as following the reasoning in section 3 we do not need to worry about any contact terms that may have been missed in this cut – any such terms do not exist for an even-point theory.

We note that since the internal pions are identical, this contribution comes dressed with an internal symmetry factor of $S_{(12|34)} = \frac{1}{2}$. Moreover, this is just the s -channel cut – to capture all channels we can sum over all cyclic permutations:

$$\mathcal{A}_{1\text{-loop}}^{\text{NLSM}} = \frac{1}{2} \begin{array}{c} 2 \\ \diagup \quad \diagdown \\ \text{---} \bullet \quad \bullet \text{---} \\ \diagdown \quad \diagup \\ 1 \quad \quad 4 \end{array} \quad 3 + \text{cyc}(2, 3, 4) \quad (4.12)$$

Now, given the appearance of loop momenta in the integrand, we must proceed to the next step in our integration procedure, tensor reduction.

Reduction Since there are up to two powers of loop momenta appearing in the integrand, it is clear that there will be dimensional dependence when applying the Passarino-Veltman integral reduction of eq. (3.23). In doing so, we can write the one-loop pion amplitude completely in terms of scalar kinematics and scalar bubble integrals:

$$\mathcal{A}_{1\text{-loop}}^{\text{NLSM}} = f_\pi^{-4} C_{(1234)}^{\text{box}} \left[\frac{s_{12} I_2^D(k_{12})}{4} \left(s_{12} + \frac{s_{14} - s_{13}}{D-1} \right) + (1 \leftrightarrow 3) \right] + \text{cyc}(2, 3, 4) \quad (4.13)$$

At this point, this is a dimensionally agnostic one-loop amplitude for NLSM. The next step is to plug particular values of D into the evaluated analytic expressions of I_2^D provided in eq. (2.46).

Integration In the study of NLSM loop-level amplitudes, we provide two examples for the integration dimension, $D = 4 - 2\epsilon$ and $D = 2 - 2\epsilon$, since the critical dimension of NLSM is $D = 2$. In an $\overline{\text{MS}}$ renormalization scheme, the ϵ -expanded bubble integrals for these two dimension choices are as follows:

$$I_2^{4-2\epsilon}(k_{ij}) = \frac{i}{16\pi^2} \left[\frac{1}{\epsilon} - \ln(-s_{ij}) \right] + \mathcal{O}(\epsilon) \quad (4.14)$$

$$I_2^{2-2\epsilon}(k_{ij}) = \frac{i}{2\pi s_{ij}} \left[\frac{1}{\epsilon} - \ln(-s_{ij}) \right] + \mathcal{O}(\epsilon) \quad (4.15)$$

Plugging these into our D -dimensional expressions, and dropping scheme dependent rational terms at subleading order, yields the following color-ordered 1-loop pion amplitudes for each respective dimension:

$$A_{(1234)}^{4-2\epsilon} = \frac{i}{12\pi^2} f_\pi^{-4} \left[\frac{\sigma_2}{\epsilon} + \left(s_{12}(s_{13} - s_{12}) \frac{\ln(-s_{12})}{8} + (1 \leftrightarrow 3) \right) \right] + \mathcal{O}(\epsilon) \quad (4.16)$$

$$A_{(1234)}^{2-2\epsilon} = -\frac{i}{2\pi} f_\pi^{-4} \left[\frac{s_{13}}{\epsilon} - s_{13} \frac{\ln(-s_{12}) + \ln(-s_{23}) - 3}{2} \right] + \mathcal{O}(\epsilon) \quad (4.17)$$

where σ_2 is the previously defined four-point permutation invariant, and the full amplitudes are recovered by summing over cyclic permutations of (2,3,4),

$$\mathcal{A}_{1\text{-loop}}^{\text{NLSM}} = C_{(1234)}^{\text{box}} A_{(1234)}^D + \text{cyc}(2, 3, 4). \quad (4.18)$$

It's worth pointing out that while the divergence in $D = 4 - 2\epsilon$ is an ultraviolet divergence, the one in $D = 2 - 2\epsilon$ is a logarithmic IR divergence, akin to that of $\mathcal{N} = 4$ super-Yang-Mills (sYM) in the critical dimension of $D = 4 - 2\epsilon$. Since all the particle states above are scalars, there are no helicity structures to map into, and thus we will bypass the final integration step of **projection**. Equipped with this one-loop warmup, we are now prepared to take on a two-loop example.

4.1.2 Two-loop

The two-loop calculation is exactly the same procedure as one-loop, with some additional details that need to be accounted for when performing the integration step. We begin just as above with integrand construction via D -dimensional unitarity.

Construction The color-decomposition becomes slightly more complicated at two-loop than the procedure outlined in the previous section at one-loop. Just as before, we will still fix the integrand on color-dressed cuts, however, now we can no longer simply decompose the full color dressed amplitude in terms of integrated color-stripped objects. At two-loop, a convenient basis of adjoint color factors happens to be the double-box and the cross-box, shown below:

$$C_{(12|34)}^{2\text{box}} = \text{Diagram 1} \quad C_{([12]|34)}^{\text{Xbox}} = \text{Diagram 2} \quad (4.19)$$

By iteratively applying Jacobi relations on internal edges, any color structure can be expressed completely in terms of functional relabelings of these two graphs. Concretely, these cubic graphs come dressed with the following color factors written in terms of group theory structure constants:

$$C_{(12|34)}^{2\text{box}} \equiv f^{b_7 a_1 b_1} f^{b_1 a_2 b_2} f^{b_2 b_3 b_4} f^{b_4 a_3 b_5} f^{b_5 a_4 b_6} f^{b_6 b_3 b_7} \quad (4.20)$$

$$C_{([12]|34)}^{\text{Xbox}} \equiv f^{b_7 a_1 b_1} f^{b_1 b_6 b_2} f^{b_2 a_2 b_3} f^{b_3 b_7 b_4} f^{b_4 a_3 b_5} f^{b_5 a_4 b_6} \quad (4.21)$$

Again, we can carefully choose a spanning set of unitarity cuts in terms of our color-dressed NLSM operators in order to land directly on this minimal color basis. In doing so, we can focus our attention to integrating the kinematics that weight each of the color basis element.

As we argued in the introduction, two-loop amplitudes for even point theories, like NLSM, are completely determined by two recursive integrals, the double-bubble and the ostrich-diagram, modulo theory-dependent kinematic numerators. For NLSM, the relevant integrals are as follows:

$$\text{Diagram 3} = \sum_{\text{states}} \int \frac{d^D l_1 d^D l_2}{(2\pi)^{2D}} \frac{\mathcal{A}_{(p_4|12|p_3)}^{\text{NLSM}} \mathcal{A}_{(\bar{p}_1|\bar{p}_4\bar{p}_3|\bar{p}_2)}^{\text{NLSM}} \mathcal{A}_{(p_2|34|p_1)}^{\text{NLSM}}}{l_1^2 (l_1 + k_{12})^2 l_2^2 (l_2 + k_{12})^2} \quad (4.22)$$

$$\text{Diagram 4} = \sum_{\text{states}} \int \frac{d^D l_1 d^D l_2}{(2\pi)^{2D}} \frac{\mathcal{A}_{(2|q_4\bar{q}_3|\bar{q}_1)}^{\text{NLSM}} \mathcal{A}_{(1|\bar{q}_4 q_3|\bar{q}_2)}^{\text{NLSM}} \mathcal{A}_{(q_2|34|q_1)}^{\text{NLSM}}}{l_1^2 (l_1 + l_2 + k_1)^2 l_2^2 (l_2 + k_{12})^2} \quad (4.23)$$

where the internal momenta appearing in the NLSM operators, $\bar{p}_i = -p_i$ and $\bar{q}_i = -q_i$, are defined in terms of the two loop momenta as follows:

$$p_1 = l_2 + k_{12} \quad p_2 = -l_2 \quad p_3 = l_1 \quad p_4 = -(l_1 + k_{12}), \quad (4.24)$$

$$q_1 = l_2 + k_{12} \quad q_2 = -l_2 \quad q_3 = l_1 \quad q_4 = -(l_1 + l_2 + k_1). \quad (4.25)$$

Due to the simplicity of scalar theories like NLSM, the state sum for the double-bubble numerator is quite simple, and can be expressed concisely below:

$$\begin{aligned}
\text{Cut} \left(\begin{array}{c} 2 \\ \diagup \quad \diagdown \\ \text{---} \text{---} \text{---} \\ \diagdown \quad \diagup \\ 1 \quad \quad 4 \end{array} \right) &= \sum_{\text{states}} \mathcal{A}_{(p_4|12|p_3)}^{\text{NLSM}} \mathcal{A}_{(\bar{p}_1|\bar{p}_4\bar{p}_3|\bar{p}_2)}^{\text{NLSM}} \mathcal{A}_{(p_2|34|p_1)}^{\text{NLSM}} \\
&= C_{(12|34)}^{2\text{box}} \left[\tau_3^{(1)} \tau_{13} \tau_1^{(3)} + \tau_3^{(1)} \tau_{23} \tau_2^{(3)} + \tau_3^{(2)} \tau_{23} \tau_1^{(3)} + \tau_3^{(2)} \tau_{13} \tau_2^{(3)} \right] \\
&\quad + C_{(12|43)}^{2\text{box}} \left[\tau_3^{(2)} \tau_{23} \tau_2^{(3)} + \tau_3^{(2)} \tau_{13} \tau_1^{(3)} + \tau_3^{(1)} \tau_{23} \tau_1^{(3)} + \tau_3^{(1)} \tau_{13} \tau_2^{(3)} \right]
\end{aligned} \tag{4.26}$$

where we have introduced the following notation above that combines internal and external momenta, $\tau_j^{(i)} = (k_i + p_j)^2$ and $\tau_{ij} = (p_i + p_j)^2$. Plugging in the color-dressed NLSM amplitudes, the same can be done for the ostrich-diagram cut, giving us

$$\begin{aligned}
\text{Cut} \left(\begin{array}{c} 2 \\ \diagup \quad \diagdown \\ \text{---} \text{---} \text{---} \\ \diagdown \quad \diagup \\ 3 \quad \quad 4 \end{array} \right) &= \sum_{\text{states}} \mathcal{A}_{(2|q_4\bar{q}_3|\bar{q}_1)}^{\text{NLSM}} \mathcal{A}_{(1|\bar{q}_4q_3|\bar{q}_2)}^{\text{NLSM}} \mathcal{A}_{(q_2|34|q_1)}^{\text{NLSM}} \\
&= C_{([12]|34)}^{\text{Xbox}} \left[\tau_1^{(3)} \tau_3^{(2)} \tau_4^{(1)} + \tau_1^{(3)} \tau_4^{(2)} \tau_3^{(1)} + \tau_2^{(3)} \tau_3^{(2)} \tau_4^{(1)} + \tau_2^{(3)} \tau_4^{(2)} \tau_3^{(1)} \right] \\
&\quad - \left(C_{(12|34)}^{2\text{box}} \tau_1^{(3)} + C_{(12|43)}^{2\text{box}} \tau_2^{(3)} \right) \left[\tau_3^{(2)} \tau_3^{(1)} + \tau_4^{(2)} \tau_4^{(1)} \right].
\end{aligned} \tag{4.27}$$

The kinematic variables $\tau_j^{(i)}$ and τ_{ij} are the same, except we have made the replacement $p_i \rightarrow q_i$. The full two-loop NLSM amplitude can thus be computed by summing over the distinct labels of the resulting integrals, each weighted by suitable internal symmetry factors:

$$\mathcal{A}_{2\text{-loop}}^{\text{NLSM}} = \frac{1}{4} \left[\begin{array}{c} 2 \\ \diagup \quad \diagdown \\ \text{---} \text{---} \text{---} \\ \diagdown \quad \diagup \\ 1 \quad \quad 4 \end{array} \right] + \frac{1}{2} \left[\begin{array}{c} 2 \\ \diagup \quad \diagdown \\ \text{---} \text{---} \text{---} \\ \diagdown \quad \diagup \\ 3 \quad \quad 4 \end{array} \right] + 4 \left[\begin{array}{c} 3 \\ \diagup \quad \diagdown \\ \text{---} \text{---} \text{---} \\ \diagdown \quad \diagup \\ 2 \quad \quad 1 \end{array} \right] + \text{cyc}(2, 3, 4) \tag{4.28}$$

We stress that the integrals appearing above are complicated by tensor integrals with many powers of loop momenta. However, as noted in the introduction, since both integrals are recursively one-loop, we can again apply a two-loop generalization of Passarino-Veltman for both the bubble and triangle integrals, stated in eq. (3.23) and eq. (3.38), respectively. With this, we proceed to the next step in the calculation.

Reduction Just as with one-loop, we will now reduce the integrals of eq. (4.28) to the a basis of D -dimensional scalar integrals using the EMU loop reduction. The double-bubble

contribution yields the following:

$$\begin{aligned}
\text{Diagram} &= f_\pi^{-6} C_{(12|34)}^{2\text{box}} \left[\frac{(s_{12} I_2^D(k_{12}))^2}{2} \left(\frac{s_{14} - s_{13}}{(D-1)^2} + s_{12} \right) \right] \\
&\quad + f_\pi^{-6} C_{(12|43)}^{2\text{box}} \left[\frac{(s_{12} I_2^D(k_{12}))^2}{2} \left(\frac{s_{13} - s_{14}}{(D-1)^2} + s_{12} \right) \right]
\end{aligned} \tag{4.29}$$

Likewise, we can perform a similar reduction to the dunce cap integrals – but with a small twist. The double-bubble integral above is completely separable, which allows one to treat the tensor reduction of each loop integral as independent. This is not so for the ostrich-diagram integral. The ostrich-diagram carries an internal bubble, $I_2^D(q)$, with a loop dependent scale factor of $q = l_2 + k_1$. Thus, we must first reduce the powers of l_1 and then perform a tensor reduction on all the remaining l_2 factors. Doing so yields the following result:

$$\begin{aligned}
\text{Diagram} &= f_\pi^{-6} C_{(12|34)}^{2\text{box}} \frac{s_{12}}{6} \left[\frac{(D-1)(D-4)s_{14} + 2(D-2)^2 s_{13}}{(D-1)(4-3D)} \right] [I_3 \circ I_2]^D(k_{12}) \\
&\quad + f_\pi^{-6} C_{(12|43)}^{2\text{box}} \frac{s_{12}}{6} \left[\frac{(D-1)(D-4)s_{13} + 2(D-2)^2 s_{14}}{(D-1)(4-3D)} \right] [I_3 \circ I_2]^D(k_{12}) \\
&\quad + f_\pi^{-6} C_{([12]|34)}^{\text{Xbox}} \left[\frac{s_{12}^2}{6} \frac{D+1}{D-1} \right] [I_3 \circ I_2]^D(k_{12})
\end{aligned} \tag{4.30}$$

where we have defined the scalar ostrich-diagram integral, $[I_3 \circ I_2]^D(k_{12})$, as a D -dimensional convolution of I_2^D and I_3^D , provided below:

$$[I_3 \circ I_2]^D(k_{12}) \equiv \int \frac{d^D l_1 d^D l_2}{(2\pi)^D} \frac{(l_2 + k_1)^2}{l_1^2 (l_1 + l_2 + k_1)^2 l_2^2 (l_2 + k_{12})^2}. \tag{4.31}$$

We have added the additional factor of $(l_2 + k_1)^2$ in the definition of $[I_3 \circ I_2]^D(k_{12})$ to simplify the final expression in eq. (4.30). We will use this as our basis integral throughout the text. This two-loop integral can be evaluated analytically using the D -dimensional single scale bubble and triangle integral expressions in eq. (2.46). Thus, we have completely reduced the full two-loop NLSM amplitude to a linear combination of scalar integrals, $I_2^D(k_{ij})$ and $[I_3 \circ I_2]^D(k_{ij})$. Now we will proceed to the final step of evaluating the amplitude in particular dimensions.

Integration While there is plenty of physics to be extracted from the combination of eq. (4.29) and eq. (4.30), we will focus on the behavior of the leading divergence for $D = 2 - 2\epsilon$ in the planar limit where $N_c \rightarrow \infty$. In this limit, the cross-box is subleading in the N_c expansion, and can be neglected. In a trace basis, the double-box can be expanded as follows:

$$C_{(12|34)}^{2\text{box}} \xrightarrow{N_c \rightarrow \infty} N_c^2 C(1234) + \mathcal{O}(N_c) \tag{4.32}$$

where we have defined the color trace factor, $C(1234) \equiv \text{tr}[T^1 T^2 T^3 T^4]$. Furthermore, the leading divergences for the loop integrals in $D = 2 - 2\epsilon$ dimensions are the following:

$$I_2^{2-2\epsilon}(k_{ij}) I_2^{2-2\epsilon}(k_{ij}) = -\frac{1}{s_{ij}^2} \frac{1}{(2\pi\epsilon)^2} + \mathcal{O}(\epsilon^{-1}) \quad (4.33)$$

$$[I_3 \circ I_2]^{2-2\epsilon}(k_{ij}) = -\frac{3}{8s_{ij}} \frac{1}{(2\pi\epsilon)^2} + \mathcal{O}(\epsilon^{-1}) \quad (4.34)$$

The analogous divergences for $D = 4 - 2\epsilon$ can be extracted directly from the integral expressions in eq. (2.46). Plugging these values into eq. (4.29) and eq. (4.30), we can extract the full leading logarithmic divergence from the full color dressed amplitude in eq. (4.28). Since we are interested in the large N_c limit, we will define a color-ordered quantity $A_{(1234)}^{2-2\epsilon}$,

$$\mathcal{A}_{2\text{-loop}}^{\text{NLSM}} = \left[C(1234) A_{(1234)}^{2-2\epsilon} + \text{cyc}(2, 3, 4) \right] + \mathcal{O}(N_c) \quad (4.35)$$

which takes on the following value upon evaluating the integrals in $D = 2 - 2\epsilon$,

$$A_{(1234)}^{2-2\epsilon} = -\frac{1}{2} \left[\frac{f_\pi^{-2} N_c}{4\pi\epsilon} \right]^2 f_\pi^{-2} s_{13} \quad (4.36)$$

We write it in this suggestive form to emphasize that the logarithmic divergence present at one-loop in eq. (4.17) appears to exponentiate! More concretely, through explicit calculation we have demonstrated that through two-loop, the leading divergence of the color ordered amplitudes in the planar limit goes as follows:

$$A^{2-2\epsilon} \Big|_{\text{div.}} = A^{\text{tree}} \left(1 + \frac{A^{1\text{-loop}}}{A^{\text{tree}}} + \frac{1}{2} \left[\frac{A^{1\text{-loop}}}{A^{\text{tree}}} \right]^2 + \dots \right) \quad (4.37)$$

It would be interesting to investigate whether this exponential structure also can be applied to the subleading logarithms in the planar limit, similar to what was found in [139, 140] in $D = 4 - 2\epsilon$ for planar $\mathcal{N} = 4$ sYM. The iterated structure of planar $\mathcal{N} = 4$ has been linked to the integrability of the theory [141–150]. We find compelling the possibility that this iterated structure of NLSM amplitudes in $D = 2 - 2\epsilon$ could indicate similar integrable behavior, as studied in [151–154]. We leave this as a direction of future study.

Now that we have walked through our procedure for computing two-loop even point theory amplitudes with NLSM as an exemplar, we are prepared to proceed to the main results of the text. While the construction of DBIVA integrands is significantly more cumbersome than constructing the simple expressions of NLSM, the general procedure is exactly the same. The only differences being additional gauge independent state sums, and longer compute time needed for the tensor reduction.

4.2 DBIVA via EMU

In the remainder of this section, we will construct four-photon matrix elements in DBIVA theories through two-loop order. While we will consider a number of different internal matter

states inside the loops, the interactions for which are not captured by the DBIVA Lagrangian eq. (2.36), we will require that all the external states are vectors. This will allow us to map our loop-level results to the basis of gauge invariant tensors described in section 3.3. Furthermore, in the last section, we will investigate how the loop level contributions turn on new operators in the EFT written above.

As we noted in the introduction, DBIVA tree-level amplitudes, which appear in the field theory limit of the abelianized open superstring, can be realized as a double copy between NLSM and sYM [48],

$$\mathcal{M}^{\text{DBIVA}} = \mathcal{A}^{\text{NLSM}} \otimes \mathcal{A}^{\text{sYM}} \quad (4.38)$$

To carry out this construction at loop level, we simply would need to replace the color factors of NLSM with color-dual loop-level numerators, and then integrate the result. At present, this procedure can only be carried out beyond one-loop with NLSM and $\mathcal{N} = 4$ sYM, for which color-dual representations are known through four-loop [6, 30]. Indeed, in the next section we will use this as a check on our $\mathcal{N} = 4$ DBIVA results of this section. Moreover, if we had access to color-dual representations for NLSM at two-loop, we could simply plug those into the sYM integrands constructed from simplified methods of supersymmetric sums [155], which would dramatically simplify our unitarity based construction.

While the double-copy procedure is presently not an option, the recursive structure of even point gauge theories saves us. As in the previous section where we computed NLSM amplitudes, the recursively one-loop structure permits us to only consider the four-point contacts when constructing the physical parts of the two-loop integrand. We will start by reproducing the known one-loop results from a completely D -dimensional framework, and then move onto our novel two-loop results.

4.2.1 One-loop DBIVA

Analogous to our procedure in the previous section where we defined $\mathcal{A}_{(1|23|4)}^{\text{NLSM}}$, first we will define a set of four-point operators for each distinct set of particle interaction. The D -dimensional contacts needed for DBIVA amplitudes at one-loop are as follows:

$$\mathcal{M}(1_\gamma, 2_\gamma, 3_\gamma, 4_\gamma) = 2\text{tr}(F_1 F_2 F_3 F_4) - \frac{1}{2}\text{tr}(F_1 F_2)\text{tr}(F_3 F_4) + \text{cyc}(1, 2, 3) \equiv t_8 F^4 \quad (4.39)$$

$$\mathcal{M}(1_\lambda, 2_\gamma, 3_\gamma, 4_{\bar{\lambda}}) = s_{13}\bar{u}_1(\not{\epsilon}_2 \not{k}_{12} \not{\epsilon}_3)\bar{v}_4 + s_{12}\bar{u}_1(\not{\epsilon}_3 \not{k}_{13} \not{\epsilon}_2)\bar{v}_4 \quad (4.40)$$

$$\mathcal{M}(1_X, 2_\gamma, 3_\gamma, 4_{\bar{X}}) = 2(k_1 F_2 F_3 k_1) + 2(k_4 F_3 F_2 k_4) \quad (4.41)$$

where we have introduced notation $(k_a F_b F_c k_a) \equiv k_a^\mu F_b^{\mu\nu} F_c^{\nu\rho} k_a^\rho$ for the mixed scalar-vector amplitude. The particle content is labeled by γ for the BI photons, λ for the VA fermions, and X for the Dirac scalars. With these tree-level amplitudes in hand, we define the following

set of operators needed for integrand construction:

$$\mathcal{M}_{(1|23|4)}^{\gamma\gamma\gamma\gamma} = \mathcal{M}(1_\gamma, 2_\gamma, 3_\gamma, 4_\gamma) \quad (4.42)$$

$$\mathcal{M}_{(1|23|4)}^{\lambda\gamma\bar{\lambda}} = \mathcal{M}(1_\lambda, 2_\gamma, 3_\gamma, 4_{\bar{\lambda}}) \quad (4.43)$$

$$\mathcal{M}_{(1|23|4)}^{X\gamma\bar{X}} = \mathcal{M}(1_X, 2_\gamma, 3_\gamma, 4_{\bar{X}}) \quad (4.44)$$

While these are a subset of the four-point operators we will use in the two-loop construction, they are sufficient for all the one-loop external-photon amplitudes. To construct the integrands, we will use the D -dimensional state sums for vectors and fermions, which we provide below:

$$\sum_{\text{states}} \varepsilon_{(l)}^\mu \varepsilon_{(-l)}^\nu = \eta^{\mu\nu} - \frac{l^\mu q^\nu + l^\nu q^\mu}{l \cdot q}, \quad (4.45)$$

$$\sum_{\text{states}} u_{(l)} \bar{v}_{(-l)} = \frac{1}{2}(1 \pm \Gamma_5) \Gamma_\mu l^\mu \quad (4.46)$$

where $q^2 = 0$ is a null-reference momentum. Here, Γ_μ are D -dimensional gamma matrices endowed with all the normal Clifford algebraic relations. Since we want to keep this as D -dimensional as possible, we define Γ_5 as the symbol representing the $(D+1)^{th}$ gamma matrix that anti-commutes with all other Γ_μ . Using this, we have added in a chiral projection state operator $P_\pm = \frac{1}{2}(1 \pm \Gamma_5)$ that will be relevant when computing the two-loop fermion contribution. To see why, we note that since we are only computing external photon amplitudes, the loop contribution must be parity even. Concretely, this means that if there is a single chiral trace, the Γ_5 contribution must integrate to zero:

$$2\text{tr}_\pm[\dots] \equiv \text{tr}[(1 \pm \Gamma_5)\dots] \xrightarrow{\int d\Pi_{\text{loop}}} \frac{1}{2}\text{tr}[\dots] \quad (4.47)$$

The property will significantly simplify the two-loop reduction in the presence of single chiral trace. However, at two-loop we can also get multi-trace contributions. In this case, the parity odd contribution (sourced by odd powers of Γ_5) must vanish after integration as follows:

$$4\text{tr}_\pm[\dots]\text{tr}_\pm[\dots] \xrightarrow{\int d\Pi_{\text{loop}}} \text{tr}[\dots]\text{tr}[\dots] + \text{tr}[\Gamma_5 \dots]\text{tr}[\Gamma_5 \dots] \quad (4.48)$$

The second term is also parity even, and will contribute D -dimensional Gram determinants in the presence of two internal fermion loops. While in principle this term is relevant for two-loop diagrams with internal fermions, due to the simplicity of $\mathcal{N} = 4$ DBIVA state sums, we won't need to account for it in our analysis at two-loop.

Before constructing the integrands, below we provide our conventions for the D -dimensional spinors and gamma matrices. We will normalize the gamma matrices as follows:

$$\text{Tr}(\Gamma_\mu \Gamma^\mu) = 2^{D/2-1} D \quad (4.49)$$

Furthermore, since we will eventually be evaluating our matrix elements in $D = 4$ after integration, we assume that the D -dimensional generalization of the Majorana condition holds throughout the calculation. That is, the \bar{u} and v spinors obey the following relationship:

$$\bar{u} = v^T \mathcal{C} \quad v = -\mathcal{C} \bar{u}^T, \quad (4.50)$$

where the D -dimensional charge conjugation operator can be defined in terms of the gamma matrices, Γ_μ , as follows:

$$\Gamma_\mu = -\mathcal{C}^{-1} \Gamma_\mu^T \mathcal{C}. \quad (4.51)$$

From this, the spinor strings obey another in addition to the normal Clifford algebra identities [156]:

$$\bar{u}(\Gamma_{\mu_1} \cdots \Gamma_{\mu_n})v = (-1)^n \bar{u}(\Gamma_{\mu_n} \cdots \Gamma_{\mu_1})v \quad (4.52)$$

This relationship essentially just imposes Fermi statistics on the identical Majorana fermions [157]. Now we are prepared to constructing the integrand with the state sums and operators defined above.

Construction Just as before, the first step in our procedure is to construct the integrand with all the internal loop dependence present. Taking the operators defined above, and applying the appropriate state sums, we obtain:

$$\text{Cut} \left(\begin{array}{c} 2 \\ \text{---} \end{array} \begin{array}{c} \text{---} \end{array} \begin{array}{c} 3 \\ \text{---} \end{array} \right) = \sum_{\text{states}} \mathcal{M}_{(q_1|12|q_2)}^{\gamma\gamma\gamma\gamma} \mathcal{M}_{(\bar{q}_2|34|\bar{q}_1)}^{\gamma\gamma\gamma\gamma} \equiv \text{Cut}(\mathcal{I}_{N_\gamma}^{1\text{-loop}}) \quad (4.53)$$

$$\text{Cut} \left(\begin{array}{c} 2 \\ \text{---} \end{array} \begin{array}{c} \text{---} \end{array} \begin{array}{c} 3 \\ \text{---} \end{array} \right) = \sum_{\text{states}} \mathcal{M}_{(q_1|12|q_2)}^{\lambda\gamma\gamma\bar{\lambda}} \mathcal{M}_{(\bar{q}_2|34|\bar{q}_1)}^{\lambda\gamma\gamma\bar{\lambda}} \equiv \text{Cut}(\mathcal{I}_{N_\lambda}^{1\text{-loop}}) \quad (4.54)$$

$$\text{Cut} \left(\begin{array}{c} 2 \\ \text{---} \end{array} \begin{array}{c} \text{---} \end{array} \begin{array}{c} 3 \\ \text{---} \end{array} \right) = \sum_{\text{states}} \mathcal{M}_{(q_1|12|q_2)}^{X\gamma\gamma\bar{X}} \mathcal{M}_{(\bar{q}_2|34|\bar{q}_1)}^{X\gamma\gamma\bar{X}} \equiv \text{Cut}(\mathcal{I}_{N_X}^{1\text{-loop}}) \quad (4.55)$$

where exposed internal particles are taken to be on-shell. Above we have defined the internal momenta as $q_1 = l$ and $q_2 = -(l_1 + k_{12})$. The vector and fermion contributions are rather complicated – however, to get a sense of what pops out of this D -dimensional construction, we provide the scalar cut below as an example:

$$\text{Cut}(\mathcal{I}^{1\text{-loop}}) = 16(q_1 F_1 F_2 q_1)(q_1 F_3 F_4 q_1) \quad (4.56)$$

Constructing the full amplitude is then just a matter of summing over all cut contributions, each weighted by symmetry factors S_α and the number, N_α , of α -type particles:

$$\mathcal{M}^{1\text{-loop}} = \sum_{\alpha} \frac{N_\alpha}{S_\alpha} \int \frac{d^D l}{(2\pi)^D} \frac{\text{Cut}(\mathcal{I}_{N_\alpha}^{1\text{-loop}})}{l^2(l + k_{12})^2} + \text{cyc}(2, 3, 4) \quad (4.57)$$

Since the scalars are complex, and the fermions are oriented, they come dressed with symmetry factors of $S_X = -S_\lambda = 1$. The minus sign is due to the presence of a single fermion loop. Furthermore, since the photons are indistinguishable, they carry an internal symmetry factor of $S_\gamma = 2$. Now we are prepared to carry out the integral reduction and evaluate each contribution to the one-loop amplitude above.

Reduction Again, the full D -dimensional integral at one-loop is rather complicated for the vectors and fermions – as we will see, it will be more enlightening to probe their contributions when projecting the final answer down to 4D helicity states. That being said, tensor reduced integrals are actually quite simple, and its worth show the result of applying eq. (3.23) to the integrands above in eq. (4.53). After the tensor reduction, we obtain

$$\begin{aligned}
\text{Diagram 1} &= \left[\begin{aligned} &\frac{(D^3 - 24D^2 + 68D + 72)}{8} f_{12} f_{34} \\ &+ \frac{(2D^2 - 3D - 8)}{2} (f_{1234} + f_{1243}) \\ &+ 3(D + 1)(f_{1324} - f_{13} f_{24} - f_{14} f_{23}) \end{aligned} \right] \frac{s_{12}^2 I_2^D(k_{12})}{D^2 - 1} \\
\text{Diagram 2} &= \left[\begin{aligned} &\frac{(D - 4)}{8} (f_{1324} - f_{13} f_{24} - f_{14} f_{23}) \\ &- \frac{(D + 8)}{8} f_{12} f_{34} + \frac{(D - 1)}{4} (f_{1234} + f_{1243}) \end{aligned} \right] \frac{s_{12}^2 I_2^D(k_{12})}{2(D^2 - 1)} 2^{D/2} \quad (4.58) \\
\text{Diagram 3} &= \left[\frac{D(D - 6)}{4} f_{12} f_{34} + (f_{1234} + f_{1243}) \right] \frac{s_{12}^2 I_2^D(k_{12})}{D^2 - 1}
\end{aligned}$$

In terms of these integrals, the full amplitude at one-loop can be expressed as a sum over all distinct permutations of external legs, with each graph weighted by their associated symmetry factors:³

$$\mathcal{M}^{\text{1-loop}} = \left[\frac{N_\gamma}{2} \text{Diagram 1} - N_\lambda \text{Diagram 2} + N_X \text{Diagram 3} \right] + \text{cyc}(2, 3, 4) \quad (4.59)$$

Now we can proceed to evaluating the integrals in the dimension of interest.

Integration While the procedure that we have employed thus far allows us to extract all of the logarithmic dependence of the loop integrals, for the remainder of this paper we are going to focus our attention to the leading order divergences in ϵ . The purpose of doing so is to identify the class of photon effective operators that we must add to the Born-Infeld action

³Equivalently, the scalars could be real, in which case they would carry a symmetry factor of $S_{\text{Re}[X]} = \frac{1}{2}$. Complex scalars are then recovered by two real scalars multiplying the symmetry factor, $2S_{\text{Re}[X]} = S_X = \frac{2}{2}$

in order to cancel off anomalous rational terms in the S -matrix. We will leave future analyses of the novel DBIVA amplitudes in this paper as a direction of future study.

In order to capture all the tensor structures that survive after integration, including the evanescent contributions, we will map our results to the basis of operators specified in section 3.3:

$$\mathcal{M}^{\text{photon-EFT}} = \sum_{x,y} a_{(x,y)}^{F^2 F^2} \mathcal{O}_{(x,y)}^{F^2 F^2} + a_{(x,y)}^{F^4} \mathcal{O}_{(x,y)}^{F^4} + a_{(x,y)}^{F^3} \mathcal{O}_{(x,y)}^{F^3} \quad (4.60)$$

We remind the reader that the photon operators given above are defined in eq. (3.53). At one-loop mass-dimension, there are only four tensor structures that contribute:

$$\mathcal{M}_{1\text{-loop}}^{\text{photon-EFT}} = a_{(2,0)}^{F^2 F^2} \mathcal{O}_{(2,0)}^{F^2 F^2} + a_{(2,0)}^{F^4} \mathcal{O}_{(2,0)}^{F^4} + a_{(0,1)}^{F^2 F^2} \mathcal{O}_{(0,1)}^{F^2 F^2} + a_{(0,1)}^{F^4} \mathcal{O}_{(0,1)}^{F^4} \quad (4.61)$$

Plugging in $D = 4 - 2\epsilon$ to the above evaluated one-loop integrals, the EFT expansion above forms a basis for all the algebraic (non-transcendental) parts of the one-loop integral. Explicitly, the Wilson coefficients above take on the following values when we expand the integral in $D = 4 - 2\epsilon$ dimensions,

$$a_{(2,0)}^{F^2 F^2} = \frac{i}{(4\pi)^2} \frac{1}{\epsilon} \left[\frac{N_\gamma}{75} (-60 + 61\epsilon) + \frac{N_X}{225} (30 + 47\epsilon) - \frac{N_\lambda}{75} (15 + \epsilon) \right] + \mathcal{O}(\epsilon) \quad (4.62)$$

$$a_{(0,1)}^{F^2 F^2} = \frac{i}{(4\pi)^2} \frac{1}{\epsilon} \left[\frac{N_\gamma}{3} (6 + 4\epsilon) - \frac{N_\lambda}{3} \epsilon \right] + \mathcal{O}(\epsilon) \quad (4.63)$$

$$a_{(2,0)}^{F^4} = \frac{i}{(4\pi)^2} \frac{1}{\epsilon} \left[\frac{N_\gamma}{75} (105 + 17\epsilon) + \frac{N_X}{225} (15 + 16\epsilon) + \frac{N_\lambda}{150} (15 - 19\epsilon) \right] + \mathcal{O}(\epsilon) \quad (4.64)$$

$$a_{(0,1)}^{F^4} = \frac{i}{(4\pi)^2} \frac{1}{\epsilon} \left[\frac{N_\gamma}{25} (-20 + 22\epsilon) - \frac{N_X}{225} (30 + 32\epsilon) - \frac{N_\lambda}{25} (5 + 2\epsilon) \right] + \mathcal{O}(\epsilon) \quad (4.65)$$

We remind the reader that while there are four D -dimensional four-photon operators, there are only three non-vanishing operators in $D = 4$. Since all of the above Wilson coefficients come dressed with a leading $1/\epsilon$ divergence for pure photon amplitudes, this indicates the inclusion of a divergent evanescent operator that will contribute at two-loop order. We will see the consequences of this when calculating the anomalous matrix elements for pure BI at the next loop order.

Projection While the expressions above capture the full behavior of the photon amplitudes, they obscure the 4D physics captured by spinor helicity variables. Rather than plugging in explicit values for D in the integral, it can be more informative to first project down onto a 4D basis of states, leaving the internal dimensional dependence untouched. Indeed, below we can see the affect of plugging in all-plus helicity configurations into the evaluated one-loop

integrals above:

$$\begin{aligned}
\frac{1}{2} \begin{array}{c} + \\ \text{---} \\ + \end{array} & \begin{array}{c} + \\ \text{---} \\ + \end{array} = \left[\frac{(D-4)(D-2)}{16(D^2-1)} s_{12}^2 [12]^2 [34]^2 I_2^D(k_{12}) \right] \frac{(D-2)}{2} \\
\begin{array}{c} + \\ \text{---} \\ + \end{array} & \begin{array}{c} + \\ \text{---} \\ + \end{array} = \left[\frac{(D-4)(D-2)}{16(D^2-1)} s_{12}^2 [12]^2 [34]^2 I_2^D(k_{12}) \right] \frac{2^{D/2-1}}{2} \\
\frac{1}{2} \begin{array}{c} + \\ \text{---} \\ + \end{array} & \begin{array}{c} + \\ \text{---} \\ + \end{array} = \left[\frac{(D-4)(D-2)}{16(D^2-1)} s_{12}^2 [12]^2 [34]^2 I_2^D(k_{12}) \right] \frac{2}{2}
\end{aligned} \tag{4.66}$$

Here we can see two characteristic properties of the anomaly cancellation that takes place when we introduce scalars and fermions into our spectrum.

- First, we can see that all integrals carry a factor of $(D-4)$. This reflects the property that in $D=4$, all the tree-level amplitudes that contribute to the cut must vanish outside the MHV sector. Thus, any contribution to the all plus matrix element must be suppressed by a factor of $\epsilon = (4-D)/2$ in order to push the logarithms to $\mathcal{O}(\epsilon)$.
- Second, we can see that the common factor in all three integrals is weighted differently depending on whether the internal particle is a boson or a fermion. Bosonic contributions are weighted by the number of particles in the loop (in this case, 2 real scalars or $(D-2)$ helicity states), whereas the fermion weight is dependent on the dimension of the gamma matrix representation, where $\text{tr}[\Gamma_\mu \Gamma^\mu] = 2^{D/2-1} D$. In $D=4$, all of these contribute equal magnitude to the full amplitude.

Putting this all together, we obtain the following non-vanishing algebraic parts of the one-loop matrix elements:

$$\mathcal{M}_{(-+++) }^{\text{DBIVA}} = \frac{i}{\epsilon} \frac{[12]^2 \langle 34 \rangle^2}{(4\pi)^2} \left[\frac{N_\gamma}{2} s_{12}^2 + \left(\frac{N_\gamma}{5} + \frac{N_\lambda}{20} + \frac{N_X}{30} \right) (s_{13}^2 + s_{14}^2) \right] + \mathcal{O}(\epsilon^0) \tag{4.67}$$

$$\mathcal{M}_{(-++++)}^{\text{DBIVA}} = 0 \tag{4.68}$$

$$\mathcal{M}_{(++++)}^{\text{DBIVA}} = -\frac{i}{(4\pi)^2} \frac{1}{60} (N_\gamma + N_X - N_\lambda) (s_{12}^4 + s_{13}^4 + s_{14}^4) \frac{[12][34]}{\langle 12 \rangle \langle 34 \rangle} + \mathcal{O}(\epsilon^1) \tag{4.69}$$

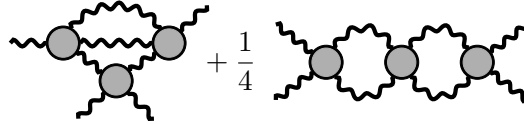
The $(-+++)$ matrix element is identically zero due to D -dimensional four-point kinematics — the only available helicity structure is $\langle 1|2|3|^2[24]^2$ which must be weighted by a mass-dimension 2 permutation invariant. The only such permutation invariant is $s+t+u=0$,

which vanishes regardless of the integration dimension. As a check, above we have reproduced the results found in [51], which used four-dimensional spinor helicity and dimension-shifting relations when performing the integration. This serves as a nice verification of our D -dimensional methods. Now we will proceed with the two-loop calculation.

4.2.2 Two-loop Born-Infeld

For all of the two-loop calculations, we will drop the header labelling which step in the process we are presenting. While we will omit these markers, our procedure is still the same: **construction**, **reduction**, **integration** and then **projection**. Due to the formidably large expressions that result from doing this calculation completely covariantly, most of our amplitudes will be presented after projecting down to 4D helicity states.

To begin, we will compute the pure Born-Infeld two-loop amplitude. Like pions, there are only two diagrams that contribute at this loop order. Including symmetry factors, the full Born-Infeld amplitude at two-loop can be expressed as follows:

$$\mathcal{M}_{2\text{-loop}}^{\text{BI}} = \frac{1}{2} \text{ (diagram 1) } + \frac{1}{4} \text{ (diagram 2) } + \text{perms} \quad (4.70)$$


As in the previous section, exposed legs implicitly sum over internal states. The grey blobs above represent D -dimensional $t_8 F^4$ operator insertions from the four-point BI tree amplitudes, which we labelled as $\mathcal{M}_{(1234)}^{\gamma\gamma\gamma\gamma}$. We give the internal loop momenta the same internal labels as we did the pions in eq. (4.26) and eq. (4.27), giving us the following integrals to evaluate for two-loop pure BI,

$$\text{ (diagram 2) } = \sum_{\text{states}} \int \frac{d^D l_1 d^D l_2}{(2\pi)^{2D}} \frac{\mathcal{M}_{(p_4 12 p_3)}^{\gamma\gamma\gamma\gamma} \mathcal{M}_{(\bar{p}_1 \bar{p}_4 \bar{p}_3 \bar{p}_2)}^{\gamma\gamma\gamma\gamma} \mathcal{M}_{(p_2 34 p_1)}^{\gamma\gamma\gamma\gamma}}{l_1^2 (l_1 + k_{12})^2 l_2^2 (l_2 + k_{12})^2} \quad (4.71)$$

$$\text{ (diagram 1) } = \sum_{\text{states}} \int \frac{d^D l_1 d^D l_2}{(2\pi)^{2D}} \frac{\mathcal{M}_{(2q_4 \bar{q}_3 \bar{q}_1)}^{\gamma\gamma\gamma\gamma} \mathcal{M}_{(1\bar{q}_4 q_3 \bar{q}_2)}^{\gamma\gamma\gamma\gamma} \mathcal{M}_{(q_2 34 q_1)}^{\gamma\gamma\gamma\gamma}}{l_1^2 (l_1 + l_2 + k_1)^2 l_2^2 (l_2 + k_{12})^2} \quad (4.72)$$

where the internal momenta obey the same convention, $\bar{p}_i = -p_i$ and $\bar{q}_i = -q_i$. Performing the tensor reduction on the internal loop momenta and projecting to 4D helicity states yields divergent quantities for all helicity configurations. In the interest of projecting to a D -dimensional basis of operators, and analyzing the $U(1)$ anomaly present at two-loop, we will just focus on the leading divergences for each helicity configuration.

Leading (++++) divergence As we saw above, the one-loop matrix element has a rational all-plus contribution. This manifestly breaks the $U(1)$ duality invariance present at tree-level. Moreover, this will contribute to non-vanishing 4D cut of the form:

$$\text{Cut} \left[\mathcal{M}_{(++++)}^{\text{BI}, 2\text{-loop}} \right]^{D=4} = \mathcal{M}_{(++++)}^{\text{BI}, 1\text{-loop}} \times \mathcal{M}_{(--++)}^{\text{BI}, \text{tree}} \quad (4.73)$$

This cut should source a logarithmic discontinuity, and thus, the leading contribution for two-loop all-plus matrix element should diverge as $1/\epsilon$. Indeed this is what we find:

$$\mathcal{M}_{(++++)}^{\text{BI,2-loop}} = -\frac{29}{600} \frac{1}{(4\pi)^4} \frac{1}{\epsilon} (s_{12}^6 + s_{13}^6 + s_{14}^6) \frac{[12][34]}{\langle 12 \rangle \langle 34 \rangle} + \mathcal{O}(\epsilon^0) \quad (4.74)$$

In principle, this divergence could be cancelled by the addition of a counterterm at $\mathcal{O}(\alpha'^4)$ inserted into a one-loop matrix element with $t_8 F^4$ at $\mathcal{O}(\alpha'^2)$. We will explore the effect of such anomaly cancelling counterterms in the next section, and we will see that this alone is not sufficient to cancel the divergence above. As we noted in the previous section, there are additional 4D operators that appear at one-loop that will vanish when plugging in $(++++)$ physical states. These too could in principle be secretly contributing to the divergence expressed above. We can see this more clearly for the $(-+++)$ result below.

Leading $(-+++)$ divergence The same cut construction above suggests a different story for $(-+++)$ at two-loop. Indeed, the following cut should vanish when taken on-shell in $D = 4$:

$$\text{Cut} \left[\mathcal{M}_{(-+++)}^{\text{BI,2-loop}} \right]^{D=4} = \mathcal{M}_{(-+++)}^{\text{BI,1-loop}} \times \mathcal{M}_{(-+++)}^{\text{BI,tree}}, \quad (4.75)$$

However, we found that $\mathcal{M}_{(-+++)}^{\text{BI,1-loop}} = 0$ due to D -dimensional four-point kinematics. Despite this, we find similarly to the all-plus helicity configuration above in eq. (4.74), the one-minus matrix element also carries a leading order $1/\epsilon$ divergence:

$$\mathcal{M}_{(-+++)}^{\text{BI,2-loop}} = -\frac{1}{75} \frac{1}{(4\pi)^4} \frac{1}{\epsilon} (s_{12}^3 + s_{13}^3 + s_{14}^3) s_{12}^2 \langle 1|2|3 \rangle^2 [24]^2 + \mathcal{O}(\epsilon^0) \quad (4.76)$$

At first glance, this appears to be a violation of the Optical Theorem. However, this divergence is sourced by one-loop evanescent operators that vanish in $D = 4$, but carry a $1/\epsilon$ divergence in $D = 4 - 2\epsilon$. In the section 5.1, we will demonstrate this in more detail, and show how higher derivative four-photon operators can be used to cancel the $U(1)$ anomaly. In doing so, we can construct a D -dimensional quantum effective action that satisfies duality invariance in $D = 4$ through two-loop order in perturbation theory.

Leading $(--++)$ divergence Finally, we express below the leading divergence for the aligned-helicity matrix elements. After reducing to the two-loop scalar integral basis, and projecting along 4D helicity states, we obtain the following expression at leading order in the ϵ -expansion:

$$\mathcal{M}_{(--++)}^{\text{BI,2-loop}} = -\frac{1}{\epsilon^2} \frac{\langle 12 \rangle^2 [34]^2}{(4\pi)^4} \left[\frac{19}{60} s_{12}^4 + \frac{14}{75} (s_{13}^4 + s_{14}^4) \right] + \mathcal{O}(\epsilon^{-1}) \quad (4.77)$$

Similar to the one-loop result, we can see that $s_{12}^4 \langle 12 \rangle^2 [34]^2$ and $(s_{13}^4 + s_{14}^4) \langle 12 \rangle^2 [34]^2$ helicity sectors are asymmetrically weighted in pure photon amplitudes. As we will see in the next

section, these two operators carry equal weight when we introduce additional states consistent with maximal supersymmetry.

Moreover, adding additional scalar and fermion states consistent with supersymmetry is the simplest way to cancel the $U(1)$ anomaly computed above outside of the aligned helicity sectors. When summing over superfield contributions at loop level, the $U(1)$ symmetry at tree-level is promoted to a $U(1)_R$ symmetry, and thus is protected perturbatively by supersymmetric Ward Identities. We will demonstrate this explicitly in the next section by computing the two-loop four-photon matrix element in $\mathcal{N} = 4$ DBIVA via our D -dimensional unitarity methods.

4.2.3 Two-loop $\mathcal{N} = 4$ DBIVA

Much of the complication in performing a two-loop calculation in pure BI theory is the proliferation of high orders in loop momenta left over in the state sum. These factors of loop momenta not only conspire with external momenta, but also mingle with external polarizations. There are a number of integral reduction algorithms [118–125] that are very effective for reducing factors of $(k_i \cdot l)$, since they can trivially be expressed as a linear combinations of inverse propagators,

$$(k_i \cdot l) = \frac{1}{2} [(l + k_i)^2 - l^2] \quad (4.78)$$

However, the factors of $(\varepsilon_i \cdot l_j)$ can be more tedious, as they do not permit an inverse propagator expansion. This is part of the motivation for the cumbersome process of applying Passarino-Veltman to the recursively one-loop integrals present in the two-loop Born-Infeld amplitude.

Luckily, the state-sewing for maximal supersymmetry is dramatically more simple than less than maximal supersymmetry [3, 158]. This is most easily seen by considering the covariant operators we defined for one-loop DBIVA amplitudes. When one applies the conditions for maximal supersymmetry, stated below,

$$D = 10 \quad N_\lambda = 1 \quad N_X = 0 \quad (4.79)$$

$$D = 6 \quad N_\lambda = 2 \quad N_X = 1 \quad (4.80)$$

$$D = 4 \quad N_\lambda = 4 \quad N_X = 3 \quad (4.81)$$

$$D = 3 \quad N_\lambda = 8 \quad N_X = 8 \quad (4.82)$$

then the state sum is completely independent of loop momenta and precisely reproduces the supersymmetric operator $s_{12}^2(t_8 F^4)$ when cut along the s_{12} -channel. This statement holds covariantly in general dimension. Concretely, we find that for theories with maximal supersymmetry:

$$\sum_{\text{states}} (t_8 F^4)_{(12l_1l_2)}^{(\max)} (t_8 F^4)_{(\bar{l}_1\bar{l}_234)}^{(\max)} = s_{12}^2 (t_8 F^4)_{(1234)}^{(\max)} \quad (4.83)$$

This can similarly be used in the integrand construction $\mathcal{N} = 4$ super-Yang-Mills, which has been computed to six-loop order [159]. In the case of maximal supersymmetry in $D = 4$,

we can write the $(t_8 F^4)_{(1234)}^{(\max)}$ operator as a supersymmetric delta function with the all-plus permutation invariant introduced previously:

$$\mathcal{M}_{(1234)}^{\mathcal{N}=4\text{DBIVA}} = \delta^{(8)}(Q) \frac{[12][34]}{\langle 12 \rangle \langle 34 \rangle} \equiv (t_8 F^4)_{(1234)}^{(\max)} \Big|_{D=4} \quad (4.84)$$

where the delta function is a Grassmann valued polynomial of spinor-helicity variables:

$$\delta^{(8)}(Q) = \prod_{a=1}^4 \sum_{i \neq j} \langle ij \rangle \eta_i^a \eta_j^a \quad (4.85)$$

By applying this supersymmetric state sum, we find that the integrands for two-loop $\mathcal{N} = 4$ DBIVA is trivially easy to construct - even simpler than NLSM integrands. Below we represent an internal on-shell superfield with a green line, and obtain the following integrand for the double-bubble:

$$\text{Cut} \left(\text{diagram} \right) = \sum_{\text{states}} (t_8 F^4)_{(1234)}^{(\max)} (t_8 F^4)_{(1234)}^{(\max)} (t_8 F^4)_{(1234)}^{(\max)} = s_{12}^4 (t_8 F^4) \quad (4.86)$$

and similarly so for the ostrich-diagram integral contribution:

$$\text{Cut} \left(\text{diagram} \right) = \sum_{\text{states}} (t_8 F^4)_{(1234)}^{(\max)} (t_8 F^4)_{(1234)}^{(\max)} (t_8 F^4)_{(1234)}^{(\max)} = s_{12}^2 \tau_2^{(2)} \tau_1^{(1)} (t_8 F^4). \quad (4.87)$$

Since there are no loop momenta interfering with the tensor structures of the external photons, the result of integration will just be proportional to a $(t_8 F^4)$ tensor, which is manifestly $U(1)$ duality invariant. Thus, as promised, adding in $\mathcal{N} = 4$ states cancels the $U(1)$ anomaly present in the pure Born-Infeld S -matrix. After applying the tensor reduction to the ostrich-diagram, we obtain the following expression for the two diagrams:

$$\text{diagram} = s_{12}^4 (I_2^D(k_{12}))^2 (t_8 F^4) \quad (4.88)$$

$$\text{diagram} = \frac{s_{12}^3}{3} [I_3 \circ I_2]^D(k_{12}) (t_8 F^4) \quad (4.89)$$

This is easily evaluated in $D = 4 - 2\epsilon$, from which we find the following expression for the leading order divergence of the four-photon two-loop amplitude in $\mathcal{N} = 4$ DBIVA theory:

$$\boxed{\mathcal{M}_{2\text{-loop}}^{\mathcal{N}=4\text{DBIVA}} = -\frac{1}{\epsilon^2} \frac{1}{768\pi^4} (s_{12}^4 + s_{13}^4 + s_{14}^4) (t_8 F^4) + \mathcal{O}(\epsilon^{-1})} \quad (4.90)$$

With this result in hand, we will now demonstrate that the same calculation that we have performed via generalized unitarity can be reproduced using loop-level double copy construction.

4.3 DBIVA via double copy

The calculation performed above was completely agnostic to the known tree-level relationship of DBIVA amplitudes as a double copy of NLSM and super Yang-Mills. As we will now show, the amplitude above can be equivalently produced using the two-loop color-dual numerators of $\mathcal{N} = 4$ sYM, and the NLSM integrands constructed earlier in this section. This observation provides further evidence for the consistency of double-copy construction at multi-loop order in perturbation theory, and serves as an existence proof for color-dual NLSM numerators at two-loop.

At loop-level, the double-copy construction amounts to replacing the color-factors in a cubic-graph representation of the integrand with a set of color-dual numerators. That is, starting with an L -loop NLSM integrand of the form:

$$\mathcal{A}_n^{\text{NLSM}} = \int \prod_{i=1}^L \frac{d^D l_i}{(2\pi)^d} \sum_{g \in \Gamma^{(3)}} \frac{1}{S_g} \frac{C_g N_g^{\text{NLSM}}}{D_g} \quad (4.91)$$

we can construct $\mathcal{N} = 4$ DBIVA by replacing the color factors, C_g , with the kinematic numerators, $N_g^{\mathcal{N}=4}$, of sYM amplitudes:

$$C_g \rightarrow N_g^{\mathcal{N}=4} \quad \Rightarrow \quad \mathcal{M}_n^{\text{DBIVA}} = \int \prod_{i=1}^L \frac{d^D l_i}{(2\pi)^d} \sum_{g \in \Gamma^{(3)}} \frac{1}{S_g} \frac{N_g^{\mathcal{N}=4} N_g^{\text{NLSM}}}{D_g} \quad (4.92)$$

where the kinematic numerators depend on particular choice of generalized gauge. In order for this construction to work, the kinematic numerators on at least one side of the double copy must satisfy all the same algebraic relations as the color factors. Since generalized unitarity allows us to construct the integrands on-shell, this construction conjecturally holds at loop-level as long as the gauge-theory is tree-level color-dual.

While there are currently no color-dual NLSM numerators identified in the literature beyond one-loop, there are color-dual representation available for $\mathcal{N} = 4$ sYM through four-loop four-point [30]. Below are the one- and two-loop basis numerators relevant for our construction:

$$N_{\mathcal{N}=4}^{\text{box}} = \begin{array}{c} 2 \quad 3 \\ \diagdown \quad \diagup \\ \square \\ \diagup \quad \diagdown \\ 1 \quad 4 \end{array} = (t_8 F^4)_{(1234)}^{(\text{max})} \quad (4.93)$$

and similarly so at two-loop four-point for the double-box and cross-box, which take on

identical expressions:

$$N_{\mathcal{N}=4}^{(12|34)} \equiv \begin{array}{c} \text{Diagram: A square with a vertical line in the middle, representing a double bubble. External legs are labeled 1 (bottom-left), 2 (top-left), 3 (top-right), and 4 (bottom-right).} \end{array} = s_{12}(t_8 F^4)_{(1234)}^{(\max)} \quad (4.94)$$

$$N_{\mathcal{N}=4}^{([12]|34)} \equiv \begin{array}{c} \text{Diagram: A square with a diagonal line from the top-left to the bottom-right, representing a crossed box. External legs are labeled 1 (bottom-left), 2 (top-left), 3 (top-right), and 4 (bottom-right).} \end{array} = s_{12}(t_8 F^4)_{(1234)}^{(\max)} \quad (4.95)$$

These two-loop numerators can be constructed via the rung-rule [158] and the no-triangle hypothesis [160]. We can see that both the one- and two-loop kinematic numerators are completely independent of loop momenta. This allows us to take our NLSM amplitudes from earlier in the section, and simply replace the color-factors post integration. We will show the results of this procedure for both one-loop and two-loop DBIVA in the proceeding sections.

4.3.1 One-loop $\mathcal{N} = 4$ DBIVA

At one-loop, performing the double copy is a simple task. As we noted above, since the box numerator for $\mathcal{N} = 4$ sYM has no kinematic dependence on internal loop momenta, we can pull it out of the integration process. Thus, making the following replacement

$$C_{(1234)}^{\text{box}} \rightarrow N_{(1234)}^{\text{box}} \quad (4.96)$$

on the integrated NLSM four-point one-loop amplitude. This yields the following expression in $D = 4 - 2\epsilon$ for the four-point one-loop $\mathcal{N} = 4$ DBIVA matrix element:

$$\mathcal{M}_{\text{DBIVA}}^{\mathcal{N}=4} = \left[\frac{s_{12}^2}{32\pi^2} \left(\frac{1}{\epsilon} + \ln(-s_{12}) \right) + \text{cyc}(2, 3, 4) \right] (t_8 F^4)_{(1234)}^{(\max)} \quad (4.97)$$

This is in agreement with the leading divergence of $\mathcal{N} = 4$ DBIVA previously found in [51], along with our eq. (4.69) result from the previous section when taking $N_\gamma = 1$, $N_\lambda = 4$ and $N_X = 3$, in concordance with maximal $D = 4$ supersymmetry

4.3.2 Two-loop $\mathcal{N} = 4$ DBIVA

At two-loop it sufficient to show that replacing the color factors reproduces the integrals we found above with the unitarity construction. Starting with the NLSM integrands in eq. (4.29) and eq. (4.30), we make the same replacement of color factors post integration as was done at one-loop. We carry this out first for the double-bubble, and find that the full D -dimensional

NLSM integral simplifies dramatically:

$$\begin{aligned}
& \left. \begin{array}{c} 2 \\ 1 \end{array} \right\} \begin{array}{c} \text{Diagram 1: A chain of three black circles connected by black arcs. The leftmost circle has two external black lines labeled 1 and 2. The middle circle has two external black lines labeled 3 and 4. The rightmost circle has two external black lines labeled 5 and 6. The arcs connect the circles in a chain-like fashion.} \end{array} \Bigg|_{C_g \rightarrow N_g^{\mathcal{N}=4}} = N_{\mathcal{N}=4}^{(12|34)} \left[\frac{(s_{12} I_2^D(k_{12}))^2}{2} \left(\frac{s_{14} - s_{13}}{(D-1)^2} + s_{12} \right) \right] \\
& + N_{\mathcal{N}=4}^{(12|43)} \left[\frac{(s_{12} I_2^D(k_{12}))^2}{2} \left(\frac{s_{13} - s_{14}}{(D-1)^2} + s_{12} \right) \right] \quad (4.98) \\
& = s_{12}^4 (I_2^D(k_{12}))^2 (t_8 F^4)_{(1234)}^{(\max)} \equiv \begin{array}{c} \text{Diagram 2: A chain of three green circles connected by green arcs. The leftmost circle has two external wavy black lines labeled 1 and 2. The middle circle has two external wavy black lines labeled 3 and 4. The rightmost circle has two external wavy black lines labeled 5 and 6. The arcs connect the circles in a chain-like fashion.} \end{array}
\end{aligned}$$

The cancellation between dimension dependent factors is even more startling for the ostrich-diagram integral:

$$\begin{aligned}
& \text{Diagram 1} \left| \begin{array}{l} C_g \rightarrow N_g^{\mathcal{N}=4} \\ = N_{\mathcal{N}=4}^{(12|34)} \frac{s_{12}}{6} \left[\frac{(D-1)(D-4)s_{14} + 2(D-2)^2 s_{13}}{(D-1)(4-3D)} \right] [I_3 \circ I_2]^D(k_{12}) \\ + N_{\mathcal{N}=4}^{(12|34)} \frac{s_{12}}{6} \left[\frac{(D-1)(D-4)s_{13} + 2(D-2)^2 s_{14}}{(D-1)(4-3D)} \right] [I_3 \circ I_2]^D(k_{12}) \\ + N_{\mathcal{N}=4}^{([12]|34)} \left[\frac{s_{12}^2}{6} \frac{D+1}{D-1} \right] [I_3 \circ I_2]^D(k_{12}) \\ = \frac{s_{12}^3}{3} [I_3 \circ I_2]^D(k_{12}) (t_8 F^4)_{(1234)}^{(\max)} \equiv \text{Diagram 2} \end{array} \right. \\
& \text{Diagram 2}
\end{aligned}
\tag{4.99}$$

This alone is sufficient to demonstrate the validity of the double-copy, as these integrated quantities are exactly the same as those produced via generalized unitarity of $\mathcal{N} = 4$ DBIVA at two-loop in eq. (4.86) and eq. (4.87). We emphasize that based on our analysis, this consistency of the double-copy at two loop appears to hold in any dimension, as all the D -dependent prefactors drop out upon replacing the gauge theory color factors with $\mathcal{N} = 4$ numerators. Considering the consistency of these two construction, this also serves as strong evidence for the existence of color-dual representation for two-loop pion integrands. We leave identifying such valid representation as an enticing future direction worth investigation.

5 Effective Actions

In this section we demonstrate how our basis of higher-derivative four-photon operators in eq. (3.53) can be used to construct quantum effective actions that capture loop-level effects. First we study anomaly cancellation for the multi-loop photon amplitudes computed above. After this, we proceed by interpreting these higher derivative operators as double copies between NLSM and higher derivative Yang-Mills amplitudes with off-shell higher-spin modes.

As was demonstrated in previous work by the authors [50], the full set of D -dimensional four-photon operators can be constructed via adjoint double-copy, but at the cost of introducing off-shell higher spin modes in the single-copy vector theory. However, these higher-spin modes can be absorbed consistently in a double-copy framework by introducing symmetric algebraic structures. We discuss future applications of this construction in section 6.

5.1 Anomaly cancellation

Here we begin with our study of higher-derivative extensions to BI theory. Our goal is to identify the higher derivative four-photon operators that are needed to cancel the $U(1)$ anomalous matrix elements computed in the previous section. We will start with the one-loop corrections, captured by tree level insertions at $\mathcal{O}(\alpha'^4)$, and then proceed with the two loop corrections, which combine both $\mathcal{O}(\alpha'^4)$ operator insertions at one-loop and $\mathcal{O}(\alpha'^6)$ operator insertions at tree-level. In doing so, we demonstrate that cancelling the $U(1)$ anomaly through two loop order can be achieved with local finite counterterms if and only if we introduce an evanescent operator at $\mathcal{O}(\alpha'^4)$ to the Born-Infeld action.

5.1.1 One-loop

In section 4.2 we computed the one-loop matrix element for a general DBIVA theory. Plugging in the values $N_\gamma = 1$ and $N_\lambda = N_X = 0$ we obtain the following anomalous all-plus matrix element for pure Born-Infeld theory:

$$\mathcal{M}_{(++++)}^{\text{BI,1-loop}} = -\frac{i}{(4\pi)^2} \frac{1}{60} (s_{12}^4 + s_{13}^4 + s_{14}^4) \frac{[12][34]}{\langle 12 \rangle \langle 34 \rangle} + \mathcal{O}(\epsilon) \quad (5.1)$$

In ref. [51], the authors identified a candidate 4D counterterm that cancels this anomalous matrix element, which we have called $\mathcal{T}_{(++++)}^{4\text{D}}$, thereby restoring duality invariance through one-loop. As noted in the previous section, the one-loop matrix element can be mapped to our D -dimensional operator basis. In general, all available 4D tensor structures at $\mathcal{O}(\alpha'^4)$ map onto our D -dimensional basis. One particular map we provide below

$$\mathcal{T}_{(++++)}^{4\text{D}} = a_{(\text{ev.})} \mathcal{T}^{\text{ev.}} + \mathcal{T}^{4+} \quad (5.2)$$

$$\mathcal{T}_{(---+)}^{4\text{D},1} = a_{(\text{ev.})} \mathcal{T}^{\text{ev.}} + 2\mathcal{T}_{(2,0)}^{F^4} - 4\mathcal{T}_{(0,1)}^{F^2 F^2} \quad (5.3)$$

$$\mathcal{O}_{(---+)}^{4\text{D},2} = a_{(\text{ev.})} \mathcal{T}^{\text{ev.}} + 2\mathcal{T}_{(2,0)}^{F^4} + 4\mathcal{T}_{(0,1)}^{F^2 F^2} \quad (5.4)$$

where we have defined the following D -dimensional operator that projects down to the all-plus configuration,

$$\mathcal{T}^{4+} = 4\mathcal{T}_{(2,0)}^{F^2 F^2} - 2\mathcal{T}_{(2,0)}^{F^4} - 4\mathcal{T}_{(0,1)}^{F^4} \quad (5.5)$$

and all the 4D operators have the freedom to add the previously defined evanescent operator, $\mathcal{T}^{\text{ev.}}$,

$$\mathcal{T}^{\text{ev.}} = \mathcal{T}_{(2,0)}^{F^2 F^2} - \mathcal{T}_{(0,1)}^{F^2 F^2} + \mathcal{T}_{(0,1)}^{F^4} \quad (5.6)$$

Thus, we can construct the new effective photon Lagrangian, $\mathcal{L}^{\text{BI+CT}}$, with the addition of the all-plus counter-terms to our Born-Infeld Lagrangian:

$$\mathcal{L}^{\text{BI+CT}} = \mathcal{L}^{\text{BI}} + \frac{(\alpha')^4}{(4\pi)^2} \frac{1}{30} (\mathcal{T}^{4+} + a_{(\text{ev.})} \mathcal{T}^{\text{ev.}}) \quad (5.7)$$

JJ: Maybe we should explain what we mean by writing an operator in terms of mandelstams etc? Computing amplitudes from this Lagrangian yields the following one-loop matrix elements at $\mathcal{O}(\alpha'^4)$:

$$\mathcal{M}_{(- - + +)}^{\text{BI+CT}, 1\text{-loop}}|_{\alpha'^4} = \mathcal{M}_{(- - + +)}^{\text{BI}, 1\text{-loop}} \quad (5.8)$$

$$\mathcal{M}_{(- + + +)}^{\text{BI+CT}, 1\text{-loop}}|_{\alpha'^4} = 0 \quad (5.9)$$

$$\mathcal{M}_{(+ + + +)}^{\text{BI+CT}, 1\text{-loop}}|_{\alpha'^4} = \mathcal{O}(\epsilon) \quad (5.10)$$

Thus, eq. (5.7) constitutes a duality invariant photon theory through one-loop order. With this, we can identify what additional operators will be needed to cancel the anomaly through two-loop.

5.1.2 Two-loop

The first step in identifying the requisite operators needed to cancel the two-loop anomaly at $\mathcal{O}(\alpha'^6)$ is to perform another one-loop calculation at this mass dimension, which includes the counterterms of $\mathcal{L}^{\text{BI+CT}}$ defined above. The one-loop amplitude is constructed as follows:

$$\mathcal{M}_{1\text{-loop}}^{\text{BI+CT}}|_{\alpha'^6} = \frac{1}{2} \frac{\alpha'^6}{30(4\pi)^2} \begin{array}{c} \mathcal{T}^{4+} \quad t_8 F^4 \\ \text{diagram} \end{array} + \frac{a_{\text{ev.}}}{2} \begin{array}{c} \mathcal{T}^{\text{ev.}} \quad t_8 F^4 \\ \text{diagram} \end{array} + \text{perms} \quad (5.11)$$

Both of these operator insertions can be evaluated using the same D -dimensional procedure used throughout the text. The all-plus counterterm yields the following contributions to $(+ + + +)$ and $(- + + +)$ helicity configurations:

$$\begin{array}{c} + \quad \mathcal{T}^{4+} \quad t_8 F^4 \quad + \\ \text{diagram} \\ + \end{array} = \left[\frac{7}{5} + \frac{79}{150} \epsilon \right] s_{12}^4 [12]^2 [34]^2 I_2^{4-2\epsilon}(k_{12}) + \mathcal{O}(\epsilon) \quad (5.12)$$

$$\begin{array}{c} + \quad \mathcal{T}^{4+} \quad t_8 F^4 \quad + \\ \text{diagram} \\ - \end{array} = \mathcal{O}(\epsilon) \quad \begin{array}{c} + \quad \mathcal{T}^{4+} \quad t_8 F^4 \quad + \\ \text{diagram} \\ - \end{array} = 0 \quad (5.13)$$

We note that there is a distinction between the first and second $(- + + +)$ expressions. The first expression is dressed with $(D-4)^2$, which pushes the leading contribution to $\mathcal{O}(\epsilon)$. Whereas the second term is identically zero because the 4D helicity structure carries an overall factor

of $(s + t + u) = 0$. In addition, since there is a non-vanishing 4D residue for the all-plus integrand, the integral has a leading order divergence in ϵ .

Below we find it instructive to show the D -dependence of the evanescent operator insertion, which yields the following matrix element contributions:

$$\begin{array}{c}
 + \quad \mathcal{T}^{\text{ev.}} \quad t_8 F^4 \quad + \\
 \text{[Diagram: A loop with two vertices, one shaded black and one shaded grey, connected by wavy lines. The top-left vertex is labeled with a plus sign, the top-right with a plus sign, the bottom-left with a plus sign, and the bottom-right with a plus sign.] } \\
 +
 \end{array} = - \left[\frac{(D-4)(D^2-7D-4)}{32(D^2-1)} \right] s_{12}^4 [12]^2 [34]^2 I_2^D(k_{12}) \quad (5.14)$$

$$\begin{array}{c}
 + \quad \mathcal{T}^{\text{ev.}} \quad t_8 F^4 \quad + \\
 \text{[Diagram: A loop with two vertices, one shaded black and one shaded grey, connected by wavy lines. The top-left vertex is labeled with a plus sign, the top-right with a plus sign, the bottom-left with a plus sign, and the bottom-right with a minus sign.] } \\
 +
 \end{array} = - \left[\frac{(D-4)(D+2)}{8(D^2-1)} \right] s_{12}^3 \langle 4|3|2 \rangle^2 [13]^2 I_2^D(k_{12}) \quad (5.15)$$

$$\begin{array}{c}
 + \quad \mathcal{T}^{\text{ev.}} \quad t_8 F^4 \quad + \\
 \text{[Diagram: A loop with two vertices, one shaded black and one shaded grey, connected by wavy lines. The top-left vertex is labeled with a plus sign, the top-right with a plus sign, the bottom-left with a minus sign, and the bottom-right with a plus sign.] } \\
 -
 \end{array} = 0 \quad (5.16)$$

This will produce $\mathcal{O}(\epsilon^0)$ matrix elements in the $(+++-)$ helicity sector. Thus, in order to cancel the divergent part of the two-loop $(+++-)$ anomaly computed in eq. (4.76), we must weight the evanescent operator by a numerical factor that diverges in $D = 4$. Given the particular numerical value computed in the previous section, we find evanescent Wilson coefficient must take the following D -dependent value:

$$\boxed{\mathcal{L}^{\text{BI+CT}} = \mathcal{L}^{\text{BI}} + \frac{\alpha'^4}{(4\pi)^2} \frac{1}{30} \left[\mathcal{T}^{4+} + \frac{4}{(D-4)} \mathcal{T}^{\text{ev.}} \right] + \mathcal{O}(\alpha'^6)} \quad (5.17)$$

where the $(D-4)$ in the denominator cancels the factor in the numerator above. In order to further absorb the remaining rational terms, we must introduce an additional set of tree-level operators at $\mathcal{O}(\alpha'^6)$. At this this order in mass-dimension, there are seven distinct operators:

$$\{\mathcal{O}_{(4,0)}^{F^2 F^2}, \mathcal{O}_{(2,1)}^{F^2 F^2}, \mathcal{O}_{(0,2)}^{F^2 F^2}, \mathcal{O}_{(4,0)}^{F^4}, \mathcal{O}_{(2,1)}^{F^4}, \mathcal{O}_{(0,2)}^{F^4}, \mathcal{O}_{(1,0)}^{F^3}\} \quad (5.18)$$

By adding these operators to the effective lagrangian above, we have verified that there is sufficient freedom to absorb the remaining rational terms present at two-loop. Of these available operators, only the F^3 tensor structure is non-vanishing when projected along the $(-+++)$ helicity configuration. Furthermore, just as at $\mathcal{O}(\alpha'^4)$, there is a single evanescent operator, which we define below:

$$\mathcal{T}_{\alpha'^6}^{\text{ev.}} = \mathcal{O}_{(4,0)}^{F^2 F^2} - 2\mathcal{O}_{(2,1)}^{F^2 F^2} + \mathcal{O}_{(0,2)}^{F^2 F^2} + \mathcal{O}_{(2,1)}^{F^4} - \mathcal{O}_{(0,2)}^{F^4 \odot^4} \quad (5.19)$$

Thus, of the seven available D -dimensional operators, they are projected to only six distinct 4D tensor structures. We will describe the counting of 4D versus general dimension photon operators in generality at all orders in α' in more depth at the end of this section.

5.2 Double copy construction

As we have stated in the text, it is well known that DBIVA theory can be constructed at tree-level as an adjoint double copy between NLSM and sYM amplitudes. There is now a large body of literature studying double-copy construction of higher derivative gauge theory counterterms [13, 15–19, 21–24], like those used above to cancel $U(1)$ anomalous matrix elements in pure Born-Infeld theory. Indeed, recent work by the authors demonstrated that all four-photon operators can be constructed consistently via the double-copy [50]. Here we briefly describe the single-copy gauge theory that when double copied with NLSM produces the higher derivative operators of the previous section.

5.2.1 Symmetric-structure double-copy

To realize the double-copy construction that produces the counterterms above, ref. [50] first decomposed NLSM pions amplitude into symmetric structure constants using the $U(N)$ color identity

$$f^{abe} f^{ecd} = d^{ade} d^{ebc} - d^{ace} d^{ebd} \quad (5.20)$$

where the symmetric structure constant is defined as follows

$$d^{abc} = \text{tr}[T^a \{T^b, T^c\}]. \quad (5.21)$$

By applying this color algebra identity to the four-point NLSM amplitudes of eq. (4.4), one finds that pions can similarly be expressed as a symmetric-structure double copy:

$$\mathcal{M}_4^{\text{NLSM}} = \sum_{g \in \Gamma^3} \frac{c_g^{\text{dd}} n_g^{\text{dd}, \pi}}{d_g} = d^{abe} d^{ecd} s + d^{ade} d^{ebd} t + d^{ace} d^{ebd} u \quad (5.22)$$

where $c_s^{\text{dd}} \equiv d^{abe} d^{ecd}$ and the NLSM symmetric s -channel numerator is $n_g^{\text{dd}, \pi} = s^2$. By identifying a set of gauge theory numerators that obey the same algebraic relations as the color factors, one can construct consistent double copy theories.

For example, consider the two-loop divergence for the $(++++)$ anomalous matrix element in pure BI theory. The 4D helicity structure can be captured by a symmetric structure double-copy between NLSM pion numerators and a local gauge theory contact at $\mathcal{O}(\alpha'^5)$. The s -channel numerators for this symmetric-structure double copy are as follows

$$n_s^{\text{NLSM}} = s^2 \quad n_s^{\text{HD}} = s^5 \frac{[12][34]}{\langle 12 \rangle \langle 34 \rangle} \quad (5.23)$$

Double-copying these kinematic numerators yields a matrix element of the form:

$$\mathcal{M}^{\text{BI+HD}} = \sum_{g \in \Gamma^3} \frac{n_g^{\text{HD}} n_g^{\text{dd}, \pi}}{d_g} = (s^6 + t^6 + u^6) \frac{[12][34]}{\langle 12 \rangle \langle 34 \rangle} \quad (5.24)$$

While this construction lacks any algebraic relations between the four-point kinematic-factors, similar symmetric numerators were found at six-point for NLSM, which obey non-trivial

algebraic relations. As we will now show, the amplitude above that is needed to cancel the two-loop anomaly can be constructed from an equivalent adjoint double, at the cost of introducing a spin-5 off-shell mode in the single copy gauge theory.

5.2.2 Higher-spin \otimes Adler Zero

Guided by the dual description of NLSM pion amplitudes as symmetric and adjoint double copies, we can easily cast the symmetric-structure numerators back to adjoint kinematics. Due to the duality between color and kinematic factors, we construct partner adjoint numerators using the following color relation:

$$c_s^{\text{ff}} = c_t^{\text{dd}} - c_u^{\text{dd}} \quad \Leftrightarrow \quad n_s^{\text{ff}} = n_t^{\text{dd}} - n_u^{\text{dd}} \quad (5.25)$$

Applying this identity to the symmetric vector numerator needed to reproduce the two-loop all-plus counterterm yields the following adjoint color-dual s -channel numerator:

$$n_s^{\text{HD},(2)} = (t^5 - u^5) \frac{[12][34]}{\langle 12 \rangle \langle 34 \rangle} . \quad (5.26)$$

Following the argument of [21], this degree five kinematic numerator indicates that there is a spin-5 mode in on top of the s -channel pole. However, when double-copied with NLSM the residue is suppressed by the Adler zero satisfying four-point contact of pion amplitudes. Thus, this adjoint color-dual numerator serves as a consistent single-copy theory when composed with color-dual NLSM numerators.

Guided by the structure of the anomalous BI matrix elements computed through two-loop in the text, a possible guess for the single-copy HD vector numerators needed to cancel the leading L -loop divergence might go as

$$n_s^{\text{HD},(L)} \stackrel{?}{=} (t^{2L+1} - u^{2L+1}) \frac{[12][34]}{\langle 12 \rangle \langle 34 \rangle} \quad (5.27)$$

This all-loop guess mirrors the structure of the one-loop adjoint numerator identified in [50], and the two-loop counterterm numerator expressed above in eq. (5.26), in that at each loop order we would require the addition of a higher odd-integer-spin mode.

The physical picture one should have for this class of photon effective operators, is that symmetric-structure double-copy and adjoint double-copy with higher spin modes are one in the same. In exchange for constructing color-dual adjoint numerators needed adjoint double-copy, or equivalently the KLT kernel, one must admit the addition of higher spin modes. However, as long as these higher spin modes are composed via adjoint double-copy, $\overset{\text{adj.}}{\otimes}$, with contact numerators, they map to the same local vector numerators one would achieve with the symmetric double-copy kernel, $\overset{\text{sym.}}{\otimes}$,

$$\text{[Diagrammatic Equation (5.28)]} \quad (5.28)$$

It would be fascinating to determine if the resulting adjoint higher-spin theory that is sourced by the anomalous matrix elements in pure BI theory is in any way a consistent physical theory. One natural guess would be some sort of tensionless limit of string theory, where the tower of massless higher spin modes are needed for the theory to be unitary. Along these lines, there have been many recent studies into building higher-spin gauge theories constructively from general principles of locality and unitarity [161–166]. There is also a possibility that these higher-derivative operators could be required for double-copy consistency at higher-multiplicity. Such behavior was demonstrated for $\text{YM} + F^3$ gauge theory [18], where double-copy consistency demanded a tower of four-point contacts that conjecturally resums to $DF^2 + \text{YM}$ theory of Johansson and Nohle [167, 168]. More recently, similar structure was likewise identified for higher-derivative corrections to biadjoint scalar EFT [22, 23]. We see better understanding the double-copy consistency of higher-spin gauge theory as an exciting direction of future study.

5.3 Evanescent operator counting

Before concluding, in this subsection we briefly describe the evanescent operator counting at higher orders in mass dimension needed for $U(1)$ duality satisfying quantum effective actions. Hilbert series are an effective method for counting the number of independent operators at a particular order in mass dimension [169, 170], which have been used in abundance in the SMEFT literature [171–173]. Here, we construct the Hilbert series for general dimension photon operators, $\mathcal{H}^{\text{gen},D}$, and similarly so for $D = 4$ operators, $\mathcal{H}^{D=4}$, for which we are restricted to a subset of 4D helicity operators.

To construct the Hilbert series for photon operators, we will define the coefficient at order- n of a polynomial in α to be the number of operators that appear at $\mathcal{O}(\alpha^{n+2})$ in our dimensionful coupling. It turns out that there are only two integer sequences that control the operator counting, which are common feature when enumerating operator bases for 2-to-2 scattering events [174–179]. The first sequence is produced by Hilbert series that counts four-point permutation invariants, $\sigma_3^x \sigma_2^y$, which we call $\mathcal{H}^{(ijkl)}$,

$$[\mathcal{H}^{(ijkl)}] = 1, 0, 1, 1, 1, 1, 2, 1, 2, 2, 2, 3, 2, 3, 3, 3, \dots \quad (5.29)$$

and the second is the series that counts symmetric invariants, $s_{ij}^x (s_{ik} s_{jk})^y$, which we denote as $\mathcal{H}^{(ij)(kl)}$,

$$[\mathcal{H}^{(ij)(kl)}] = 1, 1, 2, 2, 3, 3, 4, 4, 5, 5, 6, 6, 7, 7, 8, 8, \dots \quad (5.30)$$

where we have defined the bracket $[\mathcal{H}]$ such that it maps Hilbert series with integer coefficients at successive orders in α into a sequence of numbers. Both of these Hilbert series are simple rational functions of α , which we state below:

$$\mathcal{H}^{(ij)(kl)} = \frac{1}{(\alpha - 1)^2(\alpha + 1)} = \alpha^0 + \alpha^2 + \alpha^3 + \alpha^4 + \alpha^5 + 2\alpha^6 + \alpha^6 + 2\alpha^8 + \dots \quad (5.31)$$

$$\mathcal{H}^{(ijkl)} = \frac{1}{(\alpha - 1)^2(\alpha + 1)(\alpha^2 + \alpha + 1)} = \alpha^0 + \alpha^1 + 2\alpha^2 + 2\alpha^3 + 3\alpha^4 + \dots \quad (5.32)$$

Using these, we can infer the operator counting for both general dimension and the $D = 4$ operators. The general dimension operator basis that we have used throughout scales as follows:

$$\mathcal{O}_{(x,y)}^{F^2 F^2} \sim s_{ij}^x (s_{ik} s_{jk})^y \quad \mathcal{O}_{(x,y)}^{F^4} \sim s_{ij}^x (s_{ik} s_{jk})^y \quad \mathcal{O}_{(x,y)}^{F^3} \sim \sigma_3^x \sigma_2^y \quad (5.33)$$

where $\mathcal{O}_{(x,y)}^{F^4}$ begins at $\mathcal{O}(\alpha'^3)$ and both $\mathcal{O}_{(x,y)}^{F^2 F^2}$ and $\mathcal{O}_{(x,y)}^{F^4}$ begin at $\mathcal{O}(\alpha'^2)$. Thus, the Hilbert series $\mathcal{H}^{\text{gen.}D}$ can be defined as follows:

$$\mathcal{H}^{\text{gen.}D} = 2\mathcal{H}^{(ij)(kl)} + \alpha\mathcal{H}^{(ijkl)} \quad (5.34)$$

In contrast, the 4D helicity structures scale as follows:

$$\mathcal{O}_{(x,y)}^{(--++)} \sim s_{ij}^x (s_{ik} s_{jk})^y \quad \mathcal{O}_{(x,y)}^{(-+++)} \sim \sigma_3^x \sigma_2^y \quad \mathcal{O}_{(x,y)}^{(++++)} \sim \sigma_3^x \sigma_2^y \quad (5.35)$$

Similar to the D -dimensional operators above, $\mathcal{O}_{(x,y)}^{(--++)}$ starts at $\mathcal{O}(\alpha'^2)$ and $\mathcal{O}_{(x,y)}^{(-+++)}$ begins the sequence at $\mathcal{O}(\alpha'^3)$. However, the all plus behavior is slightly abnormal relative to the other counting sequences. Rather than pushing of the sequence to higher orders in α' , it starts the sequence specified by $\mathcal{H}^{(ijkl)}$ at the third entry at $\mathcal{O}(\alpha'^2)$. Thus, the $D = 4$ Hilbert series can be defined as follows:

$$\mathcal{H}^{D=4} = \mathcal{H}^{(ij)(kl)} + \alpha\mathcal{H}^{(ijkl)} + (1 + \alpha - \alpha^3)\mathcal{H}^{(ijkl)} \quad (5.36)$$

Putting this all together we obtain the following expression for the general dimension and 4D four-photon operator Hilbert series:

$$\boxed{\begin{aligned} \mathcal{H}^{\text{gen.}D} &= \frac{(\alpha + 2)(\alpha + 1) + \alpha^2}{(\alpha - 1)^2(\alpha + 1)(\alpha^2 + \alpha + 1)} \\ \mathcal{H}^{D=4} &= \frac{(\alpha + 2)(\alpha + 1) - \alpha^3}{(\alpha - 1)^2(\alpha + 1)(\alpha^2 + \alpha + 1)} \end{aligned}} \quad (5.37)$$

With this, we can determine the number of evanescent operators that can contribute at each successive order in α' for four-photon matrix elements. The number of evanescent operators at each mass-dimension is just the difference between the dimension of the general dimension Hilbert series, and that of the $D = 4$ Hilbert series, $\mathcal{H}^{\text{ev.}} = \mathcal{H}^{\text{gen.}D} - \mathcal{H}^{D=4}$. Thus we obtain the following Hilbert series for the number of evanescent four-photon operators at $\mathcal{O}(\alpha'^{n+2})$:

$$\boxed{\mathcal{H}^{\text{ev.}} = \frac{\alpha^2}{(\alpha - 1)^2(\alpha^2 + \alpha + 1)}} \quad (5.38)$$

It would be interesting to determine whether the three Hilbert series stated above owe their construction to some hidden geometric origin. Indeed all of the operator counting in the SMEFT literature can be traced to the geometry of the group theory representations that underly the Standard Model [169, 170]. We leave identifying these concealed mathematical structures as an exciting direction of future study.

6 Conclusions

In this manuscript, we have carried out a detailed analysis of NLSM and DBIVA effective field theories at NNLO in the perturbative expansion. In section 2, we provided a review of the generalized unitarity and integration methods employed throughout the text. Then in section 3 we introduced and developed the on-shell constructive methods of Even-point Multi-loop Unitarity (EMU), and computed the tensor reduction for triangle and bubble integrals in D -dimensions of arbitrary rank along with a spanning set of four-photon operators needed to capture higher-loop effects. Due to the simplicity of even-point multi-loop amplitudes of NLSM and DBIVA, these methods allowed us to compute fully integrated two-loop amplitudes for NLSM, pure Born-Infeld, and $\mathcal{N} = 4$ DBIVA theory in section 4. Finally, in section 5 we studied the quantum effective actions that capture the aforementioned loop effects. In doing so, we have identified a variety of rich physical structures that we summarize below:

Exponentiation In eq. (4.29) and eq. (4.30) we computed in general dimension, D , the two contributions to NLSM two-loop amplitudes. Evaluating these diagrams in $D = 2 - 2\epsilon$, and taking the planar limit, $N_c \rightarrow \infty$, we found in eq. (4.37) that the IR divergences exponentiate through two-loop. This non-trivial property is found in theories that are conjectured to be integrable [151–154], like $\mathcal{N} = 4$ super-Yang-Mills [139, 140]. In future work, we hope to study whether this iterative structure can be further applied to the scale dependent logarithms present at multi-loop order in the theory.

Anomalies Equipped with our D -dimensional integration methods, we performed an analogous calculation at two-loop for pure Born-Infeld in section 4.2.2. In doing so, we demonstrated that the previously identified one-loop counterterm is not sufficient to cancel the two-loop anomaly. In fact, the $(- + ++)$ anomaly of eq. (4.76), which was absent at one-loop, diverges at two-loop order due to the presence of a one-loop evanescent operator in the D -dimensional formulation of Born-Infeld theory. One resolution to this anomaly comes in the form of introducing $\mathcal{N} = 4$ DBIVA superfields in the two-loop state-sum. This protects the S -matrix from anomalies by promoting the classically conserved $U(1)$ duality to a supersymmetric R-symmetry. The evaluated integrals that contribute to the $\mathcal{N} = 4$ DBIVA two-loop amplitudes are provided in eq. (4.86) and eq. (4.87).

Evanescence Another resolution to the two-loop anomaly comes in the form of higher-derivative pure-photon counterterms. To do so, we demonstrated through explicit calculation in section 5.1 that we must introduce a divergence evanescent operator at one-loop order. This is similar to the anomalies of pure Einstein-Hilbert gravity [131, 132], which vanish at one-loop since the R^2 Gauss-Bonnet term is evanescent in $D = 4$, but which diverge at two-loop order [59–61]. Given the complexity of gravity calculations at high loop order, further studies of multi-loop Born-Infeld amplitudes could serve as accessible laboratory for studying evanescent effects beyond one-loop in double-copy constructible theories. To this end, we have

used Hilbert series to count the number of four-photon evanescent operators to higher-order derivative corrections in section 5.3 to aid in future studies.

In addition to these themes woven throughout the text, we have en passant identified novel double-copy structures at two-loop. In section 4.3 we found that two-loop $\mathcal{N} = 4$ DBIVA amplitudes can be constructed via the double copy of color-dual $\mathcal{N} = 4$ sYM integrands with the generalized unitarity cuts of NLSM. This construction was D -dimensionally identical to the result obtained via generalized unitarity and maximal supersymmetric state sums. While not a proof, this provides strong evidence for the compatibility of NLSM with color-kinematics duality beyond one-loop. This result also serves as the first non-gravitational double-copy beyond one-loop, further supporting the consistency of color-kinematics duality at loop-level, which as of today remains a conjecture.

Moreover, recent work by the authors has demonstrated that color-kinematics duality can be used as a bootstrap principle to constrain higher derivative operators. This has been shown both for gauged NLSM amplitudes [19] and $\text{YM} + F^3$ theory [18], the later of which is particularly relevant for anomaly cancellation, and possibly UV completion, of both $\mathcal{N} = 4$ supergravity and the R^3 modification to Einstein-Hilbert gravity [18]. Indeed, similar structure has been recently identified in color-dual scalar theories [22–24]. This observation suggests a new paradigm that elevates color-kinematics duality from a mathematical correspondence capable of encoding IR symmetries, to a principle that probes signatures of UV physics captured by higher-derivative corrections. Guided by this new paradigm, a natural next step is to determine whether the anomaly cancelling counterterms of eq. (4.74) and eq. (4.76) source additional higher-loop counterterms constrained by double-copy consistency, in the spirit of [18]. We see this as an exciting future direction in further understanding the loop-level constraints imposed by the duality between color and kinematics.

Acknowledgments The authors would like to thank Rafael Aoude, Alex Edison, Kezhu Guo, Ian Low, James Mangan, Frank Petriello, Nia Robles, Radu Roiban, Aslan Seifi, and Suna Zekioglu for insightful conversations, related collaboration, and encouragement throughout the completion of this work. This work was supported by the DOE under contract DE-SC0015910 and by the Alfred P. Sloan Foundation. N.H.P. additionally acknowledges the Northwestern University Amplitudes and Insight group, the Department of Physics and Astronomy, and Weinberg College for their generous support.

References

- [1] Z. Bern, L.J. Dixon, D.C. Dunbar and D.A. Kosower, *One loop n -point gauge theory amplitudes, unitarity and collinear limits*, *Nucl. Phys.* **B425** (1994) 217 [[hep-ph/9403226](#)].
- [2] Z. Bern, L.J. Dixon, D.C. Dunbar and D.A. Kosower, *Fusing gauge theory tree amplitudes into loop amplitudes*, *Nucl. Phys.* **B435** (1995) 59 [[hep-ph/9409265](#)].
- [3] Z. Bern, L.J. Dixon and D.A. Kosower, *Progress in one loop QCD computations*, *Ann. Rev. Nucl. Part. Sci.* **46** (1996) 109 [[hep-ph/9602280](#)].

- [4] D. Forde, *Direct extraction of one-loop integral coefficients*, *Phys. Rev. D* **75** (2007) 125019 [[0704.1835](#)].
- [5] Z. Bern, J.J.M. Carrasco and H. Johansson, *New relations for gauge-theory amplitudes*, *Phys. Rev. D* **78** (2008) 085011 [[0805.3993](#)].
- [6] Z. Bern, J.J.M. Carrasco and H. Johansson, *Perturbative quantum gravity as a double copy of gauge theory*, *Phys. Rev. Lett.* **105** (2010) 061602 [[1004.0476](#)].
- [7] A. Adams, N. Arkani-Hamed, S. Dubovsky, A. Nicolis and R. Rattazzi, *Causality, analyticity and an IR obstruction to UV completion*, *JHEP* **10** (2006) 014 [[hep-th/0602178](#)].
- [8] C. Cheung, K. Kampf, J. Novotny and J. Trnka, *Effective Field Theories from Soft Limits of Scattering Amplitudes*, *Phys. Rev. Lett.* **114** (2015) 221602 [[1412.4095](#)].
- [9] C. Cheung, K. Kampf, J. Novotny, C.-H. Shen and J. Trnka, *On-Shell Recursion Relations for Effective Field Theories*, *Phys. Rev. Lett.* **116** (2016) 041601 [[1509.03309](#)].
- [10] C. Cheung, K. Kampf, J. Novotny, C.-H. Shen and J. Trnka, *A Periodic Table of Effective Field Theories*, *JHEP* **02** (2017) 020 [[1611.03137](#)].
- [11] C. Cheung, K. Kampf, J. Novotny, C.-H. Shen, J. Trnka and C. Wen, *Vector Effective Field Theories from Soft Limits*, *Phys. Rev. Lett.* **120** (2018) 261602 [[1801.01496](#)].
- [12] I. Low and Z. Yin, *Soft Bootstrap and Effective Field Theories*, *JHEP* **11** (2019) 078 [[1904.12859](#)].
- [13] J.J.M. Carrasco, L. Rodina, Z. Yin and S. Zekioglu, *Simple encoding of higher derivative gauge and gravity counterterms*, *Phys. Rev. Lett.* **125** (2020) 251602 [[1910.12850](#)].
- [14] N. Arkani-Hamed, T.-C. Huang and Y.-t. Huang, *The EFT-Hedron*, *JHEP* **05** (2021) 259 [[2012.15849](#)].
- [15] J.J.M. Carrasco, L. Rodina and S. Zekioglu, *Composing effective prediction at five points*, *JHEP* **06** (2021) 169 [[2104.08370](#)].
- [16] H.-H. Chi, H. Elvang, A. Herderschee, C.R.T. Jones and S. Paranjape, *Generalizations of the double-copy: the KLT bootstrap*, *JHEP* **03** (2022) 077 [[2106.12600](#)].
- [17] Q. Bonnefoy, G. Durieux, C. Grojean, C.S. Machado and J. Roosmale Nepveu, *The seeds of EFT double copy*, *JHEP* **05** (2022) 042 [[2112.11453](#)].
- [18] J.J.M. Carrasco, M. Lewandowski and N.H. Pavao, *The color-dual fates of F^3 , R^3 , and $\mathcal{N} = 4$ supergravity*, [2203.03592](#).
- [19] J.J.M. Carrasco, M. Lewandowski and N.H. Pavao, *Double-copy towards supergravity inflation with α -attractor models*, *JHEP* **02** (2023) 015 [[2211.04441](#)].
- [20] D. Green, Y. Huang and C.-H. Shen, *Inflationary Adler conditions*, *Phys. Rev. D* **107** (2023) 043534 [[2208.14544](#)].
- [21] N.H. Pavao, *Effective observables for electromagnetic duality from novel amplitude decomposition*, *Phys. Rev. D* **107** (2023) 065020 [[2210.12800](#)].
- [22] A.S.-K. Chen, H. Elvang and A. Herderschee, *Emergence of String Monodromy in Effective Field Theory*, [2212.13998](#).

- [23] A.S.-K. Chen, H. Elvang and A. Herderschee, *Bootstrapping the String KLT Kernel*, [2302.04895](#).
- [24] T.V. Brown, K. Kampf, U. Oktem, S. Paranjape and J. Trnka, *Scalar BCJ Bootstrap*, [2305.05688](#).
- [25] Z. Bern, J.J. Carrasco, M. Chiodaroli, H. Johansson and R. Roiban, *The Duality Between Color and Kinematics and its Applications*, [1909.01358](#).
- [26] Z. Bern, J.J. Carrasco, M. Chiodaroli, H. Johansson and R. Roiban, *The SAGEX Review on Scattering Amplitudes, Chapter 2: An Invitation to Color-Kinematics Duality and the Double Copy*, [2203.13013](#).
- [27] T. Adamo, J.J.M. Carrasco, M. Carrillo-González, M. Chiodaroli, H. Elvang, H. Johansson et al., *Snowmass White Paper: the Double Copy and its Applications*, in *2022 Snowmass Summer Study*, 4, 2022 [[2204.06547](#)].
- [28] Z. Bern, J.J.M. Carrasco, L.J. Dixon, H. Johansson and R. Roiban, *Simplifying Multiloop Integrands and Ultraviolet Divergences of Gauge Theory and Gravity Amplitudes*, *Phys. Rev. D* **85** (2012) 105014 [[1201.5366](#)].
- [29] Z. Bern, J.J.M. Carrasco, L.J. Dixon, H. Johansson and R. Roiban, *The complete four-loop four-point amplitude in $\mathcal{N} = 4$ super-Yang-Mills theory*, *Phys. Rev. D* **82** (2010) 125040 [[1008.3327](#)].
- [30] Z. Bern, J.J. Carrasco, L.J. Dixon, H. Johansson and R. Roiban, *The ultraviolet behavior of $\mathcal{N} = 8$ supergravity at four loops*, *Phys. Rev. Lett.* **103** (2009) 081301 [[0905.2326](#)].
- [31] N.E.J. Bjerrum-Bohr, T. Dennen, R. Monteiro and D. O’Connell, *Integrand Oxidation and one-loop colour-dual numerators in $\mathcal{N} = 4$ gauge theory*, *JHEP* **07** (2013) 092 [[1303.2913](#)].
- [32] A. Edison, S. He, O. Schlotterer and F. Teng, *One-loop Correlators and BCJ Numerators from Forward Limits*, *JHEP* **09** (2020) 079 [[2005.03639](#)].
- [33] A. Edison, S. He, H. Johansson, O. Schlotterer, F. Teng and Y. Zhang, *Perfecting one-loop BCJ numerators in SYM and supergravity*, *JHEP* **02** (2023) 164 [[2211.00638](#)].
- [34] C. Cheung and C.-H. Shen, *Symmetry for flavor-kinematics duality from an action*, *Phys. Rev. Lett.* **118** (2017) 121601 [[1612.00868](#)].
- [35] S. He, O. Schlotterer and Y. Zhang, *New BCJ representations for one-loop amplitudes in gauge theories and gravity*, *Nucl. Phys. B* **930** (2018) 328 [[1706.00640](#)].
- [36] Z. Bern, S. Davies, T. Dennen, Y.-t. Huang and J. Nohle, *Color-kinematics duality for pure Yang-Mills and gravity at one and two Loops*, *Phys. Rev. D* **92** (2015) 045041 [[1303.6605](#)].
- [37] G. Mogull and D. O’Connell, *Overcoming Obstacles to Colour-Kinematics Duality at Two Loops*, *JHEP* **12** (2015) 135 [[1511.06652](#)].
- [38] Z. Bern, S. Davies and J. Nohle, *Double-Copy Constructions and Unitarity Cuts*, *Phys. Rev. D* **93** (2016) 105015 [[1510.03448](#)].
- [39] Y. Geyer, R. Monteiro and R. Stark-Muchão, *Two-Loop Scattering Amplitudes: Double-Forward Limit and Colour-Kinematics Duality*, *JHEP* **12** (2019) 049 [[1908.05221](#)].
- [40] H. Johansson, G. Kälin and G. Mogull, *Two-loop supersymmetric QCD and half-maximal supergravity amplitudes*, *JHEP* **09** (2017) 019 [[1706.09381](#)].

- [41] G. Chen, H. Johansson, F. Teng and T. Wang, *On the kinematic algebra for BCJ numerators beyond the MHV sector*, *JHEP* **11** (2019) 055 [[1906.10683](#)].
- [42] G. Chen, H. Johansson, F. Teng and T. Wang, *Next-to-MHV Yang-Mills kinematic algebra*, *JHEP* **10** (2021) 042 [[2104.12726](#)].
- [43] A. Brandhuber, G. Chen, H. Johansson, G. Travaglini and C. Wen, *Kinematic Hopf Algebra for Bern-Carrasco-Johansson Numerators in Heavy-Mass Effective Field Theory and Yang-Mills Theory*, *Phys. Rev. Lett.* **128** (2022) 121601 [[2111.15649](#)].
- [44] C. Cheung and J. Mangan, *Covariant color-kinematics duality*, *JHEP* **11** (2021) 069 [[2108.02276](#)].
- [45] M. Ben-Shahar and H. Johansson, *Off-shell color-kinematics duality for Chern-Simons*, *JHEP* **08** (2022) 035 [[2112.11452](#)].
- [46] C. Cheung, J. Mangan, J. Parra-Martinez and N. Shah, *Non-perturbative Double Copy in Flatland*, *Phys. Rev. Lett.* **129** (2022) 221602 [[2204.07130](#)].
- [47] M. Ben-Shahar, L. Garozzo and H. Johansson, *Lagrangians Manifesting Color-Kinematics Duality in the NMHV Sector of Yang-Mills*, [2301.00233](#).
- [48] F. Cachazo, S. He and E.Y. Yuan, *Scattering Equations and Matrices: From Einstein To Yang-Mills, DBI and NLSM*, *JHEP* **07** (2015) 149 [[1412.3479](#)].
- [49] J.J.M. Carrasco, C.R. Mafra and O. Schlotterer, *Abelian Z-theory: NLSM amplitudes and α' -corrections from the open string*, *JHEP* **06** (2017) 093 [[1608.02569](#)].
- [50] J.J.M. Carrasco and N.H. Pavao, *Virtues of a symmetric-structure double copy*, *Phys. Rev. D* **107** (2023) 065005 [[2211.04431](#)].
- [51] H. Elvang, M. Hadjiantonis, C.R.T. Jones and S. Paranjape, *Electromagnetic Duality and D3-Brane Scattering Amplitudes Beyond Leading Order*, *JHEP* **04** (2021) 173 [[2006.08928](#)].
- [52] Z. Bern, J.J. Carrasco, D. Forde, H. Ita and H. Johansson, *Unexpected Cancellations in Gravity Theories*, *Phys. Rev. D* **77** (2008) 025010 [[0707.1035](#)].
- [53] J.J.M. Carrasco, R. Kallosh, R. Roiban and A.A. Tseytlin, *On the $U(1)$ duality anomaly and the S -matrix of $N=4$ supergravity*, *JHEP* **07** (2013) 029 [[1303.6219](#)].
- [54] N. Craig, I. Garcia Garcia and G.D. Kribs, *The UV fate of anomalous $U(1)$ s and the Swampland*, *JHEP* **11** (2020) 063 [[1912.10054](#)].
- [55] R. Monteiro, R. Stark-Muchão and S. Wikeley, *Anomaly and double copy in quantum self-dual Yang-Mills and gravity*, [2211.12407](#).
- [56] Z. Bern, A. Edison, D. Kosower and J. Parra-Martinez, *Curvature-squared multiplets, evanescent effects, and the $U(1)$ anomaly in $\mathcal{N}=4$ supergravity*, *Phys. Rev.* **D96** (2017) 066004 [[1706.01486](#)].
- [57] Z. Bern, J. Parra-Martinez and R. Roiban, *Canceling the $U(1)$ Anomaly in the S Matrix of $N=4$ Supergravity*, *Phys. Rev. Lett.* **121** (2018) 101604 [[1712.03928](#)].
- [58] Z. Bern, D. Kosower and J. Parra-Martinez, *Two-loop n -point anomalous amplitudes in $\mathcal{N}=4$ supergravity*, [1905.05151](#).

- [59] M.H. Goroff and A. Sagnotti, *QUANTUM GRAVITY AT TWO LOOPS*, *Phys. Lett. B* **160** (1985) 81.
- [60] M.H. Goroff and A. Sagnotti, *The Ultraviolet Behavior of Einstein Gravity*, *Nucl. Phys. B* **266** (1986) 709.
- [61] A.E.M. van de Ven, *Two loop quantum gravity*, *Nucl. Phys. B* **378** (1992) 309.
- [62] Z. Bern, S. Davies, T. Dennen, A.V. Smirnov and V.A. Smirnov, *Ultraviolet Properties of $N=4$ Supergravity at Four Loops*, *Phys. Rev. Lett.* **111** (2013) 231302 [[1309.2498](#)].
- [63] M. Alishahiha, E. Silverstein and D. Tong, *DBI in the sky*, *Phys. Rev. D* **70** (2004) 123505 [[hep-th/0404084](#)].
- [64] P. Creminelli, A. Nicolis, L. Senatore, M. Tegmark and M. Zaldarriaga, *Limits on non-gaussianities from wmap data*, *JCAP* **05** (2006) 004 [[astro-ph/0509029](#)].
- [65] J.R. Fergusson and E.P.S. Shellard, *The shape of primordial non-Gaussianity and the CMB bispectrum*, *Phys. Rev. D* **80** (2009) 043510 [[0812.3413](#)].
- [66] J.J.M. Carrasco, R. Kallosh and A. Linde, *α -Attractors: Planck, LHC and Dark Energy*, *JHEP* **10** (2015) 147 [[1506.01708](#)].
- [67] J.J.M. Carrasco, R. Kallosh and A. Linde, *Cosmological Attractors and Initial Conditions for Inflation*, *Phys. Rev. D* **92** (2015) 063519 [[1506.00936](#)].
- [68] J.J.M. Carrasco, R. Kallosh, A. Linde and D. Roest, *Hyperbolic geometry of cosmological attractors*, *Phys. Rev. D* **92** (2015) 041301 [[1504.05557](#)].
- [69] BICEP, KECK collaboration, *Improved Constraints on Primordial Gravitational Waves using Planck, WMAP, and BICEP/Keck Observations through the 2018 Observing Season*, *Phys. Rev. Lett.* **127** (2021) 151301 [[2110.00483](#)].
- [70] R. Kallosh and A. Linde, *BICEP/Keck and cosmological attractors*, *JCAP* **12** (2021) 008 [[2110.10902](#)].
- [71] R. Kleiss and H. Kuijf, *Multi - Gluon Cross-sections and Five Jet Production at Hadron Colliders*, *Nucl. Phys. B* **312** (1989) 616.
- [72] J.J.M. Carrasco, *Gauge and gravity amplitude relations*, in *Proceedings, Theoretical Advanced Study Institute in Elementary Particle Physics: Journeys Through the Precision Frontier: Amplitudes for Colliders (TASI 2014): Boulder, Colorado, June 2-27, 2014*, pp. 477–557, WSP, WSP, 2015, DOI [[1506.00974](#)].
- [73] S.D. Badger, *Direct Extraction Of One Loop Rational Terms*, *JHEP* **01** (2009) 049 [[0806.4600](#)].
- [74] H. Elvang and Y.-t. Huang, *Scattering amplitudes*, [1308.1697](#).
- [75] G. Passarino and M.J.G. Veltman, *One Loop Corrections for $e^+ e^-$ Annihilation Into $\mu^+ \mu^-$ in the Weinberg Model*, *Nucl. Phys. B* **160** (1979) 151.
- [76] Z. Bern, L.J. Dixon and D.A. Kosower, *Dimensionally regulated pentagon integrals*, *Nucl. Phys. B* **412** (1994) 751 [[hep-ph/9306240](#)].
- [77] S. Weinberg, *Phenomenological Lagrangians*, *Physica A* **96** (1979) 327.

- [78] J. Gasser and H. Leutwyler, *Chiral Perturbation Theory to One Loop*, *Annals Phys.* **158** (1984) 142.
- [79] A.V. Manohar and V. Mateu, *Dispersion Relation Bounds for $\pi\pi$ Scattering*, *Phys. Rev. D* **77** (2008) 094019 [[0801.3222](#)].
- [80] B. Bellazzini, *Softness and amplitudes' positivity for spinning particles*, *JHEP* **02** (2017) 034 [[1605.06111](#)].
- [81] A.L. Guerrieri, J. Penedones and P. Vieira, *S-matrix bootstrap for effective field theories: massless pions*, *JHEP* **06** (2021) 088 [[2011.02802](#)].
- [82] J. Bijnens, G. Colangelo, G. Ecker, J. Gasser and M.E. Sainio, *Elastic $\pi\pi$ scattering to two loops*, *Phys. Lett. B* **374** (1996) 210 [[hep-ph/9511397](#)].
- [83] J. Bijnens, G. Colangelo, G. Ecker, J. Gasser and M.E. Sainio, *Pion-pion scattering at low energy*, *Nucl. Phys. B* **508** (1997) 263 [[hep-ph/9707291](#)].
- [84] L. Girlanda, M. Knecht, B. Moussallam and J. Stern, *Comment on the prediction of two loop standard chiral perturbation theory for low-energy $\pi\pi$ scattering*, *Phys. Lett. B* **409** (1997) 461 [[hep-ph/9703448](#)].
- [85] M. Born and L. Infeld, *Foundations of the new field theory*, *Proc. Roy. Soc. Lond. A* **144** (1934) 425.
- [86] C. de Rham and A.J. Tolley, *DBI and the Galileon reunited*, *JCAP* **05** (2010) 015 [[1003.5917](#)].
- [87] D.V. Volkov and V.P. Akulov, *Is the Neutrino a Goldstone Particle?*, *Phys. Lett. B* **46** (1973) 109.
- [88] R. Kallosh, *Volkov-Akulov theory and D-branes*, [hep-th/9705118](#).
- [89] Z. Komargodski and N. Seiberg, *From Linear SUSY to Constrained Superfields*, *JHEP* **09** (2009) 066 [[0907.2441](#)].
- [90] S.M. Kuzenko and S.J. Tyler, *Relating the Komargodski-Seiberg and Akulov-Volkov actions: Exact nonlinear field redefinition*, *Phys. Lett. B* **698** (2011) 319 [[1009.3298](#)].
- [91] M. Rocek, *Linearizing the Volkov-Akulov Model*, *Phys. Rev. Lett.* **41** (1978) 451.
- [92] R. Casalbuoni, S. De Curtis, D. Dominici, F. Feruglio and R. Gatto, *Nonlinear Realization of Supersymmetry Algebra From Supersymmetric Constraint*, *Phys. Lett. B* **220** (1989) 569.
- [93] S. Ferrara, R. Kallosh and A. Linde, *Cosmology with Nilpotent Superfields*, *JHEP* **10** (2014) 143 [[1408.4096](#)].
- [94] R. Kallosh, A. Linde and D. Roest, *Superconformal Inflationary α -Attractors*, *JHEP* **11** (2013) 198 [[1311.0472](#)].
- [95] A.A. Tseytlin, *Born-Infeld action, supersymmetry and string theory*, [hep-th/9908105](#).
- [96] E. Bergshoeff, F. Coomans, R. Kallosh, C.S. Shahbazi and A. Van Proeyen, *Dirac-Born-Infeld-Volkov-Akulov and deformation of supersymmetry*, *JHEP* **08** (2013) 100 [[1303.5662](#)].
- [97] C.R. Mafra, O. Schlotterer and S. Stieberger, *Complete N-Point Superstring Disk Amplitude I. Pure Spinor Computation*, *Nucl. Phys. B* **873** (2013) 419 [[1106.2645](#)].

- [98] C.R. Mafra, O. Schlotterer and S. Stieberger, *Complete N-Point Superstring Disk Amplitude II. Amplitude and Hypergeometric Function Structure*, *Nucl. Phys. B* **873** (2013) 461 [[1106.2646](#)].
- [99] J. Broedel, O. Schlotterer and S. Stieberger, *Polylogarithms, Multiple Zeta Values and Superstring Amplitudes*, *Fortsch. Phys.* **61** (2013) 812 [[1304.7267](#)].
- [100] J.J.M. Carrasco, C.R. Mafra and O. Schlotterer, *Semi-abelian Z-theory: NLSM+ ϕ^3 from the open string*, *JHEP* **08** (2017) 135 [[1612.06446](#)].
- [101] C.R. Mafra and O. Schlotterer, *Non-abelian Z-theory: Berends-Giele recursion for the α' -expansion of disk integrals*, *JHEP* **01** (2017) 031 [[1609.07078](#)].
- [102] H. Kawai, D.C. Lewellen and S.H.H. Tye, *A relation between tree amplitudes of closed and open strings*, *Nucl. Phys. B* **269** (1986) 1.
- [103] M.B. Green, J.H. Schwarz and L. Brink, *N=4 Yang-Mills and N=8 Supergravity as Limits of String Theories*, *Nucl. Phys. B* **198** (1982) 474.
- [104] T. Azevedo, M. Chiodaroli, H. Johansson and O. Schlotterer, *Heterotic and bosonic string amplitudes via field theory*, *JHEP* **10** (2018) 012 [[1803.05452](#)].
- [105] G. Bossard, P.S. Howe and K.S. Stelle, *Anomalies and divergences in N=4 supergravity*, *Phys. Lett. B* **719** (2013) 424 [[1212.0841](#)].
- [106] J. Novotný, *Self-duality, helicity conservation and normal ordering in nonlinear QED*, *Phys. Rev. D* **98** (2018) 085015 [[1806.02167](#)].
- [107] G.W. Gibbons and D.A. Rasheed, *Sl(2,R) invariance of nonlinear electrodynamics coupled to an axion and a dilaton*, *Phys. Lett. B* **365** (1996) 46 [[hep-th/9509141](#)].
- [108] H. Babaei-Aghbolagh and M.R. Garousi, *S-duality of tree-level S-matrix elements in D3-brane effective action*, *Phys. Rev. D* **88** (2013) 026008 [[1304.2938](#)].
- [109] E. Schrödinger, *Contributions to Born's new theory of the electromagnetic field*, *Proc. Roy. Soc. Lond. A* **150** (1935) 465.
- [110] H. Elvang, M. Haddjantonis, C.R.T. Jones and S. Paranjape, *All-Multiplicity One-Loop Amplitudes in Born-Infeld Electrodynamics from Generalized Unitarity*, [1906.05321](#).
- [111] M. Heydeman, J.H. Schwarz and C. Wen, *M5-Brane and D-Brane Scattering Amplitudes*, *JHEP* **12** (2017) 003 [[1710.02170](#)].
- [112] Z. Bern and A.G. Morgan, *Massive loop amplitudes from unitarity*, *Nucl. Phys. B* **467** (1996) 479 [[hep-ph/9511336](#)].
- [113] Z. Bern, L.J. Dixon, D.C. Dunbar and D.A. Kosower, *One loop selfdual and $\mathcal{N} = 4$ super-Yang-Mills*, *Phys. Lett. B* **394** (1997) 105 [[hep-th/9611127](#)].
- [114] J.C. Collins, *Renormalization: An Introduction to Renormalization, the Renormalization Group and the Operator-Product Expansion*, Cambridge Monographs on Mathematical Physics, Cambridge University Press (1984), [10.1017/CBO9780511622656](#).
- [115] Z. Bern, A. De Freitas, L.J. Dixon and H.L. Wong, *Supersymmetric regularization, two loop QCD amplitudes and coupling shifts*, *Phys. Rev. D* **66** (2002) 085002 [[hep-ph/0202271](#)].

- [116] Z. Bern, J.J.M. Carrasco, H. Johansson and D.A. Kosower, *Maximally supersymmetric planar Yang-Mills amplitudes at five loops*, *Phys. Rev. D* **76** (2007) 125020 [[0705.1864](#)].
- [117] J.J.M. Carrasco and I.A. Vazquez-Holm, *Extracting Einstein from the loop-level double-copy*, *JHEP* **11** (2021) 088 [[2108.06798](#)].
- [118] C. Anastasiou and A. Lazopoulos, *Automatic integral reduction for higher order perturbative calculations*, *JHEP* **07** (2004) 046 [[hep-ph/0404258](#)].
- [119] A. von Manteuffel and C. Studerus, *Reduze 2 - Distributed Feynman Integral Reduction*, [1201.4330](#).
- [120] A.V. Smirnov, *FIRE5: a C++ implementation of Feynman Integral REduction*, *Comput. Phys. Commun.* **189** (2015) 182 [[1408.2372](#)].
- [121] A. von Manteuffel and R.M. Schabinger, *A novel approach to integration by parts reduction*, *Phys. Lett. B* **744** (2015) 101 [[1406.4513](#)].
- [122] A.V. Smirnov and F.S. Chuharev, *FIRE6: Feynman Integral REduction with Modular Arithmetic*, *Comput. Phys. Commun.* **247** (2020) 106877 [[1901.07808](#)].
- [123] A.V. Smirnov and V.A. Smirnov, *How to choose master integrals*, *Nucl. Phys. B* **960** (2020) 115213 [[2002.08042](#)].
- [124] J. Usovitsch, *Factorization of denominators in integration-by-parts reductions*, [2002.08173](#).
- [125] P. Maierhöfer and J. Usovitsch, *Kira 1.2 Release Notes*, [1812.01491](#).
- [126] C. Hartmann, W. Shepherd and M. Trott, *The Z decay width in the SMEFT: y_t and λ corrections at one loop*, *JHEP* **03** (2017) 060 [[1611.09879](#)].
- [127] M. Chala, A. Díaz-Carmona and G. Guedes, *A Green's basis for the bosonic SMEFT to dimension 8*, *JHEP* **05** (2022) 138 [[2112.12724](#)].
- [128] J. Aebischer, A.J. Buras and J. Kumar, *Simple rules for evanescent operators in one-loop basis transformations*, *Phys. Rev. D* **107** (2023) 075007 [[2202.01225](#)].
- [129] J. Fuentes-Martín, M. König, J. Pagès, A.E. Thomsen and F. Wilsch, *Evanescent operators in one-loop matching computations*, *JHEP* **02** (2023) 031 [[2211.09144](#)].
- [130] G. Isidori, F. Wilsch and D. Wyler, *The Standard Model effective field theory at work*, [2303.16922](#).
- [131] Z. Bern, C. Cheung, H.-H. Chi, S. Davies, L. Dixon and J. Nohle, *Evanescent Effects Can Alter Ultraviolet Divergences in Quantum Gravity without Physical Consequences*, *Phys. Rev. Lett.* **115** (2015) 211301 [[1507.06118](#)].
- [132] Z. Bern, H.-H. Chi, L. Dixon and A. Edison, *Two-Loop Renormalization of Quantum Gravity Simplified*, *Phys. Rev. D* **95** (2017) 046013 [[1701.02422](#)].
- [133] M.J. Dugan and B. Grinstein, *On the vanishing of evanescent operators*, *Phys. Lett. B* **256** (1991) 239.
- [134] S. Herrlich and U. Nierste, *Evanescent operators, scheme dependences and double insertions*, *Nucl. Phys. B* **455** (1995) 39 [[hep-ph/9412375](#)].
- [135] G. Bell, *NNLO vertex corrections in charmless hadronic B decays: Real part*, *Nucl. Phys. B* **822** (2009) 172 [[0902.1915](#)].

- [136] T. Becher and R.J. Hill, *Loop corrections to heavy-to-light form-factors and evanescent operators in SCET*, *JHEP* **10** (2004) 055 [[hep-ph/0408344](#)].
- [137] L. Di Pietro and E. Stamou, *Operator mixing in the ϵ -expansion: Scheme and evanescent-operator independence*, *Phys. Rev. D* **97** (2018) 065007 [[1708.03739](#)].
- [138] V. Del Duca, L.J. Dixon and F. Maltoni, *New color decompositions for gauge amplitudes at tree and loop level*, *Nucl. Phys. B* **571** (2000) 51 [[hep-ph/9910563](#)].
- [139] C. Anastasiou, Z. Bern, L.J. Dixon and D.A. Kosower, *Planar amplitudes in maximally supersymmetric Yang-Mills theory*, *Phys. Rev. Lett.* **91** (2003) 251602 [[hep-th/0309040](#)].
- [140] Z. Bern, L.J. Dixon and V.A. Smirnov, *Iteration of planar amplitudes in maximally supersymmetric Yang-Mills theory at three loops and beyond*, *Phys. Rev. D* **72** (2005) 085001 [[hep-th/0505205](#)].
- [141] G.F. Sterman and M.E. Tejeda-Yeomans, *Multiloop amplitudes and resummation*, *Phys. Lett. B* **552** (2003) 48 [[hep-ph/0210130](#)].
- [142] J.A. Minahan and K. Zarembo, *The Bethe ansatz for $N=4$ superYang-Mills*, *JHEP* **03** (2003) 013 [[hep-th/0212208](#)].
- [143] I. Bena, J. Polchinski and R. Roiban, *Hidden symmetries of the $AdS(5) \times S^5$ superstring*, *Phys. Rev. D* **69** (2004) 046002 [[hep-th/0305116](#)].
- [144] N. Beisert, *The complete one loop dilatation operator of $N=4$ superYang-Mills theory*, *Nucl. Phys. B* **676** (2004) 3 [[hep-th/0307015](#)].
- [145] N. Beisert, *Higher loops, integrability and the near BMN limit*, *JHEP* **09** (2003) 062 [[hep-th/0308074](#)].
- [146] N. Beisert and M. Staudacher, *The $N=4$ SYM integrable super spin chain*, *Nucl. Phys. B* **670** (2003) 439 [[hep-th/0307042](#)].
- [147] L. Dolan, C.R. Nappi and E. Witten, *A Relation between approaches to integrability in superconformal Yang-Mills theory*, *JHEP* **10** (2003) 017 [[hep-th/0308089](#)].
- [148] G. Arutyunov and M. Staudacher, *Matching higher conserved charges for strings and spins*, *JHEP* **03** (2004) 004 [[hep-th/0310182](#)].
- [149] A.V. Ryzhov and A.A. Tseytlin, *Towards the exact dilatation operator of $N=4$ super Yang-Mills theory*, *Nucl. Phys. B* **698** (2004) 132 [[hep-th/0404215](#)].
- [150] S.A. Frolov, R. Roiban and A.A. Tseytlin, *Gauge-string duality for (non)supersymmetric deformations of $N=4$ super Yang-Mills theory*, *Nucl. Phys. B* **731** (2005) 1 [[hep-th/0507021](#)].
- [151] R. Shankar and E. Witten, *The S Matrix of the Supersymmetric Nonlinear Sigma Model*, *Phys. Rev. D* **17** (1978) 2134.
- [152] A.B. Zamolodchikov and A.B. Zamolodchikov, *Relativistic Factorized S Matrix in Two-Dimensions Having $O(N)$ Isotopic Symmetry*, *JETP Lett.* **26** (1977) 457.
- [153] A.B. Zamolodchikov and A.B. Zamolodchikov, *Factorized s Matrices in Two-Dimensions as the Exact Solutions of Certain Relativistic Quantum Field Models*, *Annals Phys.* **120** (1979) 253.

- [154] S. Komatsu, R. Mahajan and S.-H. Shao, *An Index for Quantum Integrability*, *SciPost Phys.* **7** (2019) 065 [[1907.07186](#)].
- [155] Z. Bern, J.J.M. Carrasco, H. Ita, H. Johansson and R. Roiban, *On the structure of supersymmetric sums in multi-loop unitarity cuts*, *Phys. Rev.* **D80** (2009) 065029 [[0903.5348](#)].
- [156] M. Chiodaroli, Q. Jin and R. Roiban, *Color/kinematics duality for general abelian orbifolds of $\mathcal{N} = 4$ super-Yang-Mills theory*, *JHEP* **01** (2014) 152 [[1311.3600](#)].
- [157] J.J.M. Carrasco and A. Seifi, *Loop-level double-copy for massive fermions in the fundamental*, *JHEP* **05** (2023) 217 [[2302.14861](#)].
- [158] Z. Bern, J.S. Rozowsky and B. Yan, *Two loop four-gluon amplitudes in $\mathcal{N} = 4$ superYang-Mills*, *Phys. Lett.* **B401** (1997) 273 [[hep-ph/9702424](#)].
- [159] J.J.M. Carrasco, A. Edison and H. Johansson, *Maximal Super-Yang-Mills at Six Loops via Novel Integrand Bootstrap*, [2112.05178](#).
- [160] Z. Bern, N.E.J. Bjerrum-Bohr and D.C. Dunbar, *Inherited twistor-space structure of gravity loop amplitudes*, *JHEP* **05** (2005) 056 [[hep-th/0501137](#)].
- [161] S. Caron-Huot, Z. Komargodski, A. Sever and A. Zhiboedov, *Strings from Massive Higher Spins: The Asymptotic Uniqueness of the Veneziano Amplitude*, *JHEP* **10** (2017) 026 [[1607.04253](#)].
- [162] M. Chiodaroli, H. Johansson and P. Pichini, *Compton black-hole scattering for $s \leq 5/2$* , *JHEP* **02** (2022) 156 [[2107.14779](#)].
- [163] L. Cangemi and P. Pichini, *Classical Limit of Higher-Spin String Amplitudes*, [2207.03947](#).
- [164] L. Cangemi, M. Chiodaroli, H. Johansson, A. Ochirov, P. Pichini and E. Skvortsov, *Kerr Black Holes Enjoy Massive Higher-Spin Gauge Symmetry*, [2212.06120](#).
- [165] N. Geiser and L.W. Lindwasser, *Generalized Veneziano and Virasoro amplitudes*, *JHEP* **04** (2023) 031 [[2210.14920](#)].
- [166] C. Cheung and G.N. Remmen, *Veneziano variations: how unique are string amplitudes?*, *JHEP* **01** (2023) 122 [[2210.12163](#)].
- [167] H. Johansson and J. Nohle, *Conformal Gravity from Gauge Theory*, [1707.02965](#).
- [168] H. Johansson, G. Mogull and F. Teng, *Unraveling conformal gravity amplitudes*, *JHEP* **09** (2018) 080 [[1806.05124](#)].
- [169] B. Henning, X. Lu, T. Melia and H. Murayama, *Hilbert series and operator bases with derivatives in effective field theories*, *Commun. Math. Phys.* **347** (2016) 363 [[1507.07240](#)].
- [170] L. Lehman and A. Martin, *Hilbert Series for Constructing Lagrangians: expanding the phenomenologist’s toolbox*, *Phys. Rev. D* **91** (2015) 105014 [[1503.07537](#)].
- [171] R.M. Fonseca, *Enumerating the operators of an effective field theory*, *Phys. Rev. D* **101** (2020) 035040 [[1907.12584](#)].
- [172] C. Hays, A. Martin, V. Sanz and J. Setford, *On the impact of dimension-eight SMEFT operators on Higgs measurements*, *JHEP* **02** (2019) 123 [[1808.00442](#)].
- [173] S. Alioli et al., *Theoretical developments in the SMEFT at dimension-8 and beyond*, in *Snowmass 2021*, 3, 2022 [[2203.06771](#)].

- [174] P.H. Damgaard, K. Haddad and A. Helset, *Heavy Black Hole Effective Theory*, *JHEP* **11** (2019) 070 [[1908.10308](#)].
- [175] K. Haddad and A. Helset, *Tidal effects in quantum field theory*, *JHEP* **12** (2020) 024 [[2008.04920](#)].
- [176] Z. Bern, J. Parra-Martinez, R. Roiban, E. Sawyer and C.-H. Shen, *Leading Nonlinear Tidal Effects and Scattering Amplitudes*, *JHEP* **05** (2021) 188 [[2010.08559](#)].
- [177] R. Balkin, G. Durieux, T. Kitahara, Y. Shadmi and Y. Weiss, *On-shell Higgsing for EFTs*, *JHEP* **03** (2022) 129 [[2112.09688](#)].
- [178] H. Liu, T. Ma, Y. Shadmi and M. Waterbury, *An EFT hunter’s guide to two-to-two scattering: HEFT and SMEFT on-shell amplitudes*, [2301.11349](#).
- [179] K. Haddad, *Recursion in the classical limit and the neutron-star Compton amplitude*, [2303.02624](#).